MODELING AND CONTROL OF EXHAUST RECOMPRESSION HCCI USING VARIABLE VALVE ACTUATION AND FUEL INJECTION

A DISSERTATION
SUBMITTED TO THE DEPARTMENT OF MECHANICAL ENGINEERING
AND THE COMMITTEE ON GRADUATE STUDIES
OF STANFORD UNIVERSITY
IN PARTIAL FULFILLMENT OF THE REQUIREMENTS
FOR THE DEGREE OF
DOCTOR OF PHILOSOPHY

Nikhil Ravi
August 2010

Abstract

With the growing focus on energy and environmental issues in the world today, significant efforts are being made in the automotive industry towards the development of sustainable and clean technologies that can power automobiles. One of the most promising engine technologies along these lines is homogeneous charge compression ignition (HCCI). By using variable valve actuation (VVA) to trap a portion of the exhaust gases and using this to increase the sensible energy of the reactant mixture on the next engine cycle, HCCI allows fast compression ignition of a homogeneous and diluted fuel-air mixture, leading to significantly better efficiency and emissions characteristics in comparison to current technologies. However, due to the lack of a direct combustion trigger, as well as the presence of cycle-to-cycle dynamics where the trapped exhaust from one engine cycle influences combustion on the next, closed-loop control is necessary for the operation of HCCI over a wide operating range.

This thesis presents a physical model-based control framework for controlling an HCCI engine with exhaust recompression and direct injection of fuel into the cylinder. A physical model is used to describe the HCCI process, with the model states being closely linked to the thermodynamic state of the cylinder constituents. Simple linear controllers based on this model are used to control the work output and the phasing of combustion on a cycle-by-cycle basis with the use of variable valve timings as well as variable fuel injection quantity. Experimental results from both single and multi-cylinder engine testbeds are presented, demonstrating the value of a physical model-based approach that allows an easy porting of the control structure from one engine to another. The controllers are also seen to be useful in reducing the cyclic variability of combustion at operating points with late combustion phasing, indicating

the value of this framework in potentially expanding the operating range of HCCI.

Having validated the basic model structure with simple controllers, this thesis then describes the expansion of the modeling framework to include a simple model for the effects of fuel injection during recompression. This represents the first such model of its kind, and it forms the basis for control strategies that use a split fuel injection, with a variable pilot injection timing, to control the phasing of combustion. These include a mid-ranging control scheme where constraints on a realistic implementation of valve actuation such as cam phasers are taken into account. Finally a more comprehensive control framework is developed based on the principle of model predictive control (MPC). The predictive controller is designed for fast tracking of desired load and phasing trajectories while respecting practical constraints on the different actuators as well as other system variables such as air-fuel ratio. Experimental implementation of the MPC scheme demonstrates the promise of this model-based control framework as a practical tool for HCCI control.

Acknowledgements

It is not everyday that one has the opportunity to thank the countless people that have contributed to one's life. Our lives are so interconnected that anything of any significance that we achieve is really the result of a myriad contributions from many unsung heroes. Of nothing is this more true than of the work presented in this thesis - and I would like to express my humble and sincere gratitude to all those giants on whose shoulders this work is built.

Few would argue that one's PhD advisor has maybe the single largest direct contribution to one's PhD experience - and in this aspect I feel truly blessed to have had the chance to work with Prof. Chris Gerdes. I vividly remember our first conversation, on an international call during the course of my application process to Stanford, when he put me (a nervous, wide-eyed, anxious undergraduate) completely at ease, and managed to convince me that coming to Stanford and working with him on engine control was the best decision I could make. Since that fateful day over six years ago, he has grown to become more than just an academic advisor - he has been a mentor in the true sense of the word, and ably guided me through the ups and downs of my graduate career. I have really valued his gift for being able to find the right balance, with each student, between guiding them and giving them the independence to forge their own path. I would also like to thank him for his unstinting support through the process of my qualifying exams, and for helping me with my preparation to ensure I developed the skills I needed to develop in order to move past that hurdle. Even as I graduate, I continue to learn from him, from his incredible pedagogical skills, his humility, his passion for using science and engineering to make a difference in the world, and his sincere committment to doing the very best he can in an honest

and forthright way. So for all this, and much much more - thank you.

I am also grateful to all the other people on my defense committee. Thanks to Prof. Steve Rock for agreeing to chair my committee, and asking some very insightful and thought-provoking questions. Thanks to Dr. Chen-Fang Chang, one of our prinicipal collaborators at General Motors, for flying out from Michigan to be on my committee. Over the years that we have worked together, I have really come to value both his comments on technical issues as well as his ready wit and fearless honesty - and so I am grateful that he could be on my committee and provide his own unique perspective on my work. Thanks also to Prof. Sanjay Lall and Prof. Chris Edwards, for being on my reading committee and taking the time to read and critique my dissertation. I have taken many classes with Prof. Lall and have always been struck by his intellectual rigor and the effortless way in which he seems to handle even the most mind-boggling math - and so I am grateful for the opportunity to get his feedback on my work. Prof. Edwards has been the thermodynamics guru to us controls engineers, and has been invaluable in enabling us to develop more effective ways of communicating with the thermodynamics community. And so his feedback on this thesis is particularly appreciated, for it has made it that much easier for a wider audience to grasp the intricacies of the work presented here. I would also like to thank him for all the insightful advice he has given me at various points in my graduate career, for it has definitely played a role in shaping my career at Stanford - and beyond.

Much of this work has been done in collaboration with other members of the C-unit - the Combustion Unit in the Dynamic Design Lab (DDL). I have immensely enjoyed working with Greg Shaver, Matt Roelle, Adam Jungkunz, Hsien-Hsin Liao and Stephen Erlien and have learnt much from them. Being a part of the DDL as a whole has also contributed significantly to making my Stanford experience what it has been - I feel extremely fortunate to have spent my last six years in the company of Craig Beal, Carrie Bobier, Holly Butterfield, Sam Chang, Chris Gadda, Rami Hindiyeh, David Hoffert, Judy Hsu, Adam Jungkunz, John Kegelman, Mick Kritiyakirana, Shad Laws, Hsien-Hsin Liao, Hyungchai Park, Josh Switkes and Kristin Talvala. Being a part of the DDL has given me the opportunity to interact with some

of the brightest people I know. There is also a certain intangible culture that has really kept the DDL a very vibrant and alive place over the years, something that has made it a great place to spend your working day, that has attracted a diverse cast of characters, that has created traditions such as defense party hats and sakebombs and that brought us all together to pitch in and pull off the spectacularly awesome Advances in Automotive Control conference in 2007. I can think of few better places to spend six years of a graduate career than in the DDL - and I'm glad I could be a part of it.

Thanks also to Scott Sutton and Godwin Zhang, our mechanical and electronics technicians in the engine lab - few, if any students would graduate if it were not for their able support. Both Scott and Godwin have been terrific support in the engine lab, handling any mechanical/electronics issues that come up, designing safe systems that work (unlike anything we could come up with) and really helping ensure that we, as students, spend our time doing research that can help us graduate.

Our sponsors at General Motors and Bosch have really supported all our work and I have benefitted immensely from our interactions with the research divisions at both these companies. It has been great to see how one's ideas might be applied in the real world, to be able to interact with people who see the practical side of things, and to use those interactions to guide one in doing novel academic research that also has the potential for real-world implementation.

Stanford has also been wonderful in that it has provided me with the opportunity to really take a wide variety of courses that have all contributed to my learning and growth. There is little more that I could have asked for in an educational institution, and I am grateful to all the professors who made my journey through Stanford a wholesome learning experience.

Beyond my academic life, Stanford has proved to be the breeding ground for many activities that have enriched my life in myriad ways. Foremost among these is Dhwani, the Indian music group that I was a part of. Music has always been one of my passions, and Dhwani has been one of the most exciting adventures at Stanford. From a small group of about 4-5 people meeting and singing together occasionally, it blossomed into a group as large as 25, with singers and instrumentalists, exploring

different genres of Indian music, performing regularly on campus, and generally have a wonderful time. Over the five years we were active, it really provided me with that much needed break from the rest of the world every week. It is also through Dhwani that I have made some my closest friends - Amritha Appaswami, Deepti Chatti, Nishant Garg, Bhavna Hariharan, Amruta Joshi, Neha Kumar, Dinesh Patil, Amrith Ram, Anurupa Rao, Poorvi Rao, Srikant Vaithilingam and many others have grown to be an integral part of my life and will always remain very dear.

I was also very grateful to get the opportunity to volunteer for Asha for Education, a non-profit that raises funds to support the education of underprivileged children in India. True happiness, it is often said, comes from being of service to others, and so working with them has been fulfilling and rewarding in many ways. It is also through Asha that I got the opportunity to run my one and only marathon, raising funds for them, a unique experience for which I am also grateful.

The Student Initiated Courses program at Stanford provides an opportunity for students to get involved in teaching courses on topics of interest to them - and it is through this that I was able to teach a course on social entrepreneurship, titled Brainstorming India. The entire process of planning and teaching this course was a huge learning experience for me, given that social entrepreneurship is markedly different from engine control, and I am grateful to have been a part of this along with the rest of the teaching team - Deepti Chatti, Abhishek Das, Ooshma Garg, Khurram Masood and Savil Srivastava.

I am also grateful to the Baha'i community at Stanford, and all the wonderful people I have interacted with through the activities in the community. Rohit Agarwala, Omid Azizi, Tanushree Bhushan, Shradha Budhiraja, Jiehua Chen, Roxana Daneshjou, Sachin Kalra, Paul Khavari, Ashkan Monfared, Hamid Samandari, Ehsan Talebi, Himani Tidke and William Wu have all contributed in various ways to uplifting my life, and I treasure all that I have shared with them, from the deep philosophical discussions, to the service activities, to the joyous and fun times.

Beyond these experiences, there are some enduring friendships that I will always cherish, and that have been immense pillars of support over the years. In particular I would like to thank my high school buddies Radhika Das, Nilotpal Sensarkar and

Vidita Subbarao - they have been like rocks that I could lean on anytime I needed to, and have supported me through many a tumultuous time. They have truly been the kind of friends one dreams of.

I would also like to thank three very special people - Vida Bertrand, Michelle Loyalka and Prashant Loyalka - who have had the most profound impact on my life. Little that I can say would do justice to them and the role they have played in shaping my thoughts, beliefs and actions. They have been truly inspiring mentors, and I continue to learn from them and their actions every single day. They live lives of service to society that I aspire to, and have been a never-ending source of spiritual nourishment for me. So I would like to thank them for all their love, wisdom, and patient guidance that have lit my path for me these last few years.

Of course, none of this would have been possible without the love and support of my parents and sister. They have always stood by me in all my endeavors and supported me through every major decision I have made in life. It is in no small measure due to the sacrifices my parents have made that I can look back on a successful graduate career today. They have always put the interests of their children before theirs, and have provided us a stable foundation on which we could build our lives. They set a lofty example for us in the way they led their own lives, and gave us the values that we live by today. And so the fact that this thesis even exists is really a testimony to their efforts, and their committment to giving us the best possible future they could.

Finally I would like to thank my beloved wife Casia, who in the last two years has really been the abiding joy of my life. I had always hoped to find a partner who understood me, who could support and encourage me when I needed it, with whom I would constantly be growing as an individual, with whom I could walk a path of service to the world, who would stand by me at all times and who would be an equal partner in every sense of the word and it has been such a wonderful experience finding someone who exceeds ones wildest hopes. So thank you - for always being there.

Contents

List of Tables

List of Figures

Chapter 1

Introduction

1.1 Background

Humanity in the past century has seen more change than ever before in its history. Much of this has been impelled by the remarkable progress that has been made in the fields of science and technology. Our reach has grown as the world has shrunk, bringing us together in ways never envisaged before. One of the key elements of this change has been the development of the automobile, which has facilitated the human being's fundamental need to grow, explore and form new social groups. Perhaps some insight can be gained into how the automobile satisfies a certain intrinsic need in the individual through the author E.B.White's penetrating words - "*Everything in life is somewhere else, and you get there in a car.*" From its modest beginnings in the late 19th century, the automobile has today grown to become an essential part of our lives; it has become a symbol of success, power and development; and its ubiquitous dominance of the patterns of life in most cities and communities across the world is unparalleled.

The 21st century, however, has brought with it global challenges that question these very patterns of life. Two of the most significant issues relate to the consumption of finite fossil fuel resources, and the pollution caused by using these fossil fuels as an energy resource. With about 805 million cars and light trucks on the road worldwide in 2007 [4], the automotive industry is a major contributor to these challenges. This is

particularly true in the United States, home to the largest passenger vehicle market of any country in the world. Figure 1.1 shows energy consumption in the US by source and sector for 2007. Two important facts can be gleaned from this data - one, petroleum today is the single largest energy resource in the US; and two, almost all the energy used by the transportation sector (about 95%) comes from petroleum. The

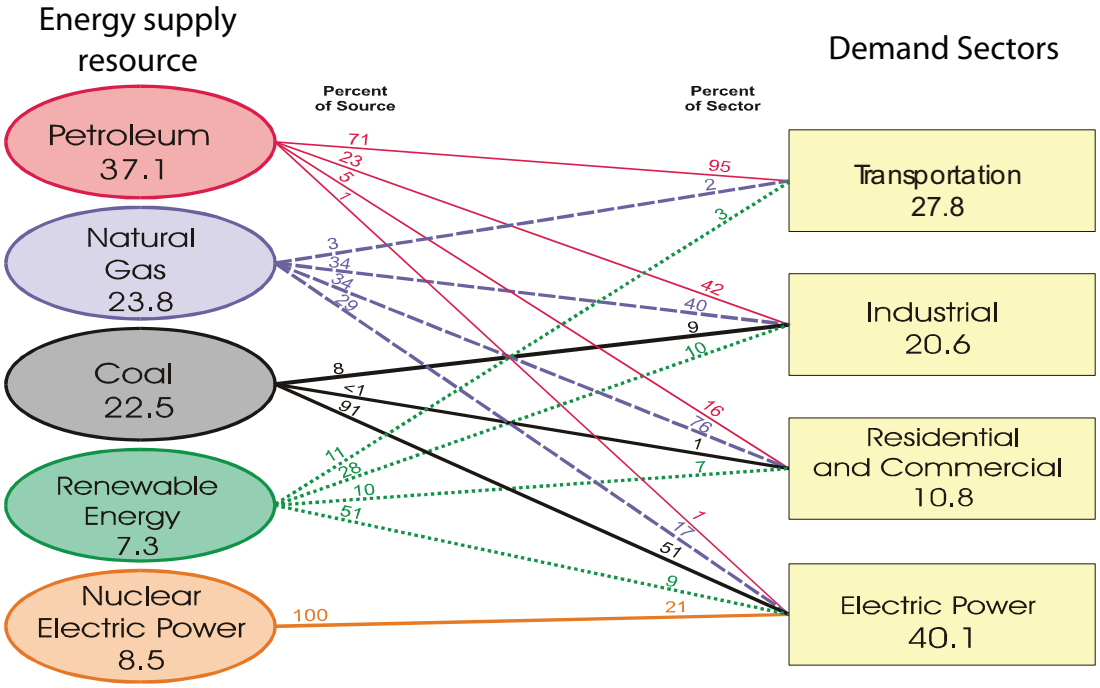

Figure 1.1: U.S. primary energy consumption by resource and sector for 2007 (quadrillion Btu), [2]

consumption of petroleum by the transportation sector has been steadily increasing over the years, and the trend is expected to continue in the coming years, as seen in Fig. 1.2.

The transportation sector is also the primary contributor to air pollution in the US. In the last decade it has overtaken the industrial sector to become the leading cause of CO_2 emissions as seen in Fig. 1.3. In spite of significant technological advances contributing to increasingly efficient engines and superior emissions-reduction systems, automobiles still contribute heavily to global CO, NO_x and hydrocarbon emissions, as shown in Table 1.1 (based on data collected in Europe).

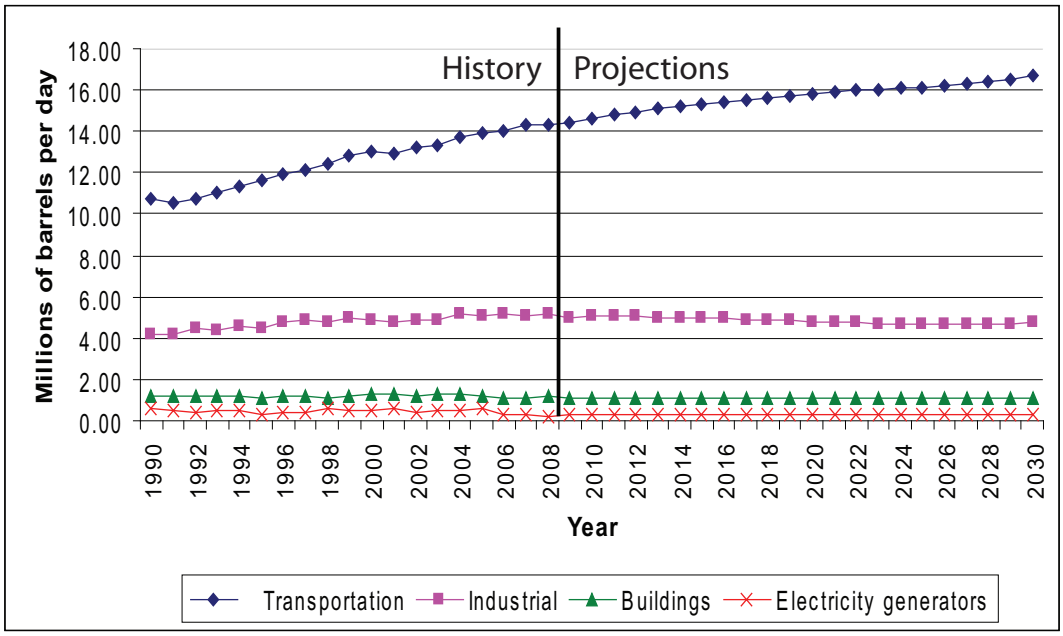

Figure 1.2: Liquid fuels consumption by sector 1990-2030 (million barrels per day), [2]

The two keywords dominating automotive powertrain research today, therefore, are efficiency and emissions - there is a strong push for cars that burn less fuel, and emit fewer pollutants. Some of the technologies in the spotlight include fuel cells, batteries, hybrid powertrains and advanced IC engine strategies. Though fuel cells and battery technologies are very promising in the long-term future, they are currently more expensive and less practical than hybrid and advanced engine strategies, and are expected to remain so in the near future. This is particularly true because of technological advances that have made electronic control systems ubiquitous in today's automobiles and have enabled combustion strategies that would not have been possible even a decade ago. One such advanced engine strategy that presents significant opportunities for reduced emissions and higher efficiencies is Homogeneous Charge Compression Ignition (HCCI).

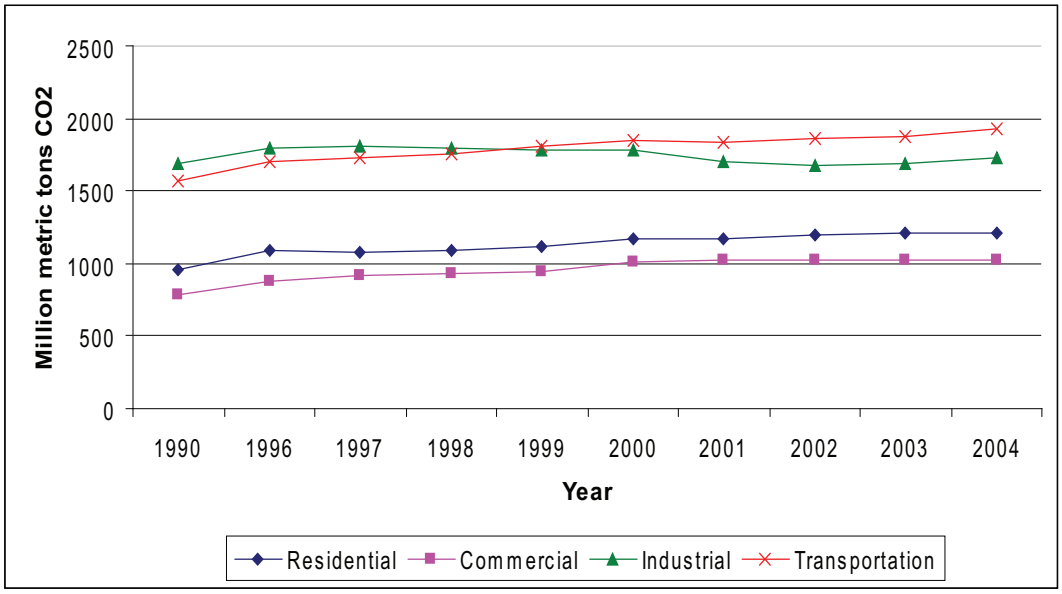

Figure 1.3: U.S. CO_2 emissions from energy consumption by end-use sector (million metric tons CO_2), [3]

1.2 Homogeneous Charge Compression Ignition

HCCI is a combustion process where a well-mixed charge of fuel and air is compressed until it autoignites. HCCI therefore has characteristics of both spark and compression ignition strategies - the fuel and air are mixed well to form a homogeneous mixture, as in spark ignition engines, but the combustion itself is initiated not by a spark but through creating a high enough temperature that leads to autoignition. HCCI engines have been shown to offer the dual benefit of high efficiency and good emissions. In particular, they have dramatically low NO_x emissions [5]. In some ways, HCCI combines the best characteristics of spark-ignited (SI) and compression-ignited (CI) engines. With low throttling losses and a typically fast combustion, it comes closer to approximating the theoretical Otto cycle. This makes HCCI much more efficient than conventional SI engines, and in fact almost as efficient as a diesel engine. At the same time the formation of homogeneous reactant mixture and low peak temperature that falls below the NO_x threshold means that it has very low particulate and NO_x emissions.

Table 1.1: Sources of major air pollutants in Europe, 2005 [1]

	CO	NO_x	HC
Gasoline vehicles	90%	52%	40%
Household	5%	3%	2%
Power stations	1%	26%	<1%
Industry	4%	11%	56%
Other	-	8%	1%

There are several ways in which HCCI can be achieved. The inducted air can be heated or pre-compressed [6, 7] in order to increase its sensible energy. Alternately, hot exhaust gases can be mixed with fresh charge to obtain a mixture with higher sensible energy. Such a strategy is known as *residual-affected HCCI*. Residual-affected HCCI can be achieved with a variable-valve actuation system in several ways. One method is to use a delayed closing of the exhaust valve to reinduct some of the exhaust from the exhaust manifold [5, 8]. Alternately, in what is known as exhaust recompression HCCI, the exhaust valve is closed early, trapping some of the exhaust within the engine cylinder. This trapped exhaust gets recompressed as the piston continues its upward stroke [8]. Though HCCI can be achieved by any (or a combination) of these various methods, this thesis focuses on the modeling and control of HCCI achieved through exhaust recompression.

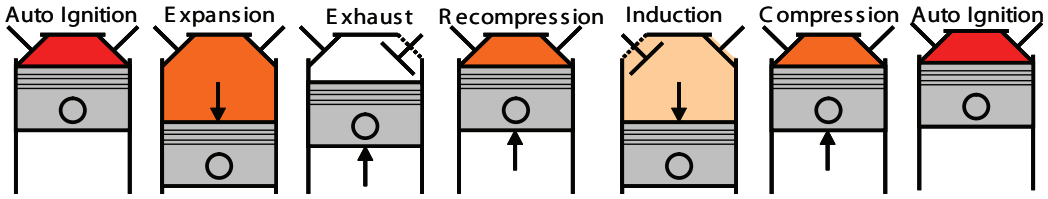

Figure 1.4: Processes in an HCCI engine cycle

A typical HCCI engine cycle with exhaust recompression can be described as shown in Figure 1.4. Combustion happens through autoignition of a homogeneous mixture of fuel, air and trapped residual, and therefore is a fast and fairly uniform process. Subsequent to this, useful work is extracted from the engine as the piston

moves down. Close to bottom dead center, the exhaust valve is opened, and a portion of the products of combustion is pushed out into the exhaust manifold during the upward stroke of the piston. The exhaust valve, however, is closed early enough to trap a significant amount of the combustion products in the cylinder, which is then recompressed as the piston reaches top dead center. With a direct fuel injection system, the fuel is injected into the cylinder, usually towards the end of this recompression stroke. The intake valve is then opened to induct fresh air that mixes with the trapped exhaust from the previous engine cycle to form a homogeneous mixture. This mixture is then compressed once the intake valve is closed, during the upward stroke of the piston, culminating in combustion.

There are, however, significant challenges in implementing HCCI in practice, some of which are listed below.

1. Unlike spark and compression ignition engines, where the combustion is initiated respectively by a spark and the injection of Diesel fuel, the combustion in an HCCI engine is more directly governed by the characteristics of the mixture in the cylinder and reaction kinetics. Therefore there is no external combustion trigger for the process, making it more difficult to ensure that combustion happens at the desired timing, or at all.

2. In the case of residual-affected HCCI, the exhaust that is carried through from one engine cycle to the next induces a cyclic coupling that complicates both steady-state and transient operation. The combustion on any engine cycle influences the combustion on the next engine cycle.

3. HCCI is fairly sensitive to the thermochemical state of the reactant mixture, and so is feasible over a narrower operating range than both spark and compression ignition strategies. Upper load limits are imposed by high rates of pressure rise, while limits at lower loads are imposed by the amount of dilution with hot exhaust gases that the system can withstand.

Therefore, in order to achieve and maintain stable HCCI, as well as to expand its range of operation, closed-loop control strategies are necessary. Without accurate

control of the pressure and temperature conditions in the cylinder, there is a distinct possibility of both misfires (which can lead to complete loss of combustion due to the lack of hot exhaust gases) and excessive peak pressure or rate of pressure rise during combustion (which can damage the engine). The work outlined in this thesis shows the development of a physical model for HCCI that is designed specifically to serve as a foundation for the development of such closed-loop controllers. Several controllers based on this model are presented, and are seen to be effective in enabling the operation of HCCI over a wide operating range.

1.3 Previous work

Since Najt et al's seminal paper on HCCI in 1983 [9] outlined the achievement of HCCI on a four-stroke engine for the first time, there has been significant research done to understand and control the combustion process in HCCI. Much of the early work in HCCI research focused on experimental tests run to investigate the feasibility, advantages and challenges in HCCI. Thring [10] extended Najt's work by running HCCI on a single cylinder engine and mapping out the operating region of HCCI in terms of the equivalence ratio and EGR rates. Christensen et al [11] compared HCCI performance with SI using three different fuels and showed its benefits in terms of efficiency and NO_x emissions. Lavy et al [12] presented experimental and numerical studies of HCCI, including visualizations of the combustion process on an optical engine. Law et al [8], Kaahaaina et al [13], Allen et al [14] and Wolters et al [15] studied the use of variable valve actuation for achieving HCCI, either through exhaust reinduction or recompression. Marriott et al [16] presented an experimental investigation of charge stratification in HCCI using a gasoline direct-injection (GDI) system, and reported very low NO_x emissions even with significant fuel heterogeneity. Zhao et al [17] evaluated the performance of a hybrid SI/HCCI engine over the European NEDC driving cycle, and showed significant improvements in efficiency and emissions when operated in the HCCI range. All these studies therefore point to the promise of HCCI as the next significant advance in automotive engine technology.

1.3.1 HCCI modeling

A wide variety of approaches have been taken to modeling combustion in HCCI, from simple zero-dimensional models to complex CFD models with detailed chemical kinetics models. While the focus of the modeling work presented in this thesis is the development of a simple model useful for controller development, it is worthwhile to take a look at some of the other strategies adopted to simulate and understand the combustion process in HCCI.

Higher order models

Much work has been done in the development of complex multi-zone and CFD models of HCCI that can simulate the combustion process with a high degree of fidelity. These models typically have detailed fluid-flow models and moderately complex to extremely comprehensive chemical models. Babajimopoulos et al [18] described one such approach where a multi-dimensional fluid mechanics code is combined with a multi-zone thermo-kinetic model to capture the effects of variable valve timing in HCCI. Another similar segregated approach was presented by Aceves et al [19]. Kong et al [20] combined detailed chemical kinetics and engine CFD computations to produce a comprehensive model of HCCI that considers the interactions between the physical and chemical process within the engine. A model of similar complexity was used by Zhang et al [21] to study the role of turbulence in HCCI. A simpler quasi-dimensional model developed by Fiveland et al [22] couples boundary layer description and crevice model with a detailed chemical model.

Several researchers such as Tanaka et al [23] have also devoted their efforts to developing reduced chemical kinetic models that still retain a fair level of accuracy in predicting the combustion process in HCCI. Zheng et al [24] developed a skeletal chemical kinetic model for HCCI combustion, that is comparatively simpler than detailed kinetics models (but still uses tens of species and reactions) as a way to include the chemistry of HCCI in CFD simulations. Another such kinetics model utilizing 38 species and 69 reactions was presented by Jia et al [25].

Somewhat simpler approaches than these higher-order models have been taken as

well, in an attempt to come up with a more tractable description of HCCI. Single zone models such as those presented by Shaver et al [26] and Sun et al [27] are much less computationally intensive while still providing valuable insights into the overall dynamics of the HCCI process.

Control-oriented models

All the above modeling approaches have proved to be valuable aids in understanding the nature of the physical and chemical processes that underlie HCCI. However, due to their complexity, they are not very useful as tools for controller synthesis - their main use from the control engineer's perspective comes from being able to enumerate and evaluate system inputs that could potentially be useful for control, and their relative efficacy. Therefore the real advances in the development of HCCI control techniques have come about only with the development of control-oriented models that focus on the dynamic nature of the HCCI process as a whole and capture the relationship between combustion on one cycle and the next. Several approaches have been taken to modeling these dynamics. Bengtsson et al [28] used system identification tools to generate a two-state model for HCCI that was shown to be useful for controller development. Shaver et al developed one of the first physical dynamic models to capture the cycle-to-cycle coupling in HCCI [29]. This has formed the basis for other control-oriented approaches such as those presented by Jia et al [30] and Widd et al [31]. Mayhew et al [32] used a similar methodology to develop a reduced order physical model that focuses on the evolution of engine states in the presence of misfires. Choi et al [33] used artifical neural networks and an ignition delay model to generate a fast estimation algorithm for the phasing of combustion that was claimed to be potentially useful for real-time HCCI control. Shahbakhti et al [34] presented a control-oriented model based on a modified knock integral model and semi-empirical correlations for gas exchange processes.

On the whole, physical models present several advantages when viewed from the standpoint of controller design and implementation. By capturing a simple description of the actual processes governing combustion, these models provide a clear link between design features of the engine (such as engine geometry) and possible control

strategies. This can be advantageous, as the engine design process could be informed by the needs of a good control strategy. Additionally, a physical model is much easier to port across different engines than a model derived from system identification as it is based on the underlying physics which are common across engines. Finally from a broader viewpoint, grounding a control-oriented model in sound thermodynamic principles serves as a bridge between the largely disparate fields of thermodynamics and control and enables better collaboration between these two disciplines towards the common goal of engine control. For these reasons, the focus of the first part of this thesis is the development of a physical control-oriented model of HCCI. The model takes as a starting point the work done by Shaver [29] in developing a control model for HCCI. This model captured the behavior of a propane-fueled HCCI engine with exhaust reinduction, and was shown to be suitable for designing controllers. However, it is only applicable to the particular HCCI strategy being modeled, and is not easily generalizable. Much of this is because the model states were defined in terms of the outputs to be controlled (peak pressure and angle of peak pressure in an engine cycle). The work presented in this thesis attempts to develop a more general physical model of HCCI that is based on a state description that is closely linked to the thermodynamic state of the in-cylinder mixture.

In addition to capturing the effects of injected fuel quantity and variable valve actuation on HCCI, this model also incorporates a simple model for the effect of fuel injected during the recompression process. While several researchers [35, 36, 37, 38] have conducted experimental studies on the effects of fuel injection during recompression, there has been no work done to date in developing a simple model of these effects that could be useful for controller development. Therefore the model presented in this thesis provides the first such opportunity for the use of fuel injection timing as a control input in HCCI.

1.3.2 HCCI control

Developing a framework for controlling HCCI over a wide operating region has been the focus of HCCI engine research for some time now. Different inputs have been

considered for control - these include control of the intake air temperature, compression ratio, external exhaust gas recirculation (EGR), internal EGR (through variable valve actuation) and fuel injection. A brief overview of some of the approaches taken to use each of these control inputs will be presented here.

Intake air heating

The application of heat exchangers to control the temperature of the intake air was investigated by Martinez-Frias et al [6]. In general this approach is seen to be too slow to meet control needs during transient operation, due to thermal inertia. However one technique that could potentially achieve cycle-by-cycle control was developed by Haraldsson et al [39]. Called Fast Thermal Management, it varies intake charge temperature by rapidly mixing hot and cold air streams. Widd et al [40] used this technique in combination with variable valve actuation to control phasing of combustion with a model predictive control strategy.

Variable compression ratio

Compression ratio can be a powerful knob to control HCCI combustion - a higher compression ratio increases charge temperature during the compression stroke, thereby advancing the phasing of combustion. Christensen et al [41] showed that variable compression ratio gives an HCCI engine great flexibility in being able to operate with almost any liquid fuel. Varying the geometric compression ratio on an engine real-time however is a challenging proposition, and no practical devices exist to date to achieve this. Effective compression ratio can be varied through actuation of the intake valve - changing its closing location can be used to change the effective compression ratio. This technique, in combination with control of the residual gas fraction, was used effectively by Shaver et al [42] to control peak pressure and angle of peak pressure in an engine cycle. However it should be noted that the range of achievable effective compression ratios is limited by the geometric compression ratio of the engine.

External and internal EGR

External EGR involves externally recirculating gases from the exhaust manifold back into the intake stream. Shi et al [43] showed that external EGR can avoid the knock combustion of HCCI at high load, and so is promising for expanding the high load limit. The main advantage of external EGR is its simplicity - many production vehicles use some form of EGR in order to meet current emissions standards. However the thermal effect of this form of control is limited due to heat loss that occurs along the EGR path. Additionally it has a slower response and so is not very useful for cycle-by-cycle control during transients.

Internal EGR on the other hand has proved to be an extremely powerful control input. The energy of the exhaust gases is captured either by closing the exhaust valve early and trapping a portion of these gases in the cylinder [8], or by closing it late and reinducting some of these gases from the exhaust manifold [5]. The latter method was used by Shaver et al [42] to achieve and control HCCI. Kang et al [44] used a combination of both internal and external EGR to get a robust HCCI controller that could control mixture temperature as well as composition. This controller has been implemented on a prototype HCCI vehicle at General Motors. In general these approaches require significant authority over valve actuation in order to achieve cycle-by-cycle control of the quantity of internal EGR. More practical approaches use cam phasers that exist in some production vehicles, but have to sacrifice fast control of transients due to the bandwidth limitations of cam phaser systems.

Variable fuel strategies

Some researchers have used dual-fuel strategies in HCCI control. Tanaka et al [23] indicated that the ignition delay and the burn rate could be independently controlled using various fuel mixtures and additives. Dual fuels with different octane numbers were also used to control the combustion timing by Bengtsson et al [45]. Olsson et al [46] demonstrated high load operation of a turbocharged dual-fuel HCCI engine.

Apart from varying the ratios of dual-fuel mixtures, total fuel quantity itself is strongly linked to the total work output of the engine. Haraldsson et al [47], for

example, used fuel quantity to vary work output while altering the ratio of two fuels to affect the phasing of combustion.

When HCCI is achieved with exhaust recompression, the timing of fuel injection can also be a powerful control input. Some researchers have pointed to the effects of fuel injection during recompression [38, 35]. However there have been no closed-loop control strategies developed that use this input to control the phasing of combustion.

Control approaches

Control approaches using any of the above actuators can broadly be divided into two categories. The first set of methodologies are based on experimentally tuned closed loop controllers. For example, Olsson et al. [48] demonstrated closed-loop control of the combustion timing in HCCI using a gain-scheduled experimentally-tuned PID controller. Agrell et al. [49] used a PID controller to control both negative valve overlap and the intake valve closing (IVC) on a single-cylinder HCCI engine. Killingworth et al [50] presented extremum seeking tuning as an effective way to tune a PID controller for combustion phasing control.

In contrast to these experimentally tuned controllers, there are a number of approaches that use model-based controllers. Some of these control frameworks have been based on models developed from an identification of the engine system, such as those presented by Strandh et al [51] and Bengtsson et al [45, 52]. Other frameworks use physical models such as those described earlier. This includes work done by Shaver et al [42, 26] and Widd et al [40].

Due to advantages offered by physical models that were described earlier, the control strategies described in this thesis are all derived from the physical control-oriented model developed here. The control strategies first use a combination of variable valve actuation and variable fuel quantity to control the phasing of combustion and work output. Simple controllers based on a split fuel injection strategy are then developed in order to exploit the effects of fuel injection during recompression. Finally a model predictive control framework is used to devise a strategy that uses all these different inputs available to control HCCI, while also respecting system constraints that one might expect in a practical implementation of HCCI.

1.4 Thesis contributions

The work presented in this thesis has been motivated by the broad objective of making HCCI practically realizable through the use of closed loop control. To this end, two primary research goals were identified:

1. To develop a physical control-oriented cycle-by-cycle model of HCCI that
    - captures the basic dynamics of the process through simplifying thermodynamic assumptions
    - is defined in terms of states that relate to the thermodynamic state of the in-cylinder mixture
    - captures the effects of various control inputs including variable valve actuation and variable fuel injection quantity and timing on the combustion process
2. To apply this model to the synthesis of robust control techniques that
    - enable control of work output and combustion phasing on every engine cycle
    - extend the operating range of HCCI by enabling operation at conditions that are otherwise unstable
    - can be easily ported across different engine testbeds

The specific contributions this thesis has made towards each of these research goals are enumerated below.

1.4.1 Control model development

1. A discrete-time nonlinear control-oriented model has been developed to describe the basic behavior of HCCI. The model states are defined in terms of the temperature and reactant concentrations of the in-cylinder mixture, providing a link to the thermodynamic state of the mixture.

2. The model captures the effects of varying the quantity of fuel injection as well as the intake and exhaust valve closing timings on the combustion process.

3. Following an iterative process of model design, insights gained from the first version of the model have been used to carefully define and locate the states at the most appropriate point in an engine cycle to allow the design of simple but accurate controllers and estimators.

4. The first simple model for the effect of fuel injection during recompression has been developed and incorporated into the overall model structure. This model considers a split injection strategy with a small pilot injection of fuel, the timing of whose injection is varied in order to control the phasing of combustion.

1.4.2 Cycle-by-cycle control of HCCI

Several control strategies based on the model have been designed and implemented in simulation and experiment.

1. An LQR controller based on the model has been used to control the peak pressure and angle of peak pressure (proxies for work output and combustion phasing) on a cycle-by-cycle basis on a single-cylinder engine. This controller is also able to reduce cyclic variation of combustion at operating points with late combustion phasing.

2. A simple control strategy that uses a combination of an empirical feedforward-integral controller to control work output with fuel quantity, and a model-based feedback controller to control phasing of combustion with valve actuation has been implemented on both a single and a multi-cylinder HCCI engine. This controller is able to track desired state trajectories accurately, and also improves combustion stability at late combustion phasing points.

3. A model-based controller that uses the timing of a pilot injection to control combustion phasing has been designed and implemented on the multi-cylinder

engine. This control input enables steady operation at low loads, which are otherwise difficult to operate at.

4. A mid-ranging controller has been designed that uses fuel injection to handle fast transients, and more slow changes in valve timing to keep the pilot injection timing in a range where it is most effective. This strategy represents the first effort at cycle-by-cycle control of HCCI that does not require fully flexible variable valve actuation, but can instead be achieved with a more slowly varying cam phaser system. This is achieved by exploiting the power of fuel injection as a high bandwidth control knob.

5. Finally, a model predictive control framework has been designed that can take actuator range and bandwidth constraints into account explicitly. This scheme also allows for the constraining of other variables not directly controlled, such as air-fuel ratio. Experimental implementation indicates that this control approach is extremely powerful as it enables fast tracking of outputs while respecting realistic constraints on the system.

1.5 Thesis outline

The work presented in this thesis can broadly be divided into four key topics:

1. The development of a physical control-oriented model for HCCI, and the generation of simple controllers based on this model to control peak pressure and angle of peak pressure in an engine cycle.

2. The description of a revised model based on insights gained from the first iteration of the model, and its use in the synthesis of simple control techniques to control work output and combustion phasing.

3. The expansion of the basic model to include a simple model for the effects of fuel injection during recompression, and control of work output and phasing using this control knob.

4. The development of a model predictive control strategy that ties together all the different control inputs and generates input commands to track desired load and phasing trajectories, while respecting actuator and output constraints.

These topics are covered over seven chapters. Brief outlines of these chapters are given below.

Chapter 2 presents a physical control-oriented model of exhaust recompression HCCI that serves as the basis for the control results presented in this thesis. The model is obtained by breaking a single HCCI cycle into several distinct stages, each of which can be described on the basis of simple thermodynamic assumptions. Based on these assumptions, this model provides a link between the thermochemical state of the mixture on one engine cycle and the next. The model states are chosen such that they capture key characteristics of the trapped exhaust gas that is carried over from one cycle to the next. Control inputs considered by the model include intake and exhaust valve timings as well as total fuel quantity, while the primary outputs are the peak pressure and the angle of peak pressure within an engine cycle. Validation of this model at an operating point is presented by comparing it with a more complex simulation model developed by Shaver [53].

Chapter 3 then uses the above model to derive a simple controller for HCCI. As the nonlinear form of the model is too complicated for direct controller synthesis, an analytical linearization about a nominal operating point is performed. An LQR controller based on the linear model is then used to control the peak pressure and angle of peak pressure. A simple Luenberger observer is also used to estimate the model states based on a measurement of the angle of peak pressure. The controller is seen to work well at tracking desired output trajectories both in simulation and on a single cylinder HCCI engine testbed. In addition, it is seen that the controller is able to reduce the cyclic variability of combustion at operating points with a significantly delayed combustion phasing. This suggests that the model is able to capture some of the dynamics in these regimes that leads to the highly variable combustion typically seen. Therefore these results serve to validate the process of model-based control described in these two chapters.

Chapter 4 takes a closer look at some of the insights gained during this process of model and controller development. It focuses on specific choices made during the model design process, their impact on the controller performance, and changes that the results suggest. Based on these insights, several revisions are made to the model - the state vector is expanded, and the definition of the states is moved to a different location in the engine cycle; thermodynamic assumptions are made more realistic; and measures of work output and combustion phasing are incorporated directly as desired control outputs. A dynamic validation of the revised model is presented by comparing state and output trajectories over step changes in inputs with the simulation model.

Chapter 5 describes the process of controller development based on the revised model, and its implementation in simulation and experiment. Here an important characteristic of the control outputs emerges - their separability with respect to the control inputs. As work output is a strong function of the total fuel quantity, a simple feedforward-integral controller commands the fuel in order to track a desired load. A feedback controller based on the physical model is then used to control the valve timings so as to track a desired combustion phasing. A standard Luenberger observer is developed as before to estimate the states based on a measurement of the combustion phasing. This simple control strategy is seen to accurately track desired output trajectories both in simulation and experiment. The value of using a physical model-based control scheme is emphasized by the easy porting of this controller from a single to a multi-cylinder engine testbed with a very quick re-parametrization. Results from these tests indicate that the controller could be very useful in balancing the performance of different cylinders on a multi-cylinder engine. Again, the controller is also able to stabilize combustion at operating points that are otherwise highly variable, underscoring its potential for widening the operating range of HCCI.

Chapter 6 then expands the framework developed in the previous chapters to include the effects of fuel injection during recompression. The inclusion of injection timing as a control input is motivated both by its potential for increasing stability at low loads, as well as the possible relaxation of bandwidth requirements on valve actuation that it would allow. As the effects of fuel injection can be complex, the modeling efforts are restricted to the consideration of a small pilot injection during

recompression. It is seen that even this small quantity of fuel can have a significant effect on combustion phasing as the timing of its injection is varied. It is seen that the relationship between injection timing and combustion phasing can be separated into a nonlinear, empirical component and a linear, analytical component that can be easily assimilated into the linear control model. Experimental data that validates the assumptions made in this process is also presented.

Chapter 7 presents two different controllers that implement a split fuel injection strategy. The first controller uses injection timing alone to control combustion phasing. Simulation and experimental results indicate that this is a very powerful control input - albeit within a limited range. Therefore a second control strategy that also uses valve actuation is developed. In addition, a first attempt is made to consider the limitations of a practical cam phaser system in terms of speed of response. A mid-ranging controller is designed where the pilot injection timing is used to respond quickly during transients, while the exhaust valve timing is varied more gradually and used to keep the injection timing within its range of effectiveness. This strategy is seen to have a wide range of operation on the multi-cylinder HCCI engine, and represents the first step towards a practical control design for HCCI.

Chapter 8 outlines the most complete control approach presented in this thesis. A model predictive control (MPC) framework is used as the basis for this control strategy. The control input is determined as the solution of a real-time optimization problem that is solved every engine cycle. Within this framework, the range limitations on injection timing and the bandwidth limitations on valve actuation are both explicitly specified. Additionally, this approach provides an opportunity to specify constraints on other system variables that are not directly controlled. As it is desirable to maintain the air-fuel ratio (AFR) within the engine cylinder within certain bounds, a measure of AFR is incorporated into the model, and constraints are defined within the optimization. Two different predictive controllers are then presented - one that controls only phasing of combustion, and another that controls both the work output and combustion phasing within the MPC scheme. The second controller is seen to perform better in simulation, and therefore it is implemented on the engine testbed. The experimental results obtained show that the controller is successful in

achieving all the control objectives, including accurate output tracking as well as constraint satisfaction. This predictive controller therefore represents the most robust and practical approach towards control of HCCI that has arisen from this work.

Chapter 9 summarizes the main insights of this thesis and points to some directions for future work that it motivates.

Chapter 2

HCCI Control Model

The first step towards designing an HCCI controller is the development of a model that captures all the relevant information about the dynamics of the HCCI process and is amenable to controller synthesis. This chapter describes the development of such a model based on a fundamental description of HCCI thermodynamics. The model states are chosen so as to represent physical quantities critical in determining the nature of HCCI combustion - reactant concentrations and temperature [29, 53]. Based on this, a recompression HCCI strategy with direct-inject gasoline is modeled. As the trapped exhaust plays a critical role in establishing the cyclic coupling, the states for the model are chosen as the moles of oxygen in the trapped exhaust and the temperature of the trapped exhaust. A discrete time approach is used to model HCCI dynamics from one engine cycle to the next, by breaking up a single HCCI cycle into several well defined stages. The engine as a thermodynamic system is therefore modeled from a controls perspective, providing a valuable tool for controller synthesis. This nonlinear model is validated in simulation against a more complex continuous-time model of HCCI developed by Shaver et al. [53].

2.1 Modeling assumptions

The primary objective of an HCCI control model is to be able to relate the dependence of combustion on a particular engine cycle to the state of the in-cylinder mixture -

which in turn depends on the characteristics of combustion on the previous engine cycle, and the inputs applied to the system. This, therefore, calls for a discrete time model, where the state of the mixture on each engine cycle can be related to the state on the previous cycle.

$$x_{k+1} = F(x_k, u_k) \tag{2.1}$$

Furthermore, this dependence is derived by considering each cycle as composed of several thermodynamically well-defined processes. Simplifying thermodynamic assumptions are used to model each process. Fresh charge induction is assumed to be adiabatic, and occurs at a constant pressure, the average pressure in the intake manifold. The compression, expansion and exhaust processes are modeled as isentropic processes. The combustion event itself, on account of the rapid nature of HCCI combustion, is assumed to be a constant volume (instantaneous) event. It is assumed that there is no early/pilot fuel injection, and consequently no possibility for fuel reactions during the recompression.

With these assumptions, an HCCI cycle can be modeled through the following six stages.

1. *Adiabatic induction* culminating in *instantaneous mixing* of fuel, air and trapped exhaust at intake valve closure (IVC)

2. *Isentropic compression* from IVC to point of combustion

3. *Isochoric combustion* occurring instantaneously and uniformly

4. *Isentropic expansion* from the point of instantaneous combustion to exhaust valve opening (EVO)

5. *Isentropic blowdown and exhaust* from EVO to exhaust valve closing (EVC)

6. *Recompression* of trapped exhaust from EVC to intake valve opening (IVO) in the next cycle

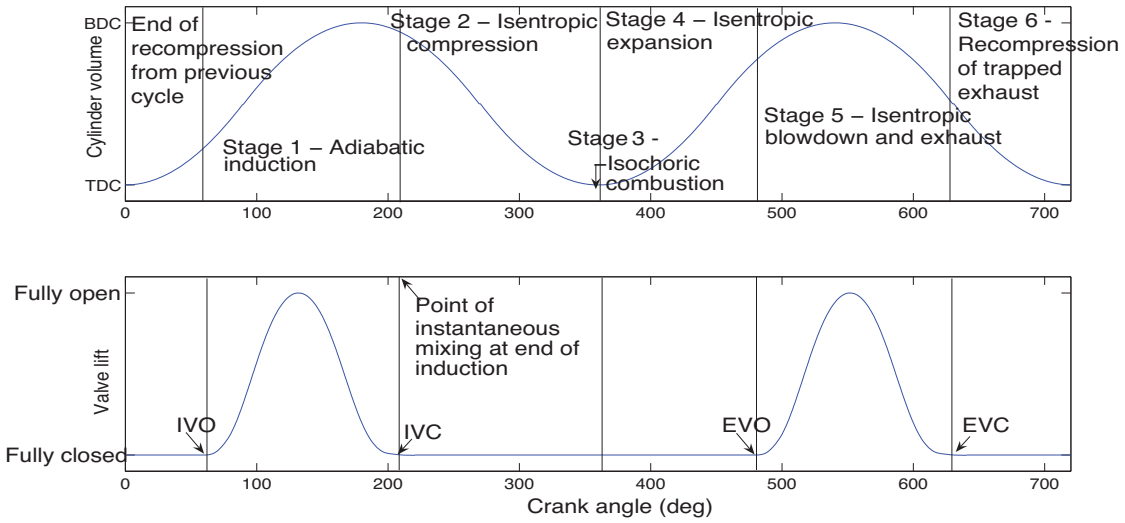

Figure 2.1: Stages in the HCCI cycle

Figure 2.1 shows these discrete stages with respect to the cylinder volume at any given position of the crank. The figure also shows typical valve lifts for the intake and exhaust valves. As seen, the exhaust valve closes significantly before top-dead center (in this figure, at 720 CAD), thereby trapping some hot exhaust gases that help initiate combustion on the subsequent engine cycle.

2.2 Definition of inputs, outputs and states

The inputs to the system in the model are assumed to be the following:

1. *Moles of fuel injected* in the current cycle, $n_{f,k}$
2. *Volume at intake valve closure*, or the point at which instantaneous mixing between air, fuel and trapped exhaust is assumed to occur, $V_{IVC,k}$
3. *Volume at exhaust valve closure*, or the point at which the states of the system are determined, $V_{EVC,k}$

The valve timings can be used to vary the relative amounts of air and trapped residual. Specifically, the EVC timing determines the quantity of trapped exhaust, while the

IVC timing determines the total quantity of the reactant mixture. A direct-inject system gives independent control of the amount of fuel in the cylinder, and is therefore a useful control knob.

In terms of the outputs of the model, what is ultimately desired is that the engine produce the amount of work required, and that combustion occur at the desired phasing. The outputs of the model are therefore chosen as quantities that are representative of these values, but are also easily measurable on an actual engine test-bed. These are

1. *Peak pressure*, $P_{3,k}$, which serves as a proxy for the net work output of the engine (given a particular combustion phasing)

2. *Angle of peak pressure*, $\theta_{23,k}$, which represents the phasing of the combustion event

In order to describe the dynamics of the HCCI process based on the framework laid down above, the states of the system need to be defined. The key thrust of this modeling work is to determine states for the HCCI process that

1. Represent a complete set of variables sufficient to describe the system dynamics to the desired level of detail for control

2. Have a physical/thermodynamic basis, ie, represent physical characteristics of the system that, at the most fundamental level, determine the nature of combustion in the engine

To this end, it would be of use to briefly examine combustion at the molecular level. The process of combustion is essentially dictated by two characteristics of the reactant mixture:

1. *Concentrations of the reactants*, which determines whether the reactant molecules are close enough to have sufficient collisions

2. *Temperature of the mixture*, which determines whether the collisions are energetic enough to cause a reaction

Choosing a set of state variables, therefore, that in some way represent these quantities, would give a fundamental basis for an HCCI model. It is easy to see why mixture temperature might play a significant role in HCCI combustion - a hotter mixture is likely to combust earlier than a cooler mixture. As for reactant concentrations, the fuel is an input to the system, and is directly controlled through the fuel injector. Therefore a measure of oxygen concentration in the mixture is a strong candidate for being a second state in the model.

The role of reactant oxygen concentration also becomes important when considering the effects of air-fuel ratio on HCCI combustion. In general HCCI is a lean combustion process, and it is desirable to stay away from rich combustion regions that would significantly degrade the fuel efficiency benefit of HCCI. Additionally, it is also necessary to stay away from very lean conditions, as the combustion becomes much more variable when fuel molecules are more scarce. Therefore any practical control strategy needs to respect these constraints, which is possible only if the controller state recognizes the oxygen concentration in the mixture. The development of such a control strategy that can use an estimate of oxygen-concentration to stay away from very lean and very rich regions will be presented in Chapter 8.

Apart from the physical reasons presented above, there is some empirical basis as well for assuming a second order physical model. Bengtsson et al. [28] show, through system identification techniques, that a model with two states captures the basic behavior of HCCI with sufficient accuracy. Therefore a second order physical model is a justifiable choice.

The final question in this regard is the decision of where exactly in the engine cycle these two states should be defined. An answer to this question can be gleaned by considering the pivotal role played by the trapped exhaust. It is the exhaust retained from the previous engine cycle that is used to heat (and dilute) the fresh charge for the current cycle, and is what induces the cycle-to-cycle coupling. This trapped exhaust, therefore, is essentially what carries information about combustion in one engine cycle through to the next.

Based on this, the states of the HCCI system can be chosen as those variables that capture the temperature and amounts of reactants in the trapped exhaust. Of

the two reactants (fuel and O_2), the fuel is an input to the system, and is directly controlled through the fuel injector. Therefore the states are chosen as:

1. Moles of oxygen in the products of combustion at EVC, $n_{O_2,k}$
2. Temperature of the trapped exhaust at EVC, $T_{e,k}$

The subscript k here denotes the k'th engine cycle, where an engine cycle is assumed to start at EVC (end of exhaust, beginning of recompression).

Figure 2.2 shows a typical HCCI pressure trace, with the locations of the different inputs, outputs and states within an engine cycle. Top dead center after recompression is taken as the 0 crank angle reference.

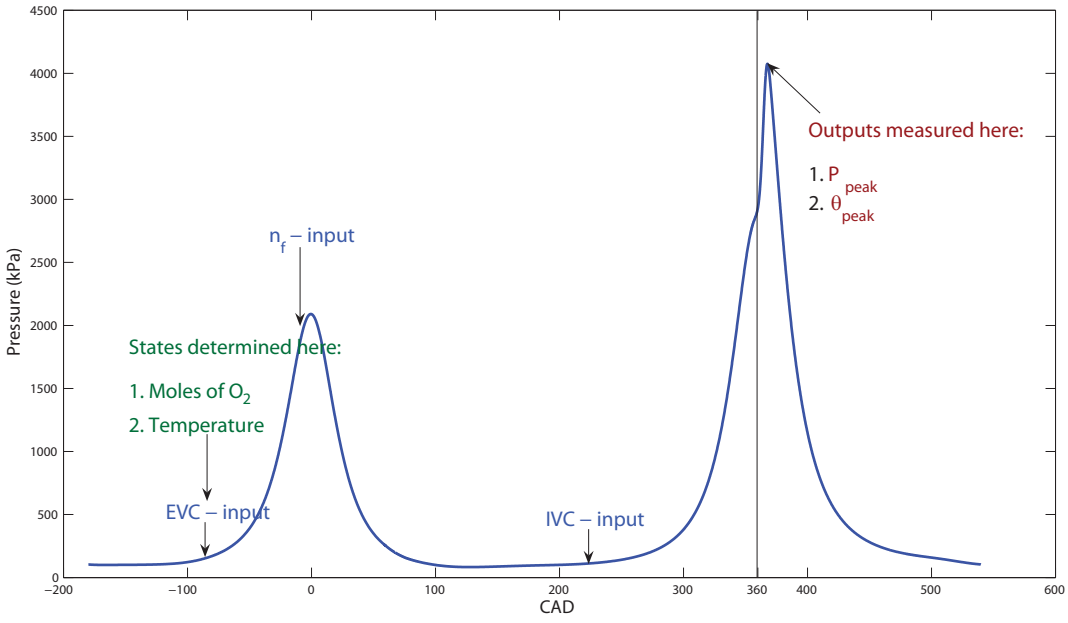

Figure 2.2: States, inputs and outputs in the HCCI model

Using these state definitions, the various stages in an HCCI cycle can now be described.

2.3 Stepping through the control model

2.3.1 Adiabatic induction followed by instantaneous mixing

At the end of the exhaust process in the previous cycle, a certain portion of the exhaust is trapped inside the cylinder by an early closing of the exhaust valve. Let total moles of exhaust in the cylinder at the point where the exhaust valve is effectively closed, EVC, be $n_{e,k}$. Then by ideal gas law

$$n_{e,k} = \frac{P_{exh} V_{EVC}}{R_u T_{e,k}} \tag{2.2}$$

where P_{exh} is the cylinder pressure at the end of the exhaust process. Here it is assumed that there is no turbocharger, and therefore this pressure is equal to the atmospheric pressure. The quantity of oxygen in the engine cylinder at the beginning of induction is given by one of the states, $n_{O_2,k}$, as there is no mass transfer during recompression (assuming no ring blowby). However, some heat transfer occurs, due to which temperature at the beginning of induction is lower than that at the beginning of recompression ($T_{e,k}$). The heat transfer during recompression can be modeled by relating temperature of trapped exhaust at the end of recompression (IVO) to the temperature at EVC by a simple zero-dimensional heat loss model:

$$T_{1,exh} = \chi T_{e,k} \tag{2.3}$$

where χ is a constant factor determined empirically and $T_{e,k}$ is one of the states. Therefore, at this point, where the exhaust valve is effectively closed, we know the total moles of trapped exhaust as well as moles of oxygen ($n_{O_2,k}$) in the cylinder, and temperature of the entire mixture (T_1). Individual concentrations of other constituents are unknown. It is, however, sufficient to know just total moles in the cylinder if we use bulk properties for the mixture, as opposed individual species properties in the thermodynamic calculations. This is a reasonable approximation because thermodynamic properties (such as specific heats) are similar for O_2, CO_2, H_2O, N_2 in the temperature ranges that are relevant [54].

The fuel is injected into the cylinder at some point towards the end of recompression. The temperature of this fuel is assumed to be constant. Let the total moles of fuel injected into the cylinder be n_f. The fuel, once injected into the cylinder, vaporizes, and so removes an amount of energy equal to $n_f h_{fg}$ from the cylinder, where h_{fg} is the heat of vaporization of gasoline. Fresh air is then inducted into the cylinder from IVO to IVC at a constant pressure and temperature. This is then assumed to mix instantaneously at IVC with the trapped exhaust and fuel. To obtain the state of the components of the cylinder after mixing, we apply the first law of thermodynamics. A constant average specific heat for the entire mixture is used. We assume that $n_{a,k}$ moles of air enter the cylinder at a fixed temperature T_i. Total moles inside the cylinder, are then given by $n_{tot,k} = n_{a,k} + n_{e,k} + n_{f,k}$.

Applying the 1st law to the mixing process based on the above assumptions

$$\bar{C}_p(n_{a,k}T_i + \chi n_{e,k}T_{e,k}) - n_{f,k}h_{fg} = \bar{C}_p\left(n_{a,k} + n_{e,k} + n_{f,k}\right)T_{1,k} \tag{2.4}$$

Here it is assumed that a part of the sensible energy is removed from the system due to vaporization of the fuel.

Rearranging Eq. (2.4),

$$T_{1,k} = \frac{n_{a,k}T_i + \chi n_{e,k}T_{e,k} - C_1 n_{f,k}}{n_{a,k} + n_{e,k} + n_{f,k}} \tag{2.5}$$

where $C_1 = h_{fg}/\bar{C}_p$.

Such a formulation also gives a very simple expression for the moles of air entering the cylinder during the current cycle. Applying the ideal gas law,

$$n_{a,k} + n_{e,k} + n_{f,k} = \frac{P_i V_{IVC,k}}{R_u T_{1,k}} \tag{2.6}$$

Substituting for $T_{1,k}$ from Eq. (2.5) and for $n_{e,k}$ from Eq. (2.2) and rearranging

$$n_{a,k} = \frac{P_i V_{IVC,k} + R_u C_1 n_{f,k} - \chi P_{exh} V_{EVC,k}}{R_u T_i} \tag{2.7}$$

Total moles of oxygen now present in the cylinder (after induction) are given by

$$n_{O_2,1} = 0.21 n_{a,k} + n_{O_2,k} \tag{2.8}$$

Using the ideal gas law and Eq. (2.7) an expression for $T_{1,k}$ is obtained in terms of the state variables

$$T_{1,k} = \frac{P_i V_{IVC,k}}{R_u (n_{a,k} + n_{e,k})} \tag{2.9}$$

Pressure and volume at this point are given by $P_{1,k} = P_i$ and $V_{1,k} = V_{IVC,k}$. Therefore the state of the mixture at the start of compression is completely known.

2.3.2 Isentropic compression

Isentropic compression is assumed, and therefore

$$T_{2,k} = \left(\frac{V_{IVC,k}}{V_{23,k}}\right)^{\gamma-1} T_{1,k} \tag{2.10}$$

$$P_{2,k} = \left(\frac{V_{IVC,k}}{V_{23,k}}\right)^{\gamma} P_i \tag{2.11}$$

Here the term $V_{23,k}$ represents the volume of the cylinder at the point where instantaneous combustion is assumed to occur. A model for determining the instant of combustion is presented subsequently.

2.3.3 Isochoric combustion

Gasoline is assumed to have the formula C_7H_{13}, representing the average stoichiometry of regular gasoline fuel. The stoichiometric combustion reaction can then be written as

$$C_7H_{13} + 10.25O_2 + 38.54N_2 \rightarrow 7CO_2 + 6.5H_2O + 38.54N_2 \tag{2.12}$$

If, instead of a stoichiometric mixture, we have n_f moles of fuel and n_a moles of

air, the reaction then is (assuming lean combustion, which is typical in HCCI)

$$\begin{aligned} n_f C_7 H_{13} + n_a(O_2 + 3.76N_2) &\rightarrow 7n_f CO_2 + 6.5n_f H_2O \\ &+ (n_a - 10.25n_f)O_2 + 3.76n_a N_2 \end{aligned} \tag{2.13}$$

HCCI combustion is typically very fast, and therefore an instantaneous, constant volume combustion can be assumed to occur. From Eq. (2.13) and (2.8), the combustion equation in terms of just the reacting species can be written as

$$\begin{aligned} n_{f,k} C_7 H_{13} + (0.21n_{a,k} + n_{O_2,k})O_2 &\rightarrow 7n_{f,k} CO_2 + 6.5n_{f,k} H_2O \\ &+ (0.21n_{a,k} - 10.25n_{f,k} + n_{O_2,k})O_2 \end{aligned} \tag{2.14}$$

Therefore the total moles of oxygen left at the end of combustion is given by

$$n_{O_2,3,k} = n_{O_2,k} + 0.21n_{a,k} - 10.25n_{f,k} \tag{2.15}$$

Applying the first law to the combustion reaction

$$m\frac{du}{dt} = \dot{Q}_{comb} - \dot{W} \tag{2.16}$$

As the combustion is assumed to occur at constant volume, the piston work, $\dot{W} = p\dot{V}$, is zero. The first law then becomes:

$$m\frac{du}{dt} = \dot{Q}_{comb} \tag{2.17}$$

Integrating this expression yields

$$U_3 - U_2 = Q_{comb} \tag{2.18}$$

Q_{comb} is a function of the energy release during combustion as well as the heat transfer to the walls.

$$Q_{comb} = Q_{er} - Q_{ht} \tag{2.19}$$

For the purpose of this first law analysis alone, combustion is assumed to be a simple heat addition process (without reaction), with the total energy release calculated on the basis of the lower heating value (on an internal energy basis) of the fuel.

$$Q_{er} = n_{f,k} LHV_f \tag{2.20}$$

The heat loss during combustion is also taken as a fraction ϵ of this fuel heating value, where ϵ is a parameter to be calibrated.

$$Q_{ht} = \epsilon n_{f,k} LHV_f \tag{2.21}$$

Substituting Eq. (2.19), (2.20) and (2.21) in Eq. (2.18), the first law then becomes

$$U_3 - U_2 = (1-\epsilon) n_{f,k} LHV_f \tag{2.22}$$

Again, assuming that all constituents (except the fuel) have the same specific heat, and substituting for U_2 and U_3

$$\begin{aligned} \left(\bar{C}_{v,f} n_{f,k} + \bar{C}_v \left(n_{a,k} + n_{e,k}\right)\right)\left(T_{2,k} - T_{ref}\right) &= \bar{C}_v (3.25 n_{f,k} + n_{a,k} + n_{e,k})(T_{3,k} - T_{ref}) \\ &- (1-\epsilon) n_{f,k} LHV_f \end{aligned} \tag{2.23}$$

where the total number of moles after combustion can be obtained from Eq. (2.14).

Rearranging,

$$T_{3,k} = \frac{C_2 n_{f,k} + \left(\bar{C}_{v,f} n_{f,k} + \bar{C}_v \left(n_{a,k} + n_{e,k}\right)\right) T_{2,k}}{\bar{C}_v (3.25 n_{f,k} + n_{a,k} + n_{e,k})} \tag{2.24}$$

where $C_2 = (1-\epsilon) LHV_f + (3.25\bar{C}_v - \bar{C}_{v,f}) T_{ref}$

Applying the ideal gas law before and after combustion,

$$\begin{aligned} N_2 &= \frac{P_2 V_{23}}{R_u T_2} \\ N_3 &= \frac{P_3 V_{23}}{R_u T_3} \end{aligned} \tag{2.25}$$

From inspection of the combustion reaction it is easy to see that $\frac{N_3}{N_2} \approx 1$. Therefore

$$P_{3,k} = P_{2,k}\frac{T_{3,k}}{T_{2,k}} \tag{2.26}$$

Rearranging Eq. (2.24) gives

$$T_{2,k} = \frac{\bar{C}_v(3.25n_{f,k} + n_{a,k} + n_{e,k})T_{3,k} - C_2 n_{f,k}}{\left(\bar{C}_{v,f}n_{f,k} + \bar{C}_v\left(n_{a,k} + n_{e,k}\right)\right)} \tag{2.27}$$

Substituting Eq. (2.27) and (4.5) in Eq. (2.26) gives an expression for the peak pressure, which is one of the model outputs:

$$P_{3,k} = \left(\frac{V_{IVC,k}}{V_{23,k}}\right)^{\gamma} \frac{\left(\bar{C}_{v,f}n_{f,k} + \bar{C}_v\left(n_{a,k} + n_{e,k}\right)\right) P_i T_{3,k}}{\bar{C}_v(3.25n_{f,k} + n_{a,k} + n_{e,k})T_{3,k} - C_2 n_{f,k}} \tag{2.28}$$

To obtain an expression for the peak pressure in terms of the states and inputs, we need to substitute for $T_{3,k}$ in Eq. (2.28). A simplification can be made here, by comparing the denominator in Eq. (2.27) with the first term in the denominator of Eq. (2.28), and recognizing that $n_{f,k} \ll n_{a,k}$. We can then assume

$$\begin{aligned} A_k &= \bar{C}_v\left\{3.25n_{f,k} + n_{a,k} + n_{e,k}\right\} \\ &\approx \bar{C}_{v,f}n_{f,k} + \bar{C}_v\left(n_{a,k} + n_{e,k}\right) \end{aligned} \tag{2.29}$$

Substituting Eq. (2.29) in Eq. (2.24) and (2.28)

$$T_{3,k} \approx \frac{C_2 n_{f,k} + A_k T_{2,k}}{A_k} \tag{2.30}$$

and

$$P_{3,k} = \left(\frac{V_{IVC,k}}{V_{23,k}}\right)^{\gamma} \frac{A_k P_i T_{3,k}}{A_k T_{3,k} - C_2 n_{f,k}} \tag{2.31}$$

Substituting for $T_{3,k}$ in Eq. (2.31) and rearranging, an expression for the output

$P_{3,k}$ in terms of the states and inputs is obtained:

$$\begin{aligned} P_{3,k} &= \frac{C_2 n_{f,k}\left(P_i V_{IVC,k} T_{e,k} + R_u C_1 n_{f,k} T_{e,k} - P_{exh} V_{EVC,k}(\chi T_{e,k} - T_i)\right)}{A V_{23,k} T_i T_{e,k}} \\ &+ \frac{\left(\frac{V_{IVC,k}}{V_{23,k}}\right)^{\gamma-1} P_i V_{IVC,k}}{V_{23,k}} \end{aligned} \tag{2.32}$$

This gives one output equation in the state space form of the model.

2.3.4 Isentropic expansion

Isentropic expansion is assumed until the opening of the exhaust valve, and so

$$T_{4,k} = \left(\frac{V_{23,k}}{V_{4,k}}\right)^{\gamma-1} T_{3,k} \tag{2.33}$$

$$P_{4,k} = \left(\frac{V_{23,k}}{V_{4,k}}\right)^{\gamma} P_{3,k} \tag{2.34}$$

2.3.5 Isentropic blowdown and exhaust

The exhaust process is modeled in two stages. First comes the blowdown process, where the gas left in the cylinder expands isentropically to the pressure in the exhaust manifold.

$$\begin{aligned} T_{5,k} &= \left(\frac{P_{exh}}{P_{4,k}}\right)^{\frac{\gamma-1}{\gamma}} T_{4,k} \\ &= \left(\frac{P_{exh}}{P_{3,k}}\right)^{\frac{\gamma-1}{\gamma}} T_{3,k} \end{aligned} \tag{2.35}$$

After blowdown, as the piston moves up till the point of exhaust valve closure, a simple mass transfer occurs where a portion of the combustion products within the cylinder are transferred to the exhaust manifold. During this mass transfer process, it is assumed that the thermodynamic state of the mixture in the cylinder remains the same.

Applying the ideal gas law at the beginning and end of the exhaust process, the

number of moles of combustion products in the cylinder before and after exhaust are obtained, the ratio of which gives an expression for the fraction of trapped exhaust, β

$$\begin{aligned} \beta &= \frac{N_5}{N_4} = \frac{V_5 P_5 T_4}{V_4 P_4 T_5} \\ &= \left(\frac{P_{exh}}{P_3}\right)^{\frac{1}{\gamma}} \frac{V_5}{V_{23}} \end{aligned} \tag{2.36}$$

From Eq. (2.14) and (2.36), the state update equation for $n_{O_2,k}$ is obtained:

$$n_{O_2,k+1} = \beta_k(0.21 n_{a,k} - 10.25 n_{f,k} + n_{O_2,k}) \tag{2.37}$$

and the temperature of trapped exhaust at EVC is equal to T_5

$$T_{e,k+1} = T_{5,k} \tag{2.38}$$

Substituting from Eq. (2.32) we get the state update equation for T_e, shown in Eq. (2.39)

$$\begin{aligned} T_{e,k+1} =& \frac{\left(P_{exh} V_{23,k} T_i T_{e,k}\right)^{\frac{\gamma-1}{\gamma}}}{A_k^{\frac{1}{\gamma}} \left\{P_i V_{IVC,k} T_{e,k} + R_u C_1 n_{f,k} T_{e,k} - P_{exh} V_{EVC,k}(\chi T_{e,k} - T_i)\right\}} \times \\ & \Bigg[A_k \left(\frac{V_{IVC,k}}{V_{23,k}}\right)^{\gamma-1} P_i V_{IVC,k} T_i T_{e,k} + C_2 n_{f,k} P_i V_{IVC,k} T_{e,k} + \\ & C_2 n_{f,k} \left\{R_u C_1 n_{f,k} T_{e,k} - P_{exh} V_{EVC,k}(\chi T_{e,k} - T_i)\right\}\Bigg]^{\frac{1}{\gamma}} \end{aligned} \tag{2.39}$$

This is the second state update equation.

2.3.6 Recompression

The total amount of trapped exhaust is given by

$$n_{e,k+1} = \frac{P_{exh} V_{EVC,k}}{R_u T_{5,k}} \tag{2.40}$$

where the cylinder pressure at the end of exhaust is assumed to be atmospheric. As described earlier, the heat transfer during recompression is modeled by relating temperature of trapped exhaust at the end of recompression to the temperature at EVC by a zero-dimensional heat loss model.

$$T_{1,exh,k+1} = \chi T_{e,k+1} \tag{2.41}$$

Therefore the state of the trapped exhaust that influences combustion on the next engine cycle is known completely.

2.3.7 Combustion phasing modeling

In order to develop a model to determine the phasing of combustion, a simple global Arrhenius rate model is used, which has been shown to be adequate to capture the dynamics affecting phasing [53]. The reaction rate for the overall combustion reaction is given as

$$RR = A_{th} e^{\left(\frac{-E_a}{R_u T}\right)} [C_7 H_{13}]^a [O_2]^b \tag{2.42}$$

where E_a is the activation energy and A_{th} is a pre-exponential factor. Values of E_a, a and b have been obtained from [55] and are, respectively, $30 kcal/mole$, 0.25 and 1.5. Integrating this global Arrhenius rate equation from IVC to the point of combustion gives an expression of the form

$$\int RR = \int_{\theta_{IVC}}^{\theta_{th}} A_{th} e^{\left(\frac{-E_a}{R_u T}\right)} [C_7 H_{13}]^a [O_2]^b dt \tag{2.43}$$

Combustion can then be modeled to begin when this integral crosses a certain threshold value, K_{th}. The point at which the peak in-cylinder pressure is reached, θ_{23} is related to the point at which the threshold is crossed as $\theta_{th} = \theta_{23} - \delta\theta$, where $\delta\theta$ is assumed to be constant as a consequence of approximating the combustion event to be a function of the crank angle. This simplification is valid around an operating point, especially as the engine speed is assumed to be constant.

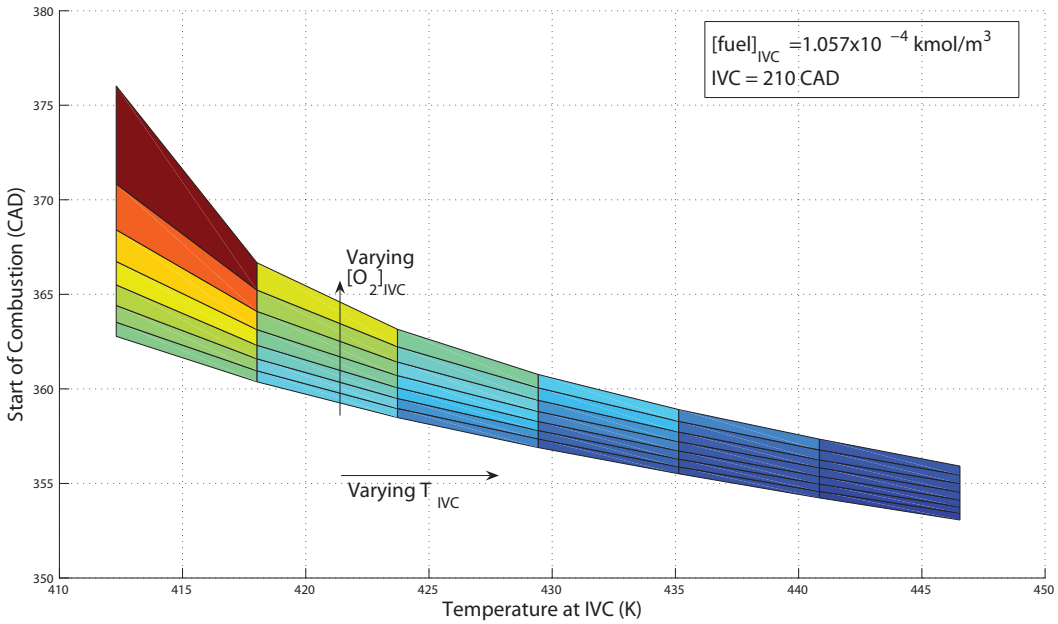

Figure 2.3: Effect of temperature and oxygen concentration on combustion phasing

The effect of oxygen concentration and temperature at the beginning of compression on the phasing of combustion can be seen in Fig. 2.3, which simulates the Arrhenius integral for a particular set of initial conditions, across a range of initial mixture temperatures and oxygen concentrations.

The integration can be simplified by approximating the integrand by its value at TDC, and beginning integration at this point, a justifiable assumption as the value of the integrand is largest at TDC. In this case a linear expression for the phasing θ_{23} is obtained in terms of the Arrhenius threshold:

$$\begin{aligned} \hat{K}_{th} &= \int_{\theta_{IVC}}^{\theta_{23}-\delta\theta} A_{th} e^{\left(\frac{-E_a}{R_u T_{TDC}}\right)} [C_7H_{13}]^a_{TDC} [O_2]^b_{TDC} d\theta/\omega_k \\ &\approx A_{th} e^{\frac{-E_a}{R_u T_{TDC}}} [C_7H_{13}]^a_{TDC} [O_2]^b_{TDC} \frac{(\theta_{23} - \theta_{TDC} - \delta\theta)}{\omega_k} \end{aligned} \tag{2.44}$$

where ω_k is the engine speed.

Here

$$\begin{aligned} T_{TDC} &= \left(\frac{V_{IVC,k}}{V_{TDC}}\right)^{\gamma-1} T_{1,k} \\ [C_7H_{13}]_{TDC} &= \frac{n_{f,k}}{V_{TDC}} \\ [O_2]_{TDC} &= \frac{0.21n_{a,k} + n_{O_2,k}}{V_{TDC}} \end{aligned} \tag{2.45}$$

Substituting Eq. (2.45) and (2.9) in Eq. (2.44) and rearranging, an expression for the combustion phasing is obtained, shown in (2.46)

$$\begin{aligned} \theta_{23,k} &= \frac{\frac{K_{th}(V_{TDC})^{a+b}\omega_k}{A_{th}(n_{f,k})^a\left(0.21n_{a,k}+n_{O_2,k}\right)^b}}{e^{\left[\frac{-E_a}{R_u}\left(\frac{V_{TDC}}{V_{IVC,k}}\right)^{\gamma-1}\left\{\frac{P_iV_{IVC,k}T_{e,k}+R_uC_1n_{f,k}T_{e,k}-P_{exh}V_{EVC,k}(\chi T_{e,k}-T_i)}{P_iV_{IVC,k}T_iT_{e,k}}\right\}\right]}} \\ &+ \theta_{TDC} + \delta\theta \end{aligned} \tag{2.46}$$

This is the second output equation in the state space form of the model. With this, there is now a closed form solution for the outputs in terms of the states and inputs, and the time-update equations for the states.

2.3.8 Model summary

A two state model of the HCCI process is obtained in the following nonlinear state-space form

$$\begin{aligned} x_{k+1} &= F(x_k, u_k) \\ y_k &= G(x_k, u_k) \end{aligned} \tag{2.47}$$

The states, inputs and outputs are given by

$$x_k = \begin{bmatrix} n_{O_2,k} \\ \tilde{T}_{e,k} \end{bmatrix}, u_k = \begin{bmatrix} n_{f,k} \\ V_{IVC,k} \\ V_{EVC,k} \end{bmatrix}, y_k = \begin{bmatrix} P_{3,k} \\ \theta_{23,k} \end{bmatrix} \tag{2.48}$$

Table 2.1: Engine parameters

Parameter	Value	Units
Engine speed	1800	rpm
Stroke	93.2	mm
Connecting rod length	147	mm
Bore diameter	81	mm
Compression ratio	13	

The two state update equations are given in Eq. (2.37) and (2.39), and the two output equations are given in Eq. (2.32) and (2.46).

2.4 Model comparison

The control model described above was validated in simulation against a continuous time simulation model of HCCI combustion developed by Shaver et al [53]. This is a ten-state model that includes much of the complex thermodynamics of the HCCI process. Valve flows are modeled using compressible flow equations, heat transfer occurs continuously throughout the engine cycle and is modeled by the extended Woschni correlation [56], and the combustion event is of finite duration, and is captured by a Wiebe function. This model is parameterized against an experimental setup, and therefore serves as a virtual testbed for HCCI.

To compare the two models, the properties of the cylinder contents at the end of each of the stages in the HCCI cycle are obtained at a particular steady-state operating condition. Of specific importance are the pressure and temperature in the cylinder at each of these locations and the location of peak pressure. These quantities are compared across the models.

The simulation is parameterized to a single cylinder engine. The base engine is a 2001 model year five-cylinder Volvo diesel engine, where just one cylinder is used for conducting tests. The other cylinders' intake and exhaust ports are blocked. A Bosch gasoline injector is used in place of the original diesel injector, to directly inject gasoline into the cylinder. Engine parameters and particular operating condition

characteristics used in simulation are shown in Tables 2.1 and 2.2 respectively. Note that all angles are referenced to 0 degrees at TDC before induction

Table 2.2: Operating point at which continuous simulation and simple control model are compared

Parameter	Value	Units
IVO	75	CAD
IVC	195	CAD
EVO	525	CAD
EVC	645	CAD
Mass of fuel injected per cycle	8	mg
Peak pressure	4350	kPa
Angle of Peak Pressure	365	CAD

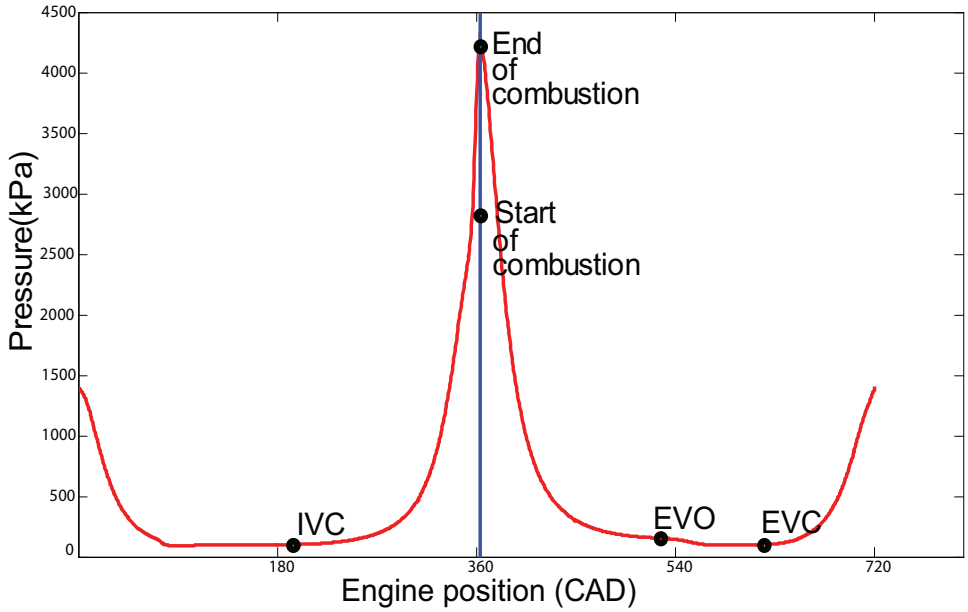

Figure 2.4: Comparison of control model and continuous time simulation - in-cylinder pressure

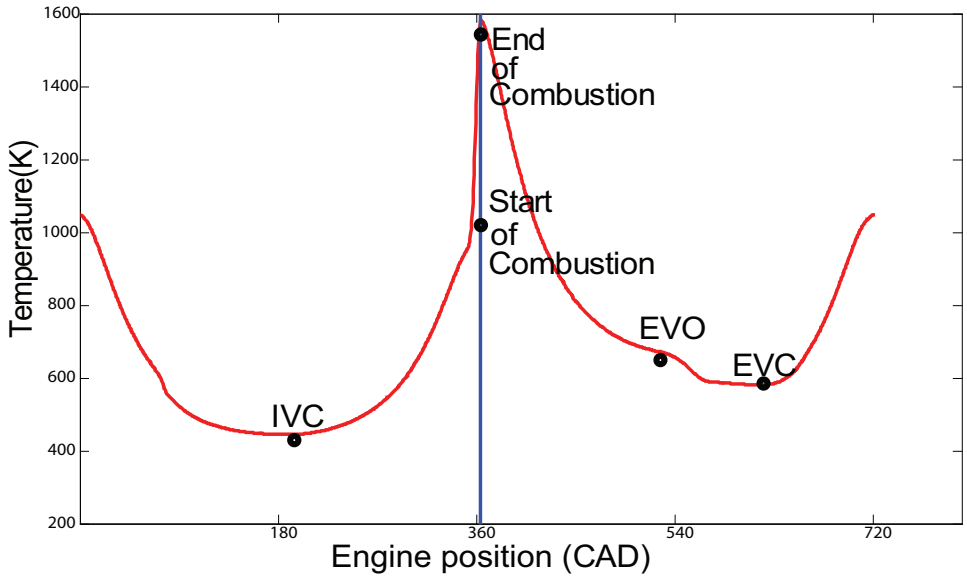

Figure 2.5: Comparison of control model and continuous time simulation - in-cylinder temperature

The particular operating condition simulated has been chosen arbitrarily as one of the test cases for which the complex simulation model was parametrized based on experiments. Figures 2.4 and 2.5 show the evolution of in-cylinder pressure and temperature respectively during one HCCI cycle as predicted by the continuous time simulation. Values obtained from the simpler control model at several discrete points are indicated on the plots. As seen, the control model accurately predicts

1. Peak pressure in the cycle
2. Crank angle at which peak pressure occurs in the cycle
3. Temperature of trapped exhaust at EVC
4. Temperatures and pressures at other points in the cycle

This comparison therefore shows a good static match between the two models at one operating condition. However a more accurate estimation of model fidelity would require a dynamic comparison between the models, and this is presented in Chapter 4.

2.5 Conclusion

The model presented in this chapter represents the first step in an approach to controlling combustion in an HCCI engine. Although HCCI is inherently an extremely complex process, the fundamental dynamics most important for control can be captured through a relatively simple two-state model. The model states were selected so as to represent mixture temperature and reactant concentrations, which are the key determinants of the nature of combustion. In addition, the trapped exhaust from one cycle represents the fundamental agent of energy transfer to the next cycle - and therefore the states for the model were chosen as moles of oxygen in, and temperature of, the trapped exhaust at EVC. The model then relates these states to the desired outputs on each engine cycle, here taken as the peak pressure and angle of peak pressure, which are proxies for the work output and phasing of combustion. As a physically motivated control model, therefore, it represents an ideal foundation for the synthesis of a variety of model-based control strategies. The next chapter describes one such simple controller structure derived from this model which is used to control HCCI over a range of conditions.

Chapter 3

Control of Peak Pressure and Angle of Peak Pressure

This chapter describes the process of controller synthesis from the model presented in Chapter 2. A linearized version of this model is used as the basis for the development of a linear controller. Since the states cannot be measured on an engine, an observer is used to obtain an estimate of the states. This observer uses a measurement of the angle of peak pressure (used as an ignition proxy) that is obtained from an in-cylinder pressure sensor. The state estimates are then used by a reference tracking LQR controller to track a desired system trajectory. This controller-observer system is first tested in simulation and then in experiment. Results show qualitative agreement between the performance of the controller in simulation and experiment. It is seen that the controller is able to track the desired trajectory around a nominal operating point with an accuracy comparable to that achieved in simulation. Some steady state error is seen in the tracking in both simulation and experiment for larger deviations from this point. This demonstrates the region for which the linearization holds. The controller is also seen to reduce the cycle-to-cycle variability of combustion significantly, particularly at a late combustion phasing.

3.1 Model linearization

Due to the highly nonlinear nature of the model, it is first linearized about an operating point, so as to allow the synthesis of linear controllers. Linear control around an operating point is a first step towards more global HCCI control. The linearization is performed analytically, with linear expressions being taken for any quantity a_k of the form

$$a_k = \bar{a}_k + \tilde{a}_k \tag{3.1}$$

where $\bar{a}_k$ represents the value of the quantity a at the nominal operating condition, and $\tilde{a}_k$ represents its deviation from that operating point. These expressions are then substituted in the nonlinear state and output update equations (given in Eq. (2.47)), and Taylor expansions to the first term give linear system equations around the particular operating condition:

$$\begin{aligned} \tilde{x}_{k+1} &= A\tilde{x}_k + B\tilde{u}_k \\ \tilde{y}_k &= C\tilde{x}_k + D\tilde{u}_k \end{aligned} \tag{3.2}$$

where A, B, C and D are matrices. As the linearization is performed analytically, this gives the form of a general linear model. Expressions for the matrices are functions of the operating point at which the system is linearized, engine parameters, and physical properties of the cylinder constituents.

3.2 Controller synthesis and implementation

The states of the system as chosen are not directly measurable. Therefore the first step in the development of a control strategy is the synthesis an observer that can be used to estimate the states. The state estimate can then be used by the controller to track a desired system trajectory.

3.2.1 Observer design

An estimator for the system can be designed using the linearized model. If the state estimate for the state $\tilde{x}_k$ is $\hat{x}_k$, the estimator dynamics are represented as

$$\hat{x}_{k+1} = A\hat{x}_k + B\tilde{u}_k + L(\tilde{y}_k - \hat{y}_k) \tag{3.3}$$

where L is the estimator, $\tilde{u}_k$ is the input (obtained from the controller), $\tilde{y}_k$ is the measured value of the output, and $\hat{y}_k$ is the estimated value of the output.

From the output equation in Eq. (3.2), $\hat{y}_k = C\hat{x}_k + D\tilde{u}_k$, and therefore

$$\begin{aligned} \hat{x}_{k+1} &= A\hat{x}_k + B\tilde{u}_k + L(\tilde{y}_k - C\hat{x}_k + D\tilde{u}_k) \\ &= (A - LC)\hat{x}_k + (B - LD)\tilde{u}_k + L\tilde{y}_k \end{aligned} \tag{3.4}$$

The estimation is however complicated by the fact that the output C matrix for the linear system is poorly conditioned. This is due to the fact that of the two outputs, the peak pressure value is a strong function of the amount of fuel injected in the cylinder, which is an input. This is particularly true once the phasing of combustion (the other output) is fixed. Therefore once the angle of peak and amount of fuel injected are known, the value of peak pressure does not give much additional information. A measurement of the net work output would suffer a similar limitation, as it is directly related to the amount of fuel injected. Hence the observer uses only the angle of peak measurement to estimate both states.

This redundancy of the peak pressure value as a measurement for this particular control strategy has several implications. Peak pressure has been used in past work by Shaver et al [42] as a reasonable substitute for work output. Control of work output, therefore, is possible through controlling peak pressure and phasing. However, it would appear that from the standpoint of estimation, peak pressure is not a very useful *measurement*, given other information (such as the angle of peak pressure). This limits the role of peak pressure as an indicator of HCCI combustion.

3.2.2 Output controller design

To track a desired output trajectory, a reference input is used as described in [57]. The control input, then, is of the form

$$u = -K_x x + (N_u + K_x N_x) r \tag{3.5}$$

where r is the reference input (representing the desired output trajectory) and K_x is the controller. N_u and N_x are feedforward matrices obtained from the following relation that specifies that the system respond with a zero steady state error to any constant input:

$$\begin{bmatrix} A - I & B \\ C & D \end{bmatrix} \begin{bmatrix} N_x \\ N_u \end{bmatrix} = \begin{bmatrix} 0 \\ I \end{bmatrix} \tag{3.6}$$

where I represents the identity matrix, and 0 the zero matrix.

Combining Eq. (3.4) and (3.5), we obtain the complete representation of the controller-observer system:

$$\begin{aligned} \tilde{u}_k &= -K_x \hat{x}_k + (N_u + K_x N_x) r_k \\ \hat{x}_{k+1} &= (A - LC)\hat{x}_k + (B - LD)\left\{-K_x \hat{x}_k + (N_u + K_x N_x) r_k\right\} + L\hat{y}_k \\ &= (A - LC - BK_x + LDK_x)\hat{x}_k + L\hat{y}_k + (B - LD)(N_u + K_x N_x) r_k \end{aligned} \tag{3.7}$$

Equation (3.7) then gives the closed loop valve commands necessary to track a desired output trajectory. Note that all inputs determined by the controller represent normalized deviations from the nominal operating point.

There are several control techniques that could be used to determine the control matrix K_x. Here an LQR controller is chosen as a representative controller. Only two of the three available inputs are used for control - the fuel quantity and the EVC timing. The LQR weights are set such as to prevent any changes in the IVC timing. This is done so as to keep the engine at an operating point where there is maximum flow into the engine through the intake valve (typically about 30-40 CAD after bottom dead center during induction [28]), while using the exhaust valve alone to vary the relative quantities of fresh air and hot exhaust. Also, the nominal conditions are

Table 3.1: Operating point at which control model is linearized

Parameter	Value	Units
IVO	80	CAD
IVC	220	CAD
EVO	480	CAD
EVC	640	CAD
Mass of fuel injected per cycle	7	mg
Peak pressure	4075	kPa
Angle of Peak Pressure	367.7	CAD

such that the mixture conditions are much more sensitive to the exhaust valve timing - even small changes in EVC lead to significant changes in cylinder volume at the beginning of recompression, leading to very different volumes of trapped exhaust.

3.2.3 Implementation in simulation

The controller-observer system is first tested on the continuous time simulation model against which the control model was validated as described in Chapter 2. Table 5.1 shows the characteristics at the particular operating condition about which the nonlinear control model has been linearized for the results shown. At this point, the eigenvalues of the linearized open-loop system are located at $(0.4213, 0.3183)$. This indicates that this operating point is stable, as both discrete-time eigenvalues lie within the unit circle. This linearized model is then used as the basis for the observer and controller synthesized and implemented in both simulation and experiment. With the controller, the closed-loop system has its eigenvalues at $(0.0013, 0.0067)$ - and therefore we expect the system to be much more stable around this point when run closed-loop.

Figure 3.1 shows the tracking achieved in simulation for a series of step changes in desired output conditions. The controller-observer system works well, with accurate tracking being achieved. Some steady state error can be observed for larger step changes, which can be attributed to the fact that the linearization of the model is

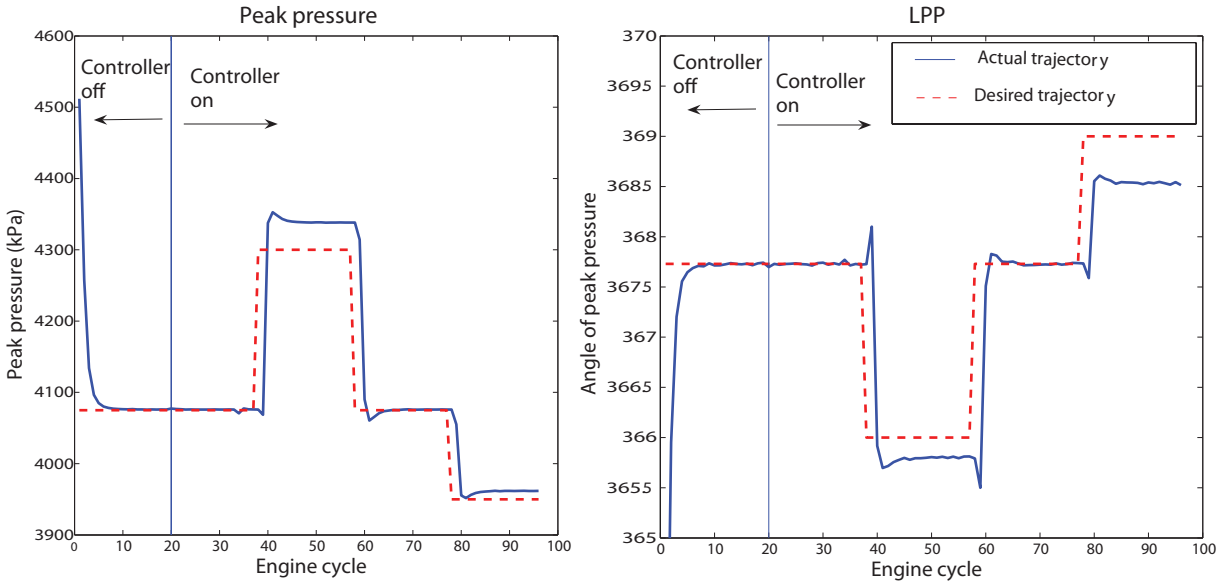

Figure 3.1: LQR output controller implemented in simulation - tracking of outputs

a little more inaccurate as we move away from the nominal operating point. Consequently, the estimation of the states is not completely accurate. This can be seen in Fig. 3.2. It is also seen that the trapped exhaust temperature is estimated more accurately than the oxygen content. This is because the phasing of combustion is a stronger function of temperature than oxygen concentration. This is evident in Eq. (2.43), where it can be seen that combustion phasing has an exponential dependence on temperature, and a polynomial dependence on fuel and oxygen concentrations. Therefore the angle of peak measurement, which is essentially a proxy for combustion phasing, gives a more accurate estimate of the trapped exhaust temperature. Some of the error in tracking also arises due to the fact that both states are being estimated using just one measurement.

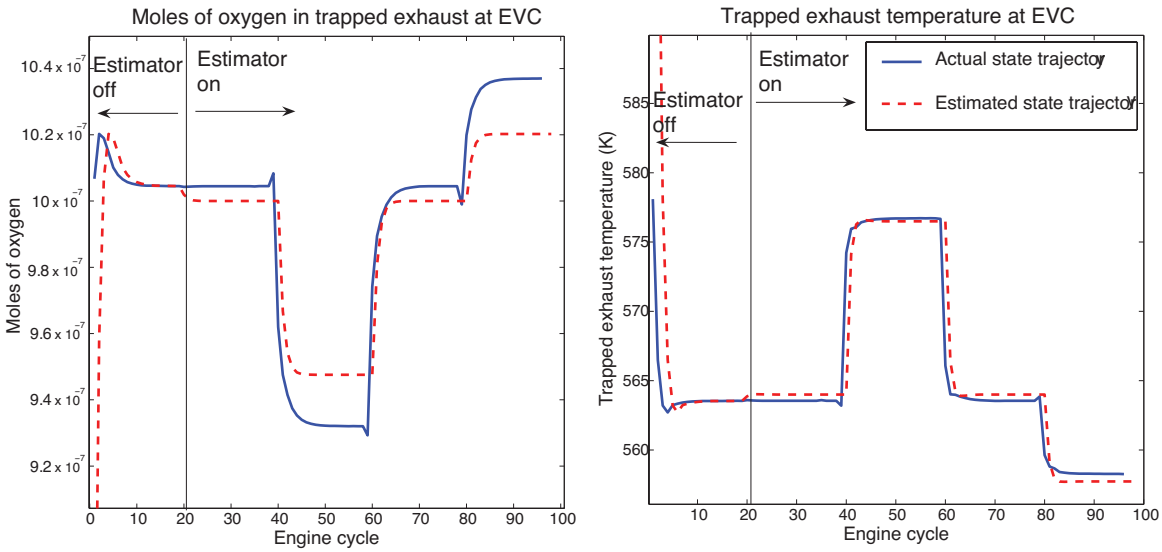

Figure 3.2: Estimator performance in simulation - evolution of states

3.3 Experimental implementation

3.3.1 Experimental apparatus

The experiments described in this chapter were performed on a single cylinder engine. The base engine is a 2001 model year five-cylinder Volvo diesel engine, where just one cylinder is used for conducting tests. A spark plug has been added in the head for the active cylinder. Additionally, a Bosch gasoline injector is used in place of the original diesel injector, to directly inject gasoline into the cylinder. Fuel is delivered to the injector at 1500 psig. The intake and exhaust valves (two each) for the active cylinder are controlled with an electro-hydraulic variable valve actuation (VVA) system. The VVA system allows fully flexible actuation of each valve independently.

The original diesel piston has been replaced with an aluminium one with a compression ratio of 13:1. The piston geometry is nearly flat with a shallow 2 mm bowl and valve cutouts that are about 0.5 mm deep. In-cylinder pressure is measured used an AVL piezoelectric pressure transducer. This information is used to calculate the outputs - peak pressure and angle of peak pressure - for control.

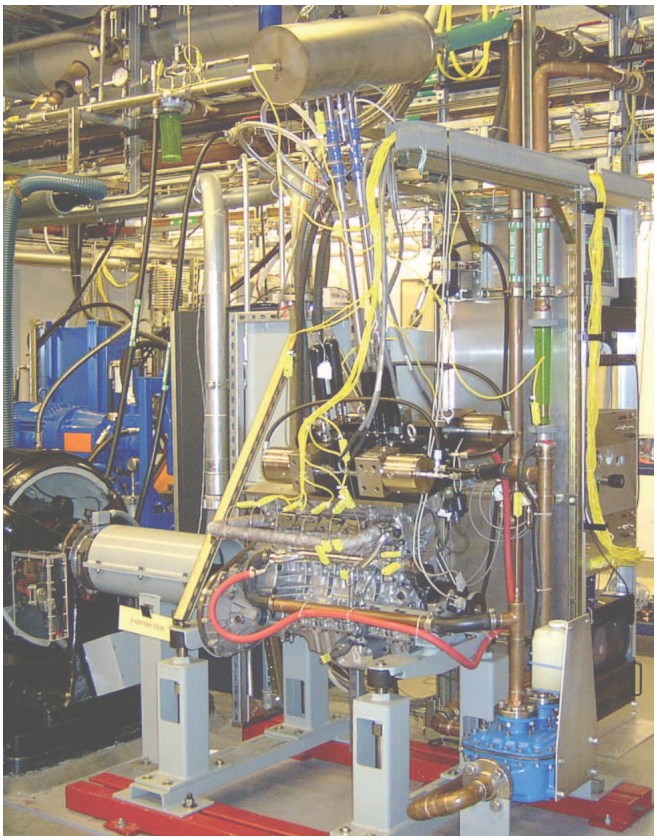

Figure 3.3: Test apparatus - single-cylinder HCCI engine

The engine is operated in Matlab's xPC-Target environment, with Simulink models used to run, control and collect information from the engine. All experiments described below were performed at 1800 RPM.

3.3.2 Experimental results

Experimental results show that the controller performs fairly reliably over a range of operating conditions around the nominal operating point. Some salient features of the controller performance include

1. Reasonable tracking within a region around the nominal operating point with an accuracy similar to that achieved in simulation

2. Some steady state error when moving further away from that point

3. Rapid response to step changes - of the order of 4-5 cycles

4. Reduction in cyclic variability

Tracking performance

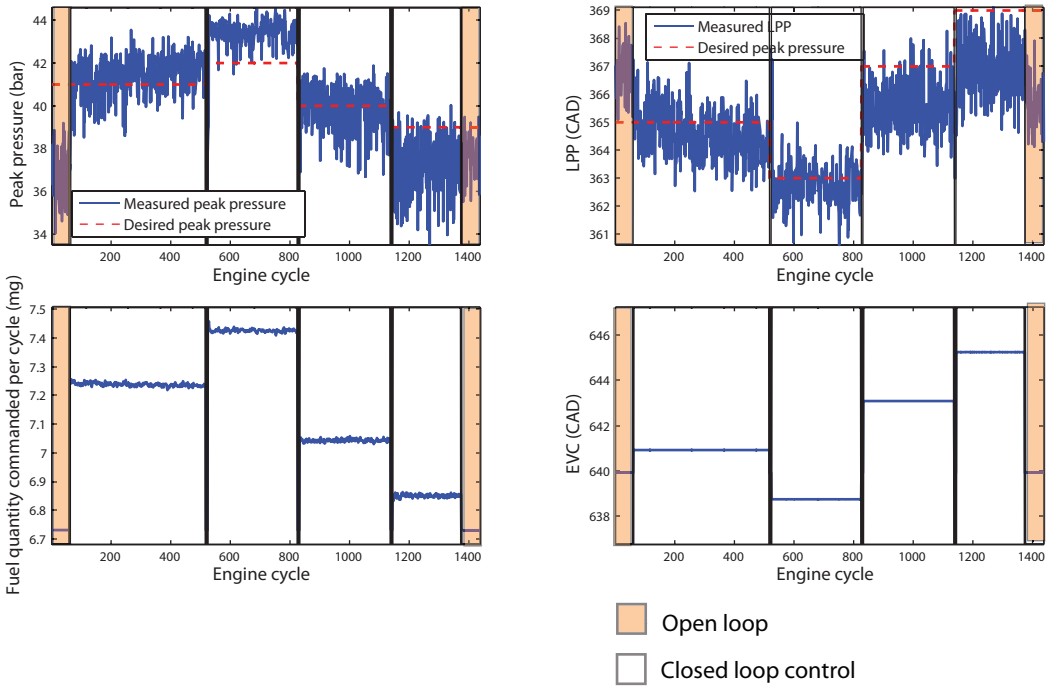

Figure 3.4: Control of HCCI - output tracking

Figure 3.4 shows the result of a particular test on the engine. The two plots on top show the desired and actual outputs - peak pressure and angle of peak pressure (LPP) - while the plots on the bottom show the commanded inputs - fuel quantity and the crank angle at exhaust valve closure (EVC). Shaded areas show when the controller is off. As seen the engine responds as soon as the controller is switched on, and then subsequently follows the desired system trajectory. There is some steady state error that we observe. The order of magnitude of the error is the same as in simulation.

Also most of the cycle-by-cycle control is performed by the fuel injection, while the valve control really becomes important only while switching from one point to another.

This is because the input cost matrix in the development of the LQR controller was set in such a way that changes in the exhaust valve timing were weighted much more than changes in fueling.

Speed of response

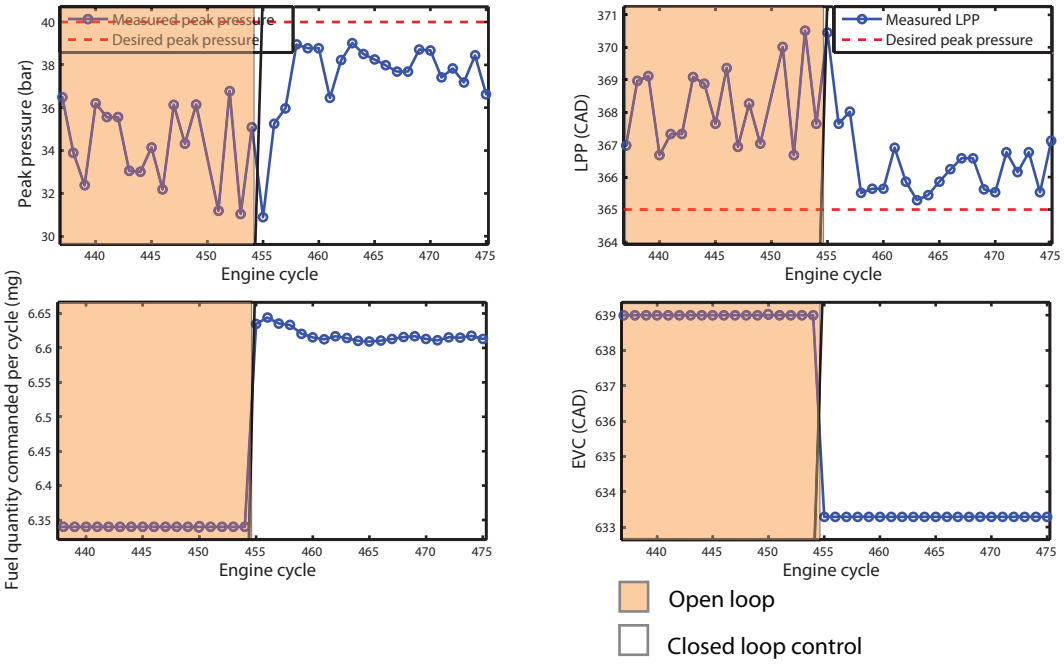

Figure 3.5: Speed of response of controller

Figure 3.5 shows a zoomed-in view of the response when the controller is switched on. As seen, the response is extremely quick, and the engine reaches the new steady state point in about 4-5 cycles.

Reduction in cyclic variability

One of the big advantages of applying cycle-by-cycle control to the HCCI process is its effect on cyclic variability. Figure 3.6 shows the results from a test where the engine is switched between open and closed-loop modes several times. This operating condition is fairly unstable open-loop, particularly due to the late phasing of combustion. The dynamics at this point are such that the combustion process is highly oscillatory from

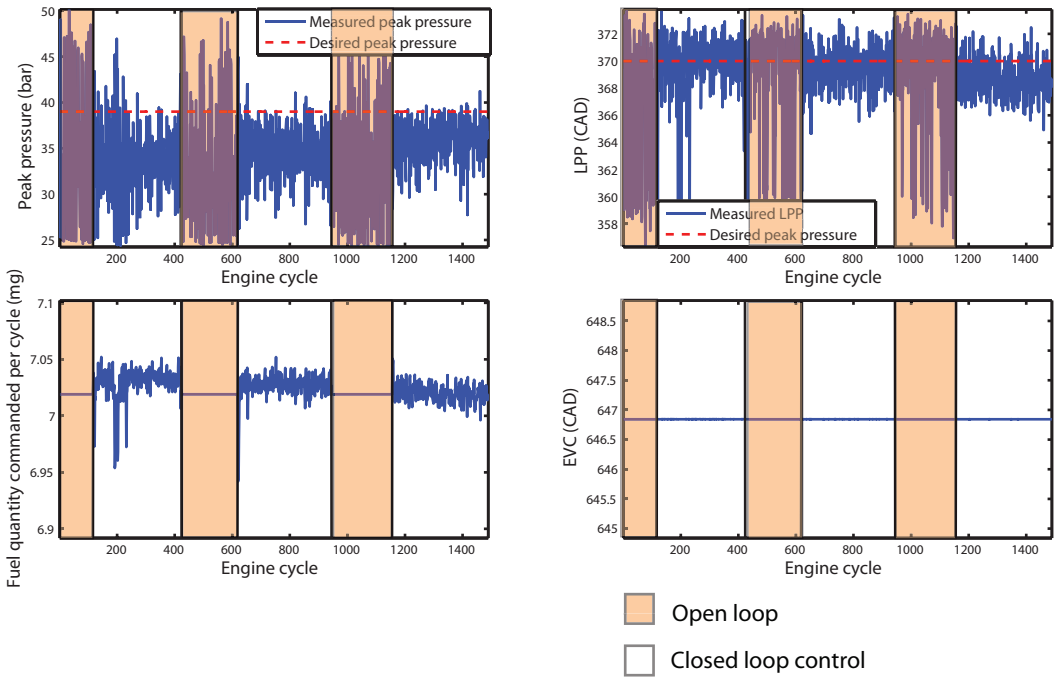

Figure 3.6: Reduction in cyclic variability

cycle to cycle, with early phasing on one cycle causing late combustion on the next due to heat transfer effects, and vice versa. However, when the controller is switched on, we see a drastic reduction in the peak-to-peak variability of both peak pressure and angle of peak pressure. This is achieved through a minimum of control effort - with practically no change in the exhaust valve timing, and just small variations in fuel quantity. However, due to the predictive nature of model-based control, these small variations in fuel quantity on a cycle-by-cycle basis are actually sufficient to prevent the oscillatory behavior from setting in.

The effect of the controller on the net work output of the engine can be seen in Fig. 3.7. Though this quantity is not directly controlled, there is a marked decrease in the variation of the net mean effective pressure (NMEP) when the controller is turned on. In open-loop, the coefficient of variation (COV) of the NMEP is 36.14%, which the controller is able to reduce in closed-loop to a significantly lower value of 2.27%. In addition, there are several instances in the open-loop case where the engine is misfiring, as evidenced by the points showing a negative value of NMEP.

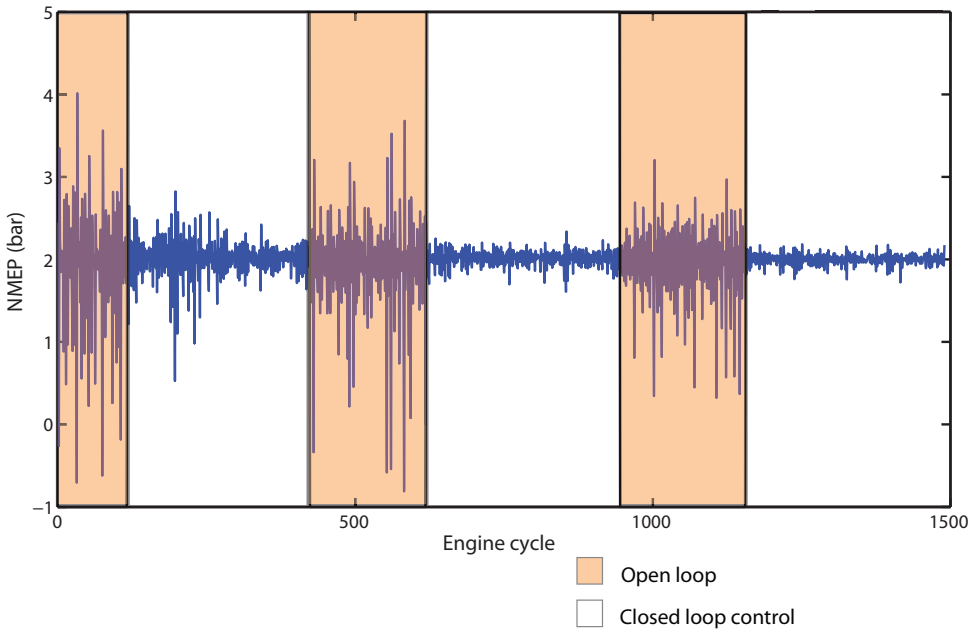

Figure 3.7: Reduction in cyclic variability - NMEP

These instances are non-existent in closed-loop mode. Therefore the controller, by reducing cycle-by-cycle variation, is actually able to prevent misfires at points that are otherwise unstable, and therefore enables more steady operation at these points.

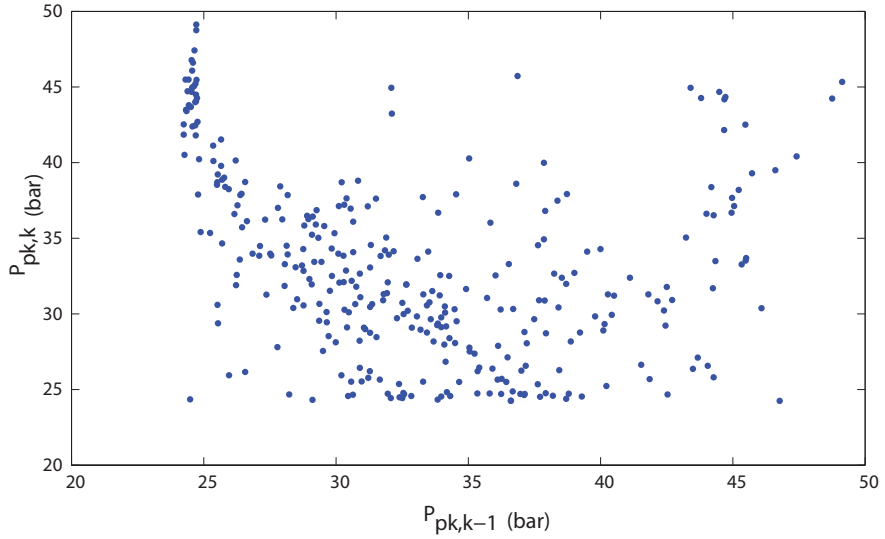

Figure 3.8: Peak pressure lag plot - Open loop

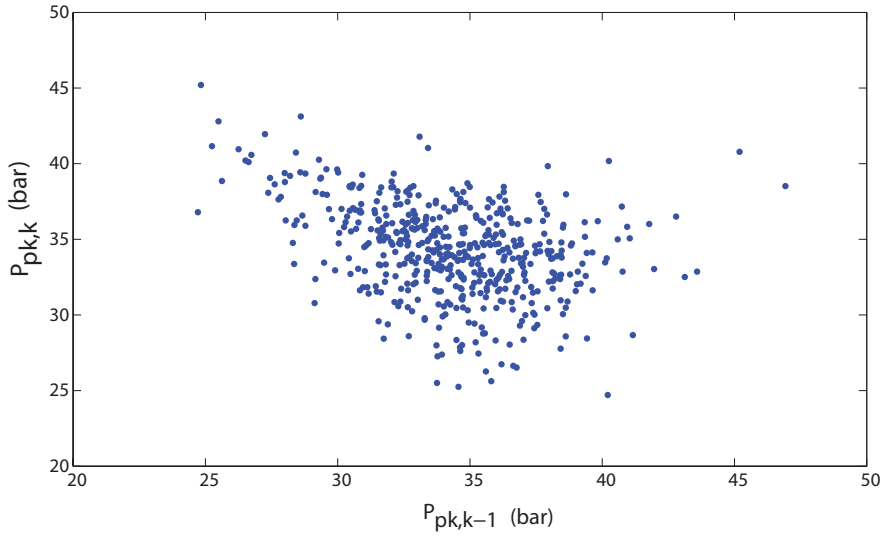

Figure 3.9: Peak pressure lag plot - Closed loop

This effect of reducing process variation can also be seen in the lag plots shown in Figs. 3.8 and 3.9. These plots show the peak pressure on cycle k as a function of the peak pressure on cycle $k-1$. In open loop, there is a lot more dispersion in these values. There are also several points that lie right at the motoring peak-pressure barrier of about 24 bar, which indicates misfires. In closed loop, however, there is much less variation, and the engine does not misfire. Whatever variation exists is centered around the mean peak pressure at this operating point, which is about 35 bar.

3.4 Conclusion

The results presented in this chapter show the value of model-based control in controlling the HCCI combustion process. The simple two state model presented in Chapter 2 is used as the basis for a linear control strategy, where state estimates generated by a linear observer are used by an LQR controller to track a desired output trajectory both in simulation and experiment. Performance is similar in both simulation and experiment, validating the use of model-based control techniques. Additionally, the model provides an insight into the redundancy of one of the measurements used by

the observer - the peak pressure in an engine cycle. It is seen that a measure of work output of the engine does not provide much information for state estimation once we have a measure of the phasing of the combustion and the quantity of fuel injected. Also, as phasing is a stronger function of the mixture temperature, the temperature state can be estimated more accurately than the oxygen concentration.

The results demonstrate two significant benefits of applying cycle-by-cycle closed loop control. First, the system is able to track a desired output trajectory reasonably within a range of conditions. More importantly, though, the controller is able to reduce the cyclic variation that is natural to HCCI, particularly at points that are prone to misfires and unsteady combustion when run open-loop. This reduction in combustion variability also prevents misfires. The controller is able to effect this reduction in variation through a minimal amount of control effort. By enabling steady operation at points that are otherwise unstable, the controller effectively widens the HCCI operating range.

The performance of the controller presented here, though reasonable within the range of operating conditions considered, is far from optimal. Subsequent controller designs presented in this thesis will show improved performance, and move towards more practical approaches that could be implemented on production vehicles.

Apart from the insights gained into the efficacy of this simple control structure, there are some other subtler observations about model structure that were made evident through this process of controller development. These observations, and the model revisions that they suggest, will be the focus of the next chapter.

Chapter 4

Model Revisions

The modeling and control results presented in Chapters 2 and 3 demonstrate that this process of physical model-based control is a useful approach for controlling HCCI around an operating point. However there are several characteristics of the model that warrant a closer look. This chapter focuses on some of these aspects of the model, choices and assumptions made while designing the structure of the model, whether they are justified, and what modifications might be called for in order to achieve better results. In particular, it is seen that while the choice of temperature and reactant concentrations as states is justified, the exact location in the engine cycle where they are defined needs to be carefully determined. Based on these observations, certain revisions made to the model are described. The work output and phasing of combustion are now directly modeled as control outputs, in terms of the net mean effective pressure (NMEP) and the point of 50 percent energy release (CA_{50}). The states are now defined at a fixed crank angle location after IVC, capturing the thermodynamic state of the reactant mixture just before combustion. Additionally, some of the thermodynamic assumptions are made more realistic - compression, expansion and exhaust processes are modeled as polytropic instead of isentropic; combustion is assumed to have a finite duration instead of infinitesimal; and the description of heat transfer during recompression is given a more physical basis by relating it to the cylinder wall temperature. This modified model is then validated against the more complex simulation model through a comparison of step responses to inputs in

addition to the static validation presented in Chapter 2.

4.1 A closer look at the control model

1. *State choices*: Several possible state choices exist for a simple HCCI model. The model developed by Shaver et al [53], for example, uses the control outputs - peak pressure and angle of peak pressure - as model states themselves. This model has been shown to be useful for control of exhaust-reinduction HCCI. However a fundamental set of states, directly linked to the thermodynamic state of the engine, is more desirable. As combustion is basically dictated by two characteristics of the reactant mixture (reactant concentrations and mixture temperature), the choice of oxygen concentration and temperature as states gives a stronger physical basis to the model.

2. *Location of the states in an engine cycle*: Each cycle in the model is broken up into several distinct processes. The exact location between these processes, where the states are defined as representative of the entire cycle, therefore, is quite important. The model presented here has its states defined at EVC. One consequence of defining the states at EVC, which is also a controlled input, is that the state then becomes very sensitive to the definition of EVC (especially since, as an input, it can change from cycle to cycle). Figure 4.1 shows the temperature profile (obtained from the continuous-time simulation) for two different exhaust valve closure conditions - 645 and 655 CAD. As seen, with a later EVC, the temperature at any particular crank angle location is lower. However, comparing the temperature at the actual commanded EVC for each condition, the trend is actually reversed. This would then lead to an incorrect response to a step change in EVC.

   The problem, though, is really one of the definition of EVC. The flow through the exhaust valve is effectively closed about 20-30 degrees before the actual commanded EVC due to the gradual valve profile. Therefore, a more accurate definition of EVC would be this "*effective*" EVC location. Defining the state

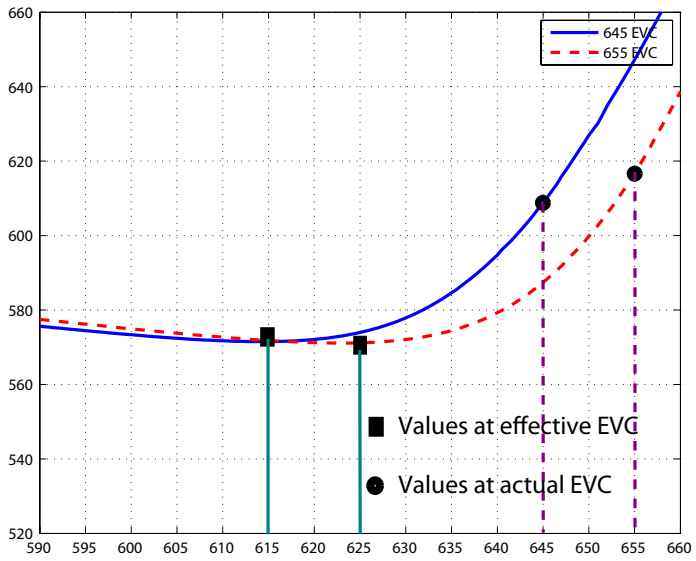

Figure 4.1: Temperature profile before and after EVC step change - values at actual and effective EVC

at this location, as shown in Fig. 4.1, gives the right step response to a change in EVC, and is therefore more representative of the state of the mixture.

The results presented earlier were obtained with the states defined at the "*effective*" EVC, and therefore this issue did not exist. However, this sensitivity of the states to the definition of the input is undesirable. It is therefore preferable to define the states at a fixed crank angle location rather than being tied to the location of an input.

3. *Ease of estimation*: In addition to defining states at a fixed crank angle location, it is also desirable to define them at a location where they are more closely tied to the measured outputs. This would significantly simplify estimation strategies. By defining the states close to EVC, the relationship between the states and outputs becomes a function of the recompression and induction models. In order to have a more direct link between the states and the outputs, they are now defined at a *fixed location after IVC*. The state of the reactant mixture after IVC

is directly related to the phasing of combustion through the Arrhenius equation (2.43). This therefore makes estimation easier and simple linear observers more robust.

4. *Direct input feed-through*: With the definition of states as presented earlier, there is a direct feed-through term from the inputs to the outputs. This manifests as a non-zero D matrix in the linearized system, complicating controller development. This is because of the fundamental model structure, where each *model cycle* really corresponds to several definite stages within one *engine cycle*. Due to this, the states at the beginning of each model cycle need to capture not only all the relevant information about the mixture at that instant (the oxygen concentration and temperature states defined earlier), but also the effects of inputs that occur earlier in the engine cycle that can independently influence the output. Figure 4.2 gives a graphical picture of this with reference to the in-cylinder pressure during successive engine cycles. As seen, each model cycle begins at a fixed location after IVC. The outputs are determined after combustion. Two of the inputs - the fuel quantity and the cylinder volume at IVC - effect not just the states but also the outputs directly. Therefore the state vector needs to be expanded to include these in order to avoid a direct feed-through.

5. *Control outputs*: One of the important objectives of HCCI control research is the development of strategies to control the work output and the phasing of combustion. The results presented earlier demonstrate control of proxies for these quantities - peak pressure and the angle of peak pressure. These however are not solely related to work output and combustion phasing respectively. For example, it is possible to have the same peak pressure for very different values of work output by varying the phasing of combustion. Therefore it is desirable to control these quantities directly instead of through proxies.

6. *Linearizing the right things*: In the process of linearizing a nonlinear model, it is important to consider whether everything should be linearized, or whether well-defined nonlinearities can be preserved. For example, the crank angle -

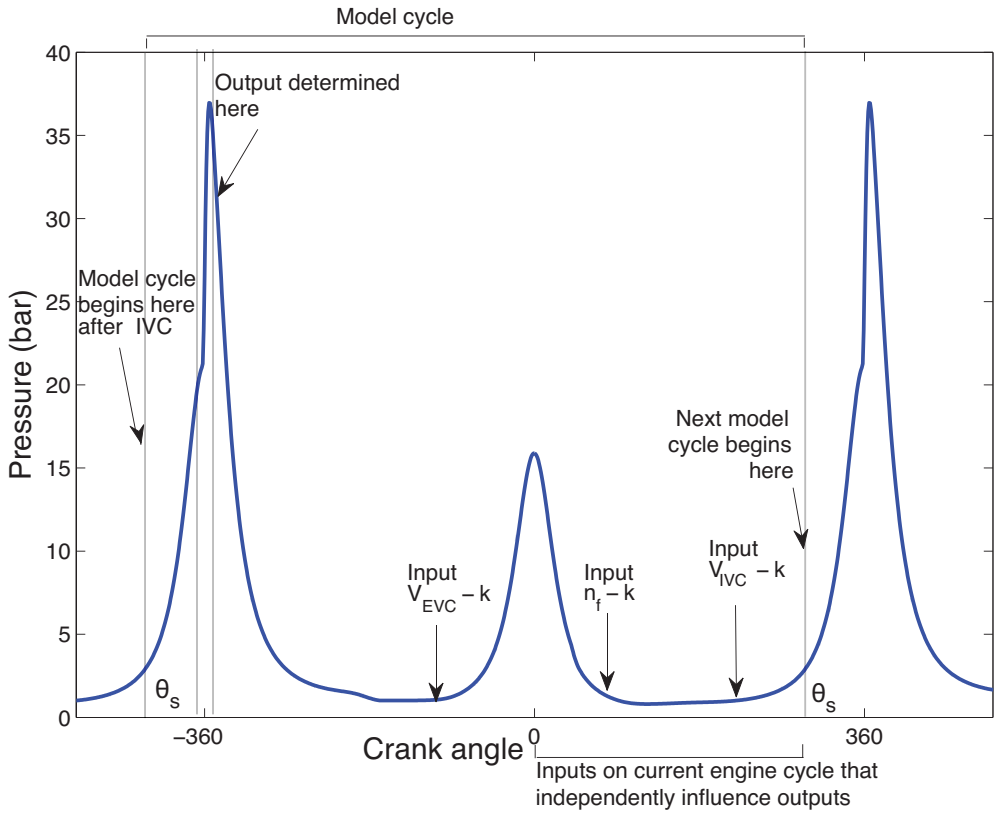

Figure 4.2: Model cycle and location of inputs that influence outputs directly

cylinder volume relationship is a highly nonlinear relationship, but one that is perfectly known. Defining inputs in terms of the cylinder volumes at intake and exhaust valve closure, as done here, essentially takes the volume equation out of the linearized model.

Linearizing the other processes in an HCCI cycle works because around an operating point, these processes can be approximated as linear. Quantities of trapped exhaust and fresh air are fairly linear with respect to the cylinder volume at EVC and IVC. The energy release is roughly proportional to the quantity of fuel injected into the cylinder. Consequently, the temperature increase due to combustion is also proportional to the fuel injected. Also, assuming lean and complete combustion, the amount of oxygen left in the exhaust stream is a linear function of the fuel injected. Heat transfer and combustion phasing are

nonlinear over the HCCI operating region, but are locally linear. This justifies the linearization of the model around an operating condition.

4.2 Revisions to the control model

Based on the above discussion several revisions were made to the control model. This section gives an overview of the model, focusing on the changes made from the version presented in Chapter 2.

4.2.1 Model states

The model states are defined at a fixed crank angle location after intake valve closure - this represents a point where both valves are closed, and all the reactants are present in the cylinder, ready for combustion. This point can be chosen as an arbitrary fixed point after intake valve closure, and is here chosen as θ_s=300 CAD (60 CAD before TDC-combustion). The particular states are chosen as

1. Concentration of oxygen at θ_s, $[O_2]_{s,k}$
2. Temperature of mixture at θ_s, $T_{s,k}$
3. Concentration of fuel at θ_s, $[f]_{s,k}$
4. Cylinder volume at intake valve closure, $V_{IVC_s,k}$

Of these states, the first two - oxygen concentration and mixture temperature - capture the essential dynamics of the HCCI process, as was shown earlier. The other two states complete the description of the thermodynamic state of the cylinder, by providing a measure of the quantity of fuel in the cylinder, and a proxy for the total amount of reactants.

Cylinder volume at the point of state definition is designated as V_1. The fuel concentration state is directly related to the fuel input occurring in the previous model cycle. Likewise, if the intake and exhaust valves are commanded independently, the IVC volume state is equal to the input IVC determined on the previous cycle.

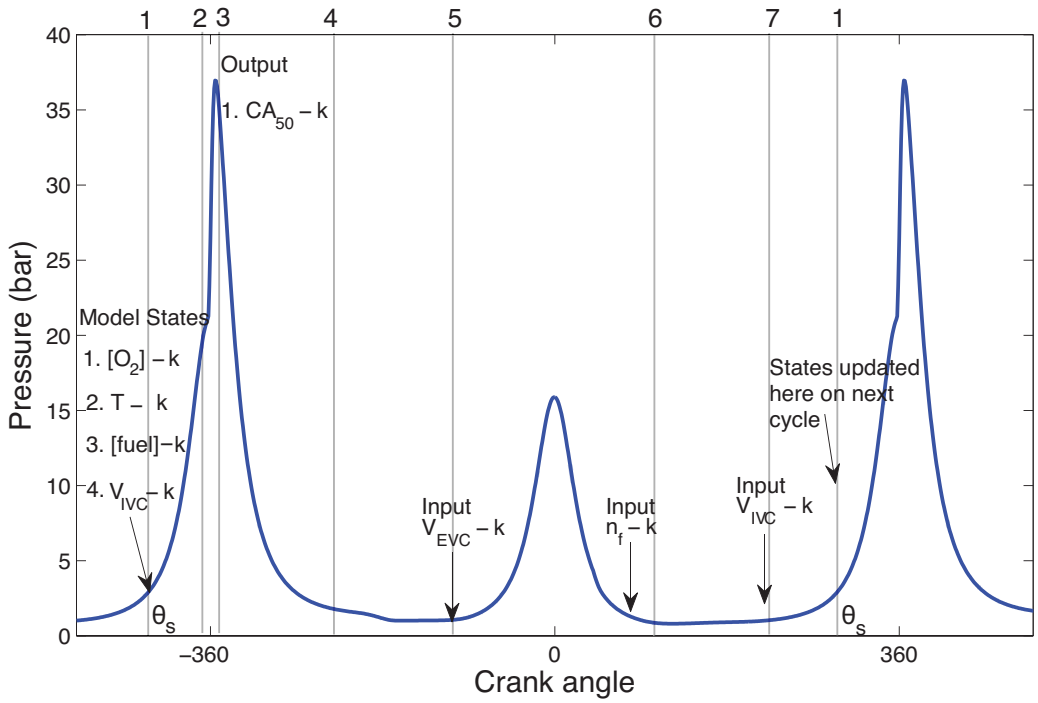

Figure 4.3: States in the control model

A graphical picture of the model is shown in Fig. 4.3 with reference to the evolution of the cylinder pressure. The states, as seen, are defined at a fixed location after the intake valve has closed, which is where the k'th cycle is assumed to begin. Each of the stages in the model as detailed below are labeled above the plot from $1-7$.

The main outputs of this model are measures of the work output and phasing of combustion. In this work, the work output is quantified in terms of the net mean effective pressure ($NMEP$) during an engine cycle. The phasing of combustion is measured as the crank angle location where 50% of the energy from combustion has been released, CA_{50}. This choice is made as it gives a robust indication of the combustion phasing - as the rate of energy release is maximum at the CA_{50}, small errors in the calculation of the point of 50% energy release lead to very small errors in combustion phasing [58].

4.2.2 Revised HCCI control model

As described earlier, a single HCCI cycle can be split into several distinct processes, each of which can be easily modeled based on certain simplifying assumptions. The states are defined at θ_s on cycle k, with cylinder volume V_1. The pressure $P_{1,k}$ is a function of the intake manifold pressure, P_i and the IVC state, assuming polytropic compression from IVC to θ_s. This is a more realistic assumption than an isentropic compression model and captures the heat transfer during the compression process.

$$P_{1,k} = \left(\frac{V_{IVC,k}}{V_1}\right)^{n_c} P_i \tag{4.1}$$

Here n_c is the polytropic exponent. Using the ideal gas law, the total moles inside the cylinder, and the number of moles of fuel and oxygen can be obtained from the state values:

$$N_{1,k} = \frac{P_{1,k}V_1}{R_u T_{s,k}} \tag{4.2}$$

$$n_{f,1,k} = [f]_{s,k}V_1 \tag{4.3}$$

$$n_{O_2,1,k} = [O_2]_{s,k}V_1 \tag{4.4}$$

1. *Polytropic compression*: Instead of an isentropic assumption, compression from θ_s to the point where combustion just begins, $\theta_{2,k}$, is assumed to be polytropic. Therefore at end of compression, pressure and temperature are given by

$$P_{2,k} = \left(\frac{V_1}{V_{2,k}}\right)^{n_c} P_{1,k} \tag{4.5}$$

$$T_{2,k} = \left(\frac{V_1}{V_{2,k}}\right)^{n_c-1} T_{1,k} \tag{4.6}$$

   The amounts of various constituents in the cylinder remain the same during the process as there is no gas exchange or reaction.

2. *Phasing of combustion*: The global Arrhenius rate equation presented in Fig.

(2.43) is used to model the phasing of combustion. However instead of approximating the integrand by its value at TDC to get a simplified analytical expression for the integral, it is preserved in its original form. On integrating the equation from intake valve closure to the point of combustion,

$$\begin{aligned}\int RRdt &= \int A_{th}e^{\left(\frac{E_a}{R_uT}\right)}[C_7H_{13}]^a[O_2]^b dt \\ &= \int_{\theta_{IVC}}^{\theta_{2,k}} A_{th}e^{\left(\frac{E_a}{R_uT}\right)}[C_7H_{13}]^a[O_2]^b \frac{dt}{d\theta}d\theta \\ &= \int_{\theta_{IVC}}^{\theta_{s}} \frac{A_{th}e^{\left(\frac{E_a}{R_uT}\right)}[C_7H_{13}]^a[O_2]^b}{\omega}d\theta \\ &+ \int_{\theta_{s}}^{\theta_{2,k}} \frac{A_{th}e^{\left(\frac{E_a}{R_uT}\right)}[C_7H_{13}]^a[O_2]^b}{\omega}d\theta \end{aligned} \tag{4.7}$$

where $\theta_{2,k}$ is the crank angle location at start of combustion.

The first integral in the last equation ≈ 0. This is because both the temperature and concentrations change relatively slowly during the initial compression, and rapidly closer to top dead center (TDC). Therefore, especially due to the exponential dependence on temperature, the integrand only becomes significant in the later part of compression. The equation then reduces to

$$\int RRdt = \int_{\theta_{s}}^{\theta_{2,k}} \frac{A_{th}e^{\left(\frac{E_a}{R_uT}\right)}[C_7H_{13}]^a[O_2]^b}{\omega}d\theta \tag{4.8}$$

When the integral in equation (4.8) crosses a threshold, K_{th}, combustion is modeled to have begun. The integral can be condensed into a map that gives the phasing of combustion as a function of the reactant concentrations and temperature at the point of state definition. This map is easier to handle than the analytical expression for the integrated Arrhenius rate in its nonlinear form.

$$\theta_{2,k} = F_1([O_2]_{s,k}, T_{s,k}, [f]_{s,k}) \tag{4.9}$$

3. *Combustion over a finite duration*: Combustion is now modeled as a finite

duration event rather than an instantaneous one. The duration of combustion in HCCI is a strongly monotonic function of the phasing of combustion [59]. Here this duration, $\theta_{durn,k}$ is approximated as a simple linear function of the start-of-combustion crank angle location, $\theta_{2,k}$. This approximation is seen to be valid around an operating point. The CA_{50}, then, can be calculated as being half the combustion duration after the start of combustion:

$$CA_{50,k} = \theta_{2,k} + 0.5\theta_{durn,k} \tag{4.10}$$

This phasing of combustion is the main output of this model. The first law of thermodynamics is applied as earlier to obtain the state of the mixture after combustion, as well as the in-cylinder pressure and temperature. A lumped heat transfer is assumed during combustion, modeled as a factor of the lower heating value of the fuel.

4. *Polytropic expansion*: Polytropic expansion is assumed until the opening of the exhaust valve, and so

$$T_{4,k} = \left(\frac{V_{3,k}}{V_{4,k}}\right)^{n_e-1} T_{3,k} \tag{4.11}$$

$$P_{4,k} = \left(\frac{V_{3,k}}{V_{4,k}}\right)^{n_e} P_{3,k} \tag{4.12}$$

where n_e is the polytropic exponent for the expansion process.

5. *Polytropic blowdown and exhaust*: The exhaust process is again split into two stages - first, the blowdown, where the exhaust gases left in the cylinder are assumed to undergo a polytropic process, and then a mass transfer to the exhaust manifold (with no change in thermodynamic state). Based on this, temperature at the point of exhaust valve closure is:

$$T_{5,k} = \left(\frac{P_{exh}}{P_{4,k}}\right)^{\frac{n_e-1}{n_e}} T_{4,k}$$

The fraction of trapped exhaust, β can be obtained from applying the ideal gas law at the beginning and end of the exhaust process:

$$\beta = \frac{N_{5,k}}{N_{4,k}} = \frac{V_{EVC,k} P_{exh} T_{4,k}}{V_{4,k} P_{4,k} T_{5,k}}$$

6. *Recompression*: During the recompression process, there is no inflow/outflow of species as the valves are closed. The fuel is injected at the end of recompression. This fuel vaporizes and takes away a portion of the energy of the cylinder contents. It is assumed that there is no early/pilot fuel injection, and consequently no possibility for fuel reforming or exothermic reaction during the recompression. The quantity of the fuel that is injected, $n_{f,k}$, is one of the inputs on this cycle. Additionally, some heat transfer occurs to the walls. Assuming an average wall temperature of T_w, an average mixture temperature of T_{avg} and using the first law of thermodynamics, the internal energy of the cylinder constituents before and after recompression can be related

$$U_{start} - hA_{avg}(T_{avg} - T_w)\Delta t_{recomp} - n_{f,k} h_{fg,fuel} = U_{end} \tag{4.13}$$

The average temperature during recompression can be approximated by taking the average of an isentropic temperature profile with no heat transfer. The time for recompression, Δt_{recomp} is a function of the valve timings and engine speed. Equation (4.13) can then be used to solve for the temperature at the end of recompression, $T_{6,k}$. Though the heat transfer during recompression is not a linear process as might be suggested by using a single average temperature to characterize the trapped exhaust, this simplified heat transfer model represents a first attempt at including the effects of cylinder wall temperature and would need to be further refined in future work.

7. *Adiabatic induction*: Fresh air is inducted into the cylinder from IVO to IVC at a constant pressure (average pressure in the intake manifold, here assumed to be atmospheric) and temperature. This is then assumed to mix instantaneously

at IVC with the trapped exhaust and fuel. On mixing,

$$n_{total} = n_{air} + n_{tr.exh} + n_{fuel} \tag{4.14}$$

Also, applying the 1st law to the mixing process,

$$u_{sensible,before} = u_{sensible,after}$$

Using the ideal gas law,

$$n_{total} = \frac{P_{7,k}V_{7,k}}{R_u T_{7,k}} \tag{4.15}$$

where $P_{7,k}$ (atmospheric pressure) and $T_{7,k}$ are pressure and temperature of the mixture at IVC. Here, the volume at IVC, $V_{7,k}$ is the final input on this cycle. These equations can be solved to obtain the amount of air inducted into the cylinder, and the final temperature of the mixture.

8. *Polytropic compression from IVC to θ_s*: Finally, the mixture is polytropically compressed to θ_s, where the states are then updated. At this point, the next cycle, $k+1$, begins.

$$P_{1,k+1} = \left(\frac{V_{7,k}}{V_1}\right)^{n_c} P_{7,k} \tag{4.16}$$

$$T_{1,k+1} = \left(\frac{V_{7,k}}{V_1}\right)^{n_c-1} T_{7,k} \tag{4.17}$$

Stepping through the above processes gives a four state nonlinear state space model that maps the inputs on one engine cycle to the outputs on that same cycle through the states.

$$\begin{aligned} x_{k+1} &= F(x_k, u_k) \\ y_k &= G(x_k) \end{aligned} \tag{4.18}$$

The states, inputs and outputs are given by

$$x_k = \begin{bmatrix} [O_2]_{s,k} \\ T_{s,k} \\ [f]_{s,k} \\ V_{IVC_s,k} \end{bmatrix}, u_k = \begin{bmatrix} n_{f,k} \\ V_{IVC,k} \\ V_{EVC,k} \end{bmatrix}, y_k = \begin{bmatrix} CA_{50,k} \end{bmatrix} \tag{4.19}$$

This nonlinear model can be linearized as detailed in Chapter 3 to aid the synthesis of a linear controller to control the phasing of combustion, CA_{50}. The other quantity of interest that needs to be controlled accurately is the work output of the engine, or $NMEP$. The relationship between the states and $NMEP$ can be derived from the model based on the in-cylinder pressure at different points during the cycle. However, the work output is strongly dependent on the quantity of fuel injected into the cylinder when the engine is operating as desired. Therefore control of $NMEP$ can be handled based on an empirically derived relationship between fuel quantity and work output, instead of through an explicit analytical relationship to the states of the nonlinear model.

4.2.3 Model comparison

The nonlinear and linear control models are compared to the continuous time simulation model. Instead of the static validation presented in Chapter 2, a dynamic validation is presented here in terms of the responses of the various models to input changes.

Figure 4.4 shows the evolution of the oxygen and temperature states, as well as the combustion phasing predicted by the three models (continuous-time simulation, nonlinear control model and linear control model) with a step change in EVC. As seen, all three models exhibit a similar characteristic during the step change. The control model is seen to be more sensitive to the change in input than the simulation model in terms of the change in state values. This is however not a significant issue as the CA_{50} change in all three models is very similar (the difference is well within the range of the variance seen on the engine around a steady-state operating point).

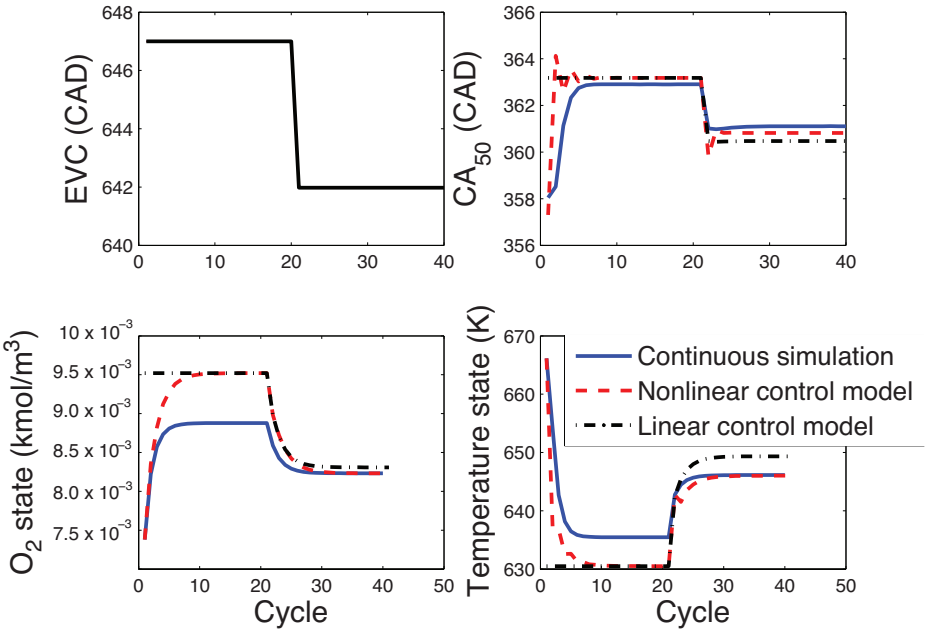

Figure 4.4: Comparison of control and simulation models over a step change in EVC

Additionally, the directionality of the response is more critical than the absolute magnitude, which can be compensated for in feedback.

Figure 4.5 shows the response of the three models to a step change in fuel quantity. Again, all models match reasonably well in terms of the magnitude and directionality of response.

4.3 Conclusion

Though the original control model presented in this thesis enabled control of peak pressure and angle of peak pressure around an operating point, there were several aspects of its structure underscored in this chapter that needed modification. Most importantly, it was seen that the states and their location in the engine cycle had to be carefully designed to meet multiple requirements:

1. They should have a physical basis and link to the thermodynamic state

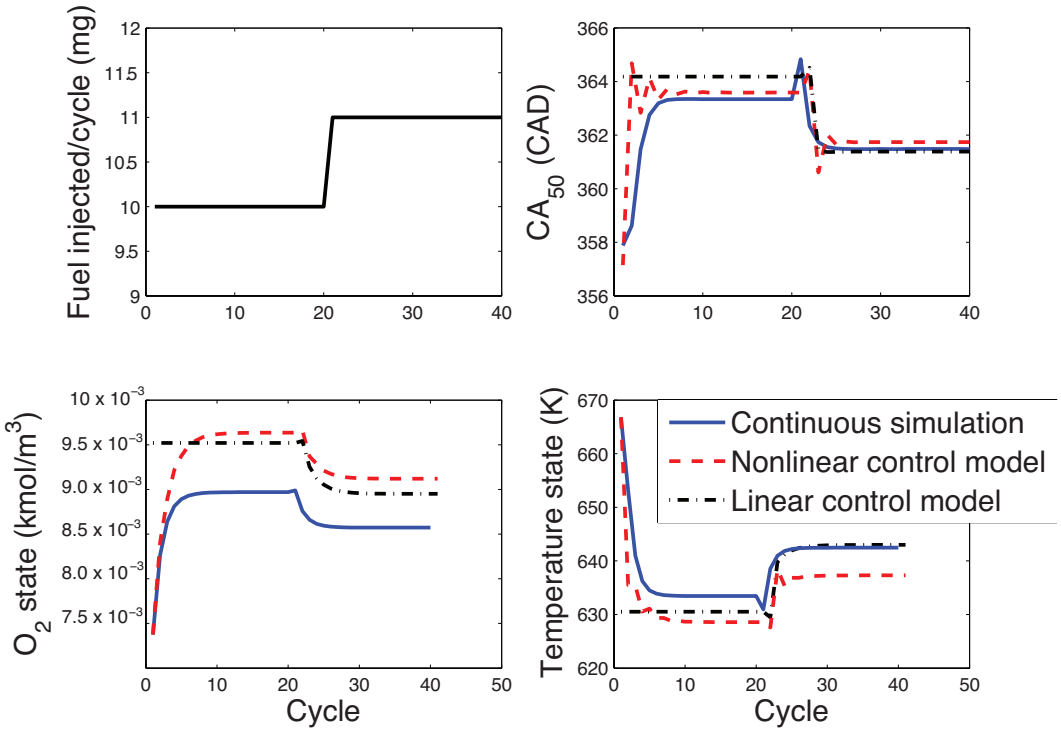

Figure 4.5: Comparison of control and simulation models over a step change in fuel

2. They should capture the effects of inputs that independently influence the outputs on each engine cycle

3. Their definition should not be tied to a varying input

4. They should be closely linked to the measured output in order to simplify estimation

These requirements motivated a four state model with the states defined at a fixed location after IVC. Additionally some of the more simplifying assumptions in the model were relaxed in favor of thermodynamically more realistic ones - compression and expansion were assumed to be polytropic instead of isentropic, a finite duration combustion event was assumed, and a more complex heat transfer model during recompression was developed. The following chapter now discusses how this model can be used to develop a controller that will directly control the outputs of interest - work output and combustion phasing.

Chapter 5

Control of Work Output and Combustion Phasing

This chapter presents results demonstrating control of work output and combustion phasing based on the revised model described in Chapter 4. The two desired outputs are seen to be separable with respect to the inputs. The work output is a very strong function of the fuel quantity. The phasing of combustion, on the other hand, is mostly related to the characteristics of the trapped exhaust - total quantity, oxygen concentration and temperature. Therefore these outputs are controlled independently. A simple feedforward map and integral controller command the fuel to achieve the desired $NMEP$. A model-based feedback controller similar to the one presented in Chapter 3 is used to control CA_{50}. The states as chosen are not directly measurable on an actual engine setup, and so an observer that generates an estimate of the states based on the available measurements is also developed.

This controller is implemented first on a single-cylinder engine, where it effectively tracks a series of desired step changes in $NMEP$ and CA_{50} over a wide range. The controller is also seen to compensate for some existing calibration errors in actuators such as the fuel injector. The real value of this physical model-based control structure, however, is brought out in its ease of portability across engine testbeds. A simple re-parametrization enables the implementation of this controller on a multi-cylinder

HCCI engine, where each cylinder is controlled independently of the others. Experimental results indicate a similar level of performance as compared to tests on the single-cylinder engine. The controller works over a fairly wide range of operating conditions, despite being based on a linearization about a single point. This seemingly surprising result can be clearly explained in terms of specific choices made during the modeling process, which were discussed in Chapter 4. The controller is seen to balance differences between the cylinders, bringing them all to the desired set-point by commanding different inputs on each. In addition, like the controller presented in Chapter 3, it is seen that the controller is able to stabilize combustion at points where the combustion is otherwise highly unstable. This could potentially aid in enlarging the operating range of HCCI.

5.1 Controller and observer synthesis

Two of the states in the four state model presented in the previous chapter - fuel concentration, $[f]_{s,k}$ and Cylinder volume at IVC, $V_{IVC_s,k}$ - are directly related to inputs on the previous model cycle and therefore known. However the other two - oxygen concentration, $[O_2]_{s,k}$ and mixture temperature, $T_{s,k}$ - are not directly measurable. Therefore a linear estimator similar to the one presented in Chapter 3 is designed, which uses the measurement of CA_{50} to estimate these two states. The output equation used by the estimator is obtained from a local linearization of the Arrhenius map described earlier.

5.1.1 Output controller design

The linear state space model can be used to design a feedback controller to track a desired combustion phasing trajectory. The other quantity of interest that needs to be controlled accurately is the work output of the engine, or $NMEP$. The relationship between the states and $NMEP$ can be derived from the model based on the in-cylinder pressure at different points during the cycle. However, the work output is strongly dependent on the quantity of fuel injected into the cylinder when the engine

is operating as desired. Therefore control of $NMEP$ can be handled based on an empirically derived relationship between fuel quantity and work output.

In addition, the phasing of combustion on a particular engine cycle is seen to have a negligible dependence on the amount of fuel injected on that cycle. This is easy to see analytically from the Arrhenius expression in Eq. (2.43) - the dominant effect is one of temperature (an exponential dependence), in addition to which the exponent on the fuel concentration term is much smaller than that on the oxygen concentration ($a = 0.25$ and $b = 1.5$, [55]). This result is borne out in experiment, as seen in Fig. 5.1 which shows the effect of fuel quantity on combustion phasing. The injected fuel quantity is varied according to a uniform random distribution on each cycle. As seen, there is almost no discernible effect on CA_{50} on that cycle.

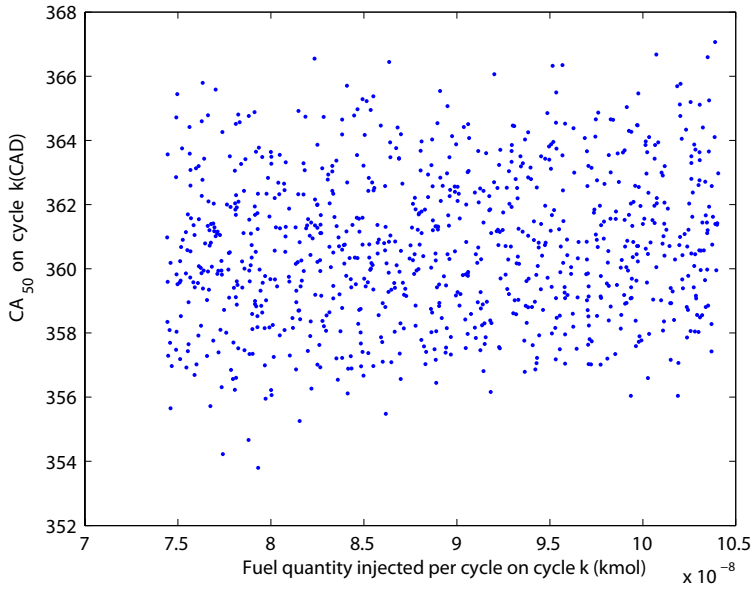

Figure 5.1: Variation of combustion phasing with injected fuel quantity on current cycle

However there is a significant effect of the fuel injected on the previous cycle on the combustion phasing on the current cycle, as seen in Fig. 5.2. This is because the quantity of fuel injected on one cycle affects the combustion and temperature of the trapped exhaust on that cycle, which then influences the temperature of the reactant

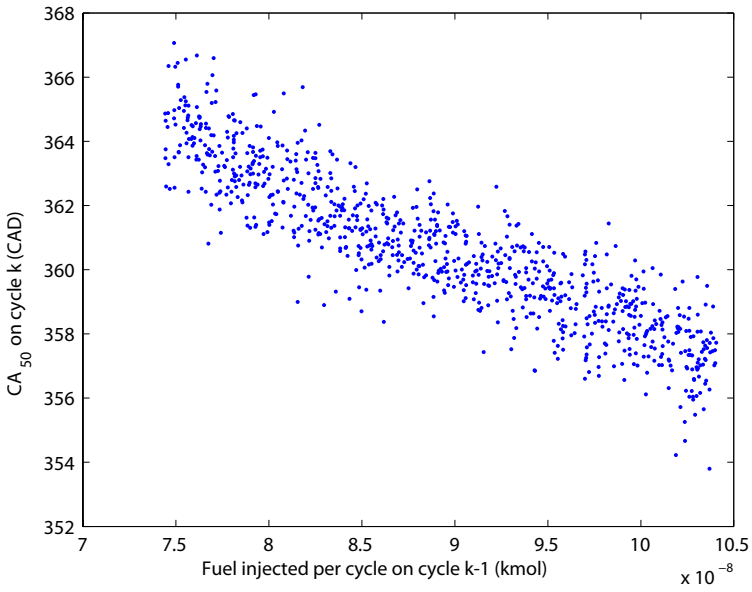

Figure 5.2: Variation of combustion phasing with injected fuel quantity on previous cycle

mixture on the next cycle. This effect is also described by Fischer et al [60].

This separability between the two outputs to be controlled suggests a control strategy where they are controlled independently. The quantity of fuel injected can be used to control the work output of the engine, while the valve timings can be used to control the phasing of combustion.

A simple feedforward-feedback controller is used to control the $NMEP$. A map relating fuel quantity to $NMEP$ derived empirically is the feedforward portion of this controller. It should be noted that in general, $NMEP$ also depends on combustion phasing - however, for the range of CA_{50} considered here, it is fuel quantity that has the dominant effect on $NMEP$. A closed-loop integral controller is then added to correct this map in feedback to get the exact $NMEP$ desired.

To control the phasing with valves, the fuel and valve inputs need to be separated

out in the linear model:

$$\begin{aligned} \tilde{x}_{k+1} &= A\tilde{x}_k + B_1\tilde{u}_{1k} + B_2\tilde{u}_{2k} \\ \tilde{y}_k &= C\tilde{x}_k \end{aligned} \tag{5.1}$$

where $\tilde{u}_{1k} = \tilde{n}_{f,k}$, which is commanded by the $NMEP$-fuel map controller, and $\tilde{u}_{2k} = \begin{bmatrix} \tilde{V}_{IVC,k} \\ \tilde{V}_{EVC,k} \end{bmatrix}$, which is used to control the combustion phasing. A reference input is used as described in Chapter 3. The matrices N_x and N_u are defined such that in steady state, the output follows the reference, with a corresponding reference state value.

$$N_x r = x_{ss}, N_u r = u_{ss} \tag{5.2}$$

The control input, then, is of the form

$$\tilde{u}_{2k} = -K_x(\tilde{x}_k - x_{ss}) + u_{ss} = -K_x\tilde{x}_k + (N_u + K_x N_x)r_k \tag{5.3}$$

where r is the reference input (representing the desired output trajectory) and K_x is the controller gain matrix. N_u and N_x are obtained from the following relation that specifies that the system respond with a zero steady state error to any constant input.

$$\begin{bmatrix} A - I & B_2 \\ C & 0 \end{bmatrix} \begin{bmatrix} N_x \\ N_u \end{bmatrix} = \begin{bmatrix} -\frac{B_1 u_1}{r} \\ I \end{bmatrix} \tag{5.4}$$

where I represents the identity matrix, and 0 the zero matrix. Equation (5.4) is obtained from Eq. (5.1) using Eq. (5.2).

An integral controller based on the deviation in measured output is added to this closed-loop controller so as to compensate for any steady-state errors that would arise due to linearization, such as those seen in the results presented in Chapter 3.

This controller can now be combined with the estimator to give a complete controller-observer system, which can then be used to track a desired $NMEP - CA_{50}$ trajectory. The controller matrix K_x can be designed using a variety of techniques

that would give different weights to the different inputs. In all results described in this chapter, a pole-placement controller is used. The poles for this controller have been chosen somewhat arbitrarily and so are not optimized for any particular metric. All the three available inputs (fuel quantity, IVC and EVC) are controlled, unlike the controller presented earlier where only fuel quantity and EVC were used to control peak pressure and angle of peak pressure.

5.2 Single-cylinder HCCI engine control

5.2.1 Simulation results

The control model is parameterized by matching it with the continuous time simulation model at one operating condition as described earlier. The characteristics of the operating point around which the system has been linearized are given in Table 5.1.

Table 5.1: Operating point at which control model is linearized

Parameter	Value	Units
Engine speed	1800	rpm
IVO	65	CAD
IVC	205	CAD
EVO	480	CAD
EVC	640	CAD
Mass of fuel injected per cycle	10	mg
$NMEP$	2.5	bar
CA_{50}	363	CAD

The characteristics of this operating condition can be substituted in the expressions for the analytical linearization to obtain a specific linear model for this point. The matrices that define this operating condition are shown in Eq. (5.5).

$$
\begin{aligned}
A &= \begin{bmatrix} 0.43 & -1.16 & -0.27 & -0.11 \\ -0.03 & 0.25 & 0.13 & -0.37 \\ 0 & 0 & 0 & 0 \\ 0 & 0 & 0 & 0 \end{bmatrix} \\
B &= \begin{bmatrix} 0.02 & 1.90 & -0.92 \\ -0.02 & -0.18 & 0.45 \\ 1 & 0 & 0 \\ 0 & 1 & 0 \end{bmatrix} \\
C &= \begin{bmatrix} -0.04 & -0.34 & -0.0063 & 0 \end{bmatrix}
\end{aligned} \tag{5.5}
$$

As seen, the bottom two rows of the A matrix are zero, as the fuel and IVC states depend purely on the inputs on the previous cycle. Additionally the output, CA_{50}, depends only on the first three states as seen from Eq. (4.10). Therefore, though IVC does not directly affect the output, it affects the oxygen and temperature states, which in turn influence CA_{50} on the next cycle.

The nonzero eigenvalues of A are 0.56 and 0.12; and so the system is stable at this point, which is borne out by experiments run on the engine at the same point.

This process of linearization and controller development is performed only at one operating point. Once a set of controller/observer matrices are obtained, those are taken as fixed and used at all other operating points.

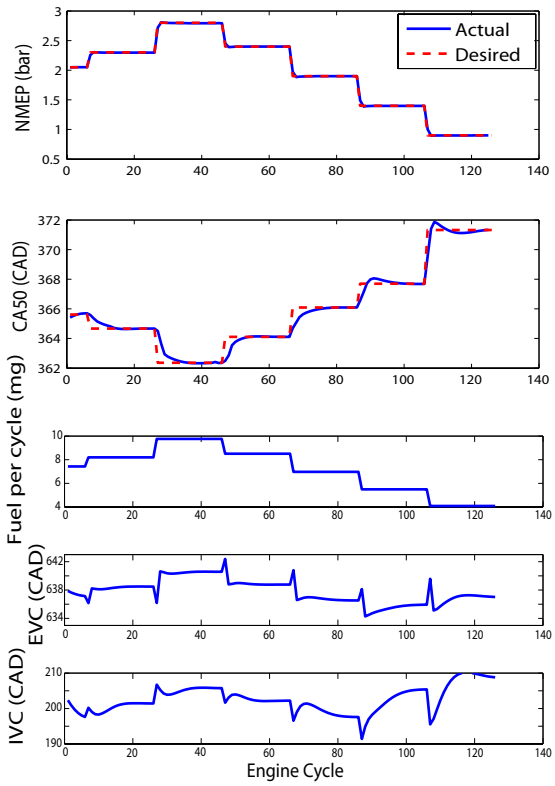

Figure 5.3: Controller implemented in simulation - outputs and inputs

The results from simulation of the linear controller are shown in Fig. 5.3. These results are obtained by running the controller on the continuous time simulation. As seen the controller is effective in tracking both the $NMEP$ and CA_{50} over a fairly wide range of step changes. As the fuel-$NMEP$ map is derived from the simulation (and as there are no dynamics between fuel and $NMEP$), there is practically no steady-state error in $NMEP$ that the integral controller has to compensate for. When it comes to the linearized model for CA_{50}, however, there are naturally some errors when compared to the nonlinear simulation, especially over such a wide range. Therefore the integral controller here modulates the valve timings, thereby enabling tracking of the desired phasing without any steady state error.

5.2.2 Experimental results

Figure 5.4 shows the results from a test run on the single cylinder HCCI engine testbed. As seen, when the controller is switched on, the engine accurately tracks the desired $NMEP - CA_{50}$ trajectory through a series of step changes.

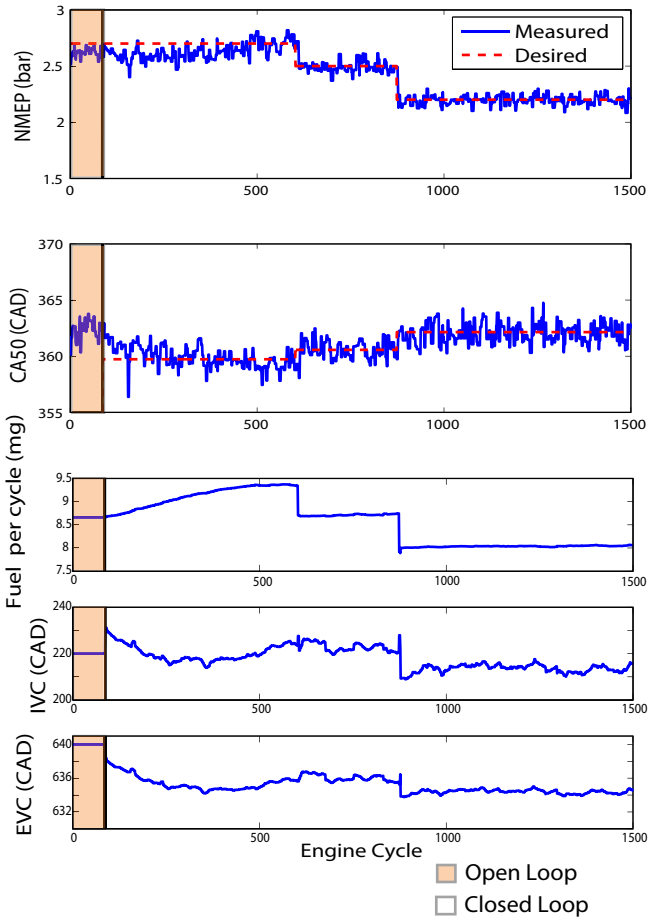

Figure 5.4: Experimental control on single cylinder HCCI engine - outputs and inputs

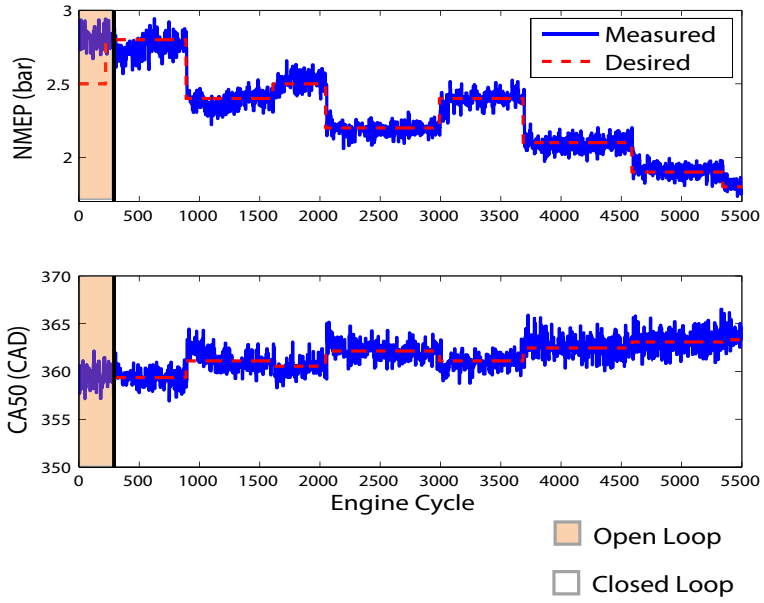

Figure 5.5: Experimental control on single cylinder HCCI engine - outputs

The inputs commanded by the controller are also shown in the same figure. When the controller is initially switched on, the integral action on the fuel controller brings the $NMEP$ to the right steady state. This initial integral action is likely due to an injector calibration error, which causes the fuel-$NMEP$ map to command the wrong amount of fuel when the controller is first turned on. However, once the integral controller has effectively "learned" this calibration error, subsequent step changes occur in the matter of a few cycles, and there is little integral action. Likewise, the CA_{50} closed-loop controller commands step changes in the valve position in order to track the desired phasing.

These experimental results show the controller's efficacy in tracking the work output. Figure 5.5 shows a series of step changes that span an $NMEP$ range from about 1.8-2.8 bar, with a phasing range of about 4 degrees. The controller also worked well with load conditions as low as 1.6 bar $NMEP$, and at speeds from 1600-2000 rpm.

5.3 Multi-cylinder HCCI control

One of the biggest advantages of a control framework based on a physical model is the ease of porting the controller from one testbed to another. A control strategy developed without a model would require a lot of tuning of controller gains in a fairly unsystematic manner. If one used system-identification techniques to identify an input-output model for a particular engine, this process would need to be repeated for a new engine. A physical HCCI engine model such as the one used here, on the other hand, is based on the fundamental thermodynamics of the HCCI process which are quite similar from engine to engine. All that is required, therefore, to develop a similar controller for another engine, is a re-parametrization of the control model to this new engine. Most of these parameters are known engine hardware constants, while a couple (such as the polytropic exponents and lumped heat transfer coefficient) are tuned with steady-state data from a single operating condition.

To demonstrate the value of this framework in controlling different engine testbeds, this controller was implemented on a multi-cylinder HCCI engine testbed with fully flexible variable valve actuation on each cylinder. Each cylinder is independently controlled, the engine essentially being treated as a series of single-cylinders. A very rudimentary parametrization of both the simulation and control models at a fixed operating condition was used. The primary objective, therefore, was not to develop the best HCCI controller for this engine, but rather to demonstrate that this control structure is robust to system changes, and modeling, parametrization and calibration errors, and works well in spite of them. As the results on the single-cylinder engine indicated that the phasing of combustion was more sensitive to the exhaust valve closing time, only the EVC control input is used to control phasing in these tests. IVC is kept fixed throughout these tests.

5.3.1 Experimental setup

The multi-cylinder engine testbed used to test the controller is a four cylinder General Motors gasoline engine modified to run HCCI. The engine runs on a compression ratio of 12:1. A common rail direct injection system is used to inject fuel directly

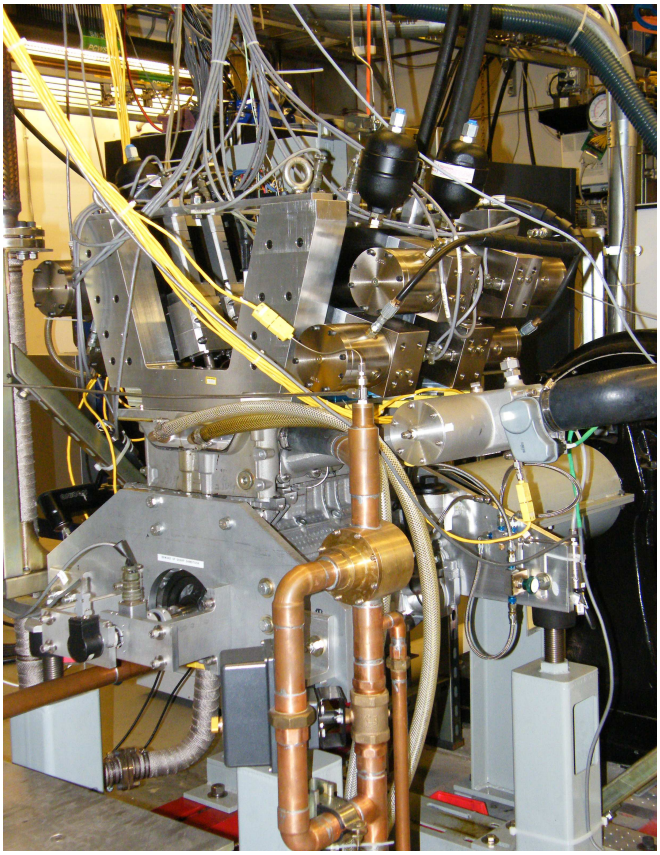

Figure 5.6: Multi-cylinder HCCI engine testbed

into each cylinder. As on the single cylinder engine, the testbed is equipped with a fully flexible VVA system that can be used to actuate the intake and exhaust valves on each cylinder independently. Air is inducted at atmospheric pressure. Though the intake system has a throttle, its position is kept fixed (at wide open) during these tests. Cylinder pressure is measured with a Kistler 6125 piezoelectric transducer in each cylinder. The software architecture used for sensing and control is similar to that on the single cylinder engine, and is based on Matlab's xPC-Target. All experiments are again run at 1800rpm.

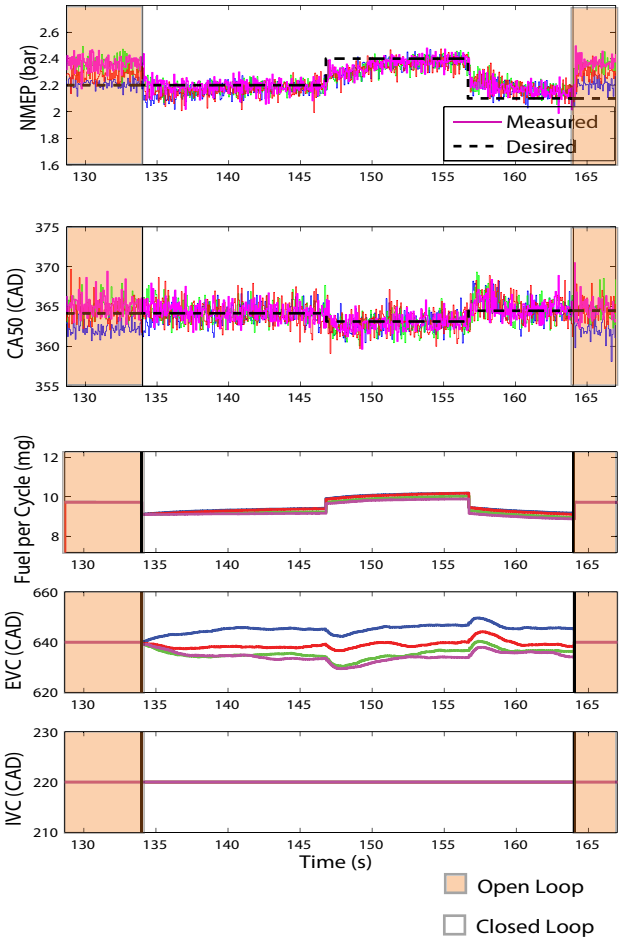

Figure 5.7: Experimental control of multi-cylinder HCCI engine - outputs and inputs

5.3.2 Experimental results

The tracking performance of the controller implemented on the multi-cylinder HCCI engine is shown in Fig. 5.7. Trajectories for each cylinder are shown in a different color. In open loop, the four cylinders are at different steady state values in $NMEP$ and CA_{50}, for the same fueling rates and valve timings. This is commonly seen in engines due to varying heat transfer and breathing characteristics in each cylinder. Once the controller is switched on, however, all the cylinders converge to the right steady-state value. Figure 5.7 also shows that the controller commands a different fuel quantity and EVC on each cylinder, thereby balancing out the cylinders. Each

cylinder is then able to track the desired step changes accurately. Again, calibration errors lead to some effort on the part of the integral controller to compensate. Once the controller is switched off, each cylinder goes back to its own steady state.

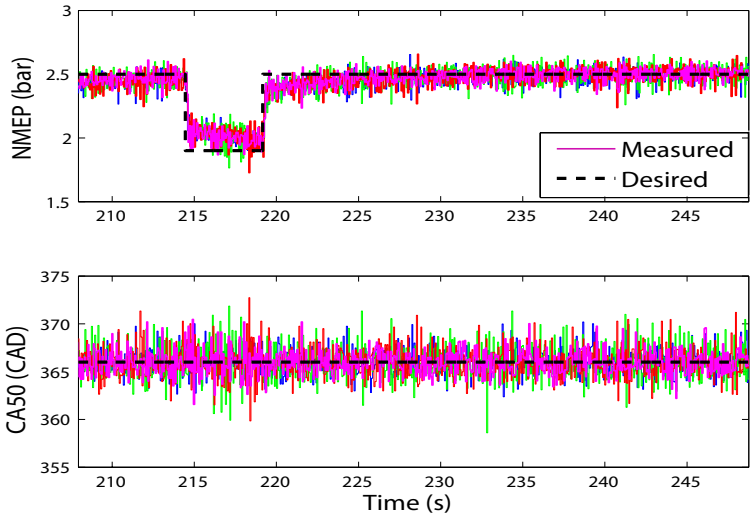

Figure 5.8: Experimental control of multi-cylinder HCCI engine, large step change - outputs

As on the single-cylinder engine, the controller works over a reasonably wide operating range, and is effective in tracking fairly large step changes in work output. This can be seen in Fig. 5.8, where a step change of about 0.6 bar is achieved at constant combustion phasing. Also, after the first step, the desired steady-state value of $NMEP$ is not reached immediately. This is because of a fuel injector calibration error, which caused the feedforward portion of the $NMEP$ controller to be inaccurate. Therefore the integral controller has to compensate for this. The slow time constant of the integral action is due to a low integral gain.

The speed of controller response when turned on can be seen in Fig. 5.9, where the output and EVC trajectories are plotted for cylinder 2. The closed-loop controller responds almost instantaneously (due to the feedforward portion) when switched on. The feedback then brings it to the appropriate steady-state within 3-4 cycles. This speed of response is representative of the controller action on all cylinders.

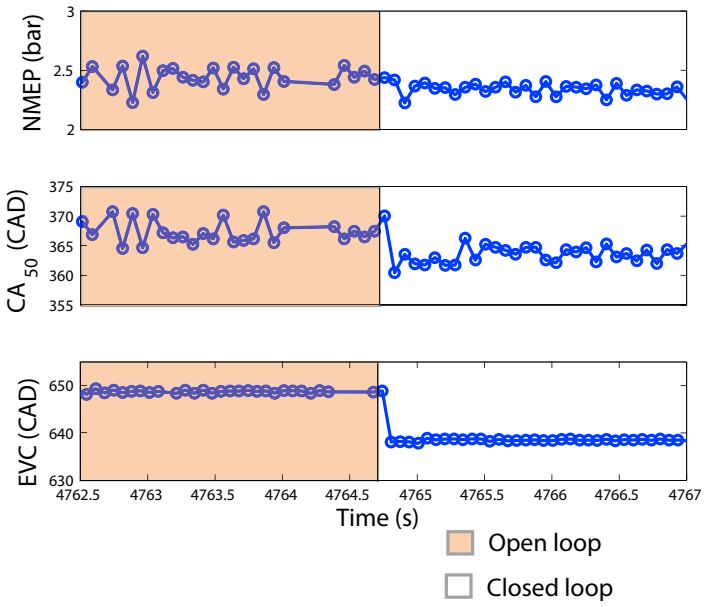

Figure 5.9: Speed of controller response on cylinder 2 - open loop to closed loop

Figure 5.10 shows the response to a step change in desired CA_{50} while in closed loop on cylinder 4. A slightly different controller with higher gains is used here. Again, the controller reaches the new steady state within a few cycles. Also, some overshoot is seen on the first cycle after the step change due to the higher controller gain. This points to one of the drawbacks of designing a feedback controller by this method of pole placement, and it might lead to controller commands that require very quick changes in valve timing that might not be feasible on a production setup. This issue will be addressed by controller schemes developed in later chapters.

The controller was able to track step changes over a fairly wide range of NMEP, from as low as about 1.6 bar to as high as 3 bar (and over a 10 degree range in CA_{50}) even though it was tuned at just a single operating point, and the fuel-injector calibrations were not entirely accurate. All these results point to the robustness of this control scheme to modeling and calibration errors.

As with the first controller presented in Chapter 3, this control strategy also provides a significant benefit in terms of combustion stabilization. Figure 5.11 shows the results of a test where operation is switched successively between open and closed

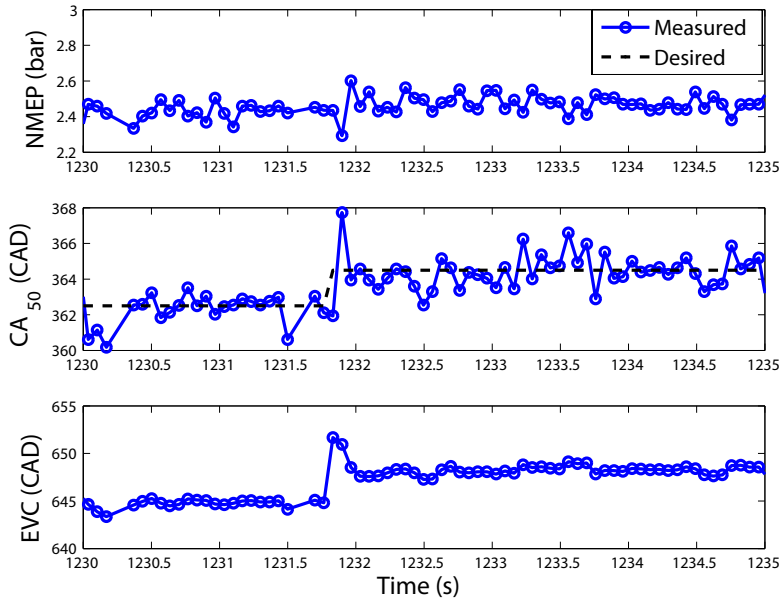

Figure 5.10: Controller response to step change on cylinder 4

loop modes at the same steady-state operating point. The two outputs and the EVC control input are shown for one of the cylinders. A marked decrease in the level of cyclic variability is seen at this late phasing point with the closed loop controller in action (shown by the regions where the EVC varies every cycle). This behavior is observed on all the other cylinders as well. This indicates that there is a systematic nature to the variation at such points which is captured by the physical model and hence corrected by the controller. Recent work done by Liao et al [61] and Jungkunz et al [62] shows that this is so - when linearized around such a late phasing operating point, the control model shows a distinct negative eigenvalue, which clearly points to the kind of oscillatory behavior seen on the engine.

5.4 Conclusion

The model revisions described in Chapter 4 result in a framework that enables direct control of work output and combustion that is robust to modeling and calibration

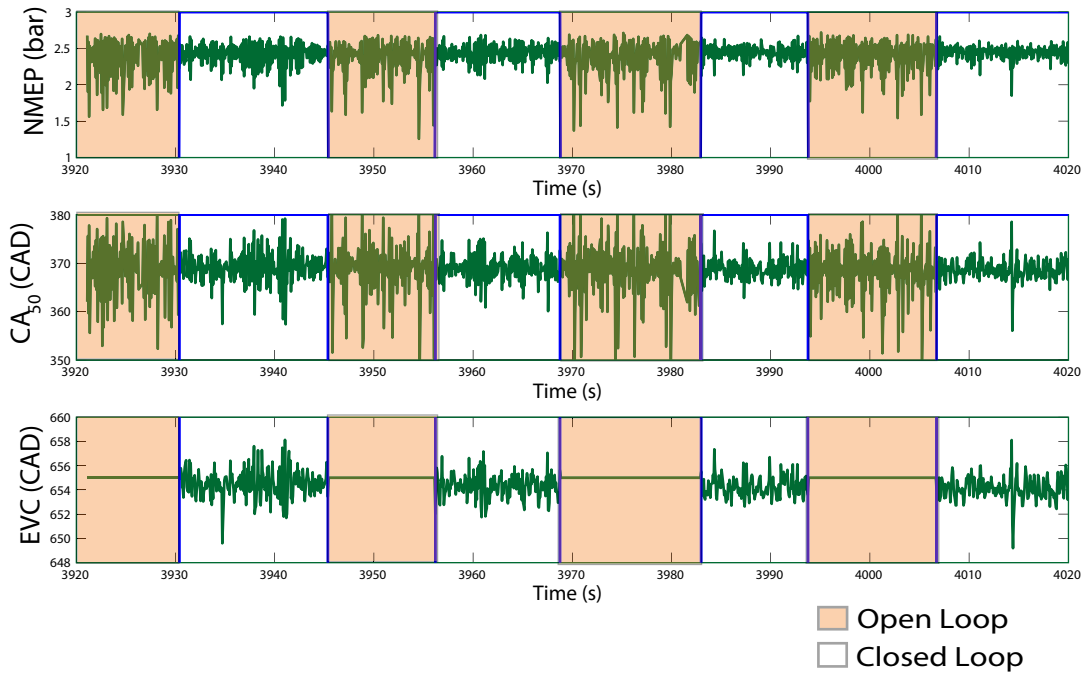

Figure 5.11: Effect of controller on cyclic variability of combustion

errors and is easily portable across engines, as evidenced by the results presented in this chapter. The recognition of the separability between the two control outputs in terms of the effects of the control inputs provides an opportunity for using a simple control structure. The fuel injection quantity is used to control the work output, while a closed-loop tracking controller based on the model is used to control the phasing of combustion through the valve timings. This control structure is seen to be useful in tracking a desired output trajectory in simulation, and on both single and multi-cylinder HCCI engines. It also balances out imbalances between different cylinders on the multi-cylinder engine, enabling smoother operation. In addition the controller is seen to reduce the cycle to cycle variability of combustion at certain points that are otherwise very unstable in open-loop. This could potentially be important in widening the operating regime of HCCI.

The results demonstrating the effectiveness of a simple linear controller on both engines provide three key insights. First, a description of HCCI in terms of mixture

temperature and reactant concentrations captures the underlying dynamics of the process, and the four state model presented earlier represents a simple and effective way of doing this. Second, though these dynamics are highly nonlinear, with appropriate state and input definitions, they can be linearized about a nominal operating point without losing their basic character. Thirdly, the use of a physical model as a basis for controller development is seen to be extremely valuable, as it enables an easy porting of the controller from one testbed to another.

Having established the modeling and control framework as an effective approach to HCCI control, the next chapter focuses on expanding this framework to include another control input - fuel injection timing. A varying injection timing can be a powerful, and relatively inexpensive, way of influencing the phasing of combustion, and so including it in the modeling framework is extremely valuable.

Chapter 6

Modeling Recompression Reactions

The previous chapters presented a framework for modeling and controlling HCCI that was seen to be very useful in modulating the work output and phasing of combustion. This chapter expands that framework to include the effect of fuel injection during recompression on the main combustion. The motivation for considering fuel injection during recompression as a possible input is twofold. First, though the results presented earlier demonstrate that variable valve actuation and fuel injection quantity are sufficient to achieve a desired $NMEP$ and CA_{50}, the control approach used requires step changes in valve timings on a cycle-by-cycle basis. This is achievable on fully flexible valve actuation systems - but these suffer from significant cost and packaging issues when implemented on vehicles on the road. Cam phasers represent a viable control knob available on several production engines, but do not have the bandwidth to achieve cycle-by-cycle control. Therefore there is a need for another fast cycle-by-cycle control input - and control of fuel injection timing during recompression has the potential for being such a control knob. This is so particularly on an HCCI engine with exhaust trapping, where the exhaust valve is closed early in the exhaust stroke to trap and recompress a portion of the hot combustion prodcuts. Fuel injected into the moderately high pressure-temperature environment created in the engine cylinder during recompression can undergo physical/chemical transformations that affect the combustion on the subsequent engine cycle [38].

In addition to this, emissions and stability have both been shown to improve near

the low-load limit by optimizing the timing of fuel injection [63, 37]. Therefore understanding the behavior of fuel injection during recompression is potentially useful in controlling HCCI combustion at low loads. This is particularly important as there can be significant cyclic variation in combustion, as well as cylinder-to-cylinder variation at low loads [64], which could be abated with cylinder-individual control of fuel injection timing.

This chapter aims to study and model the effect of fuel injection during recompression on HCCI combustion within the framework of the control model already developed. As the effects of fuel injection can be complex, the model focuses on combustion around a set of operating conditions. A split injection strategy is used, with the injection timing of a small quantity of pilot fuel (1mg) used to control combustion phasing, which is modeled with a global Arrhenius reaction rate equation as presented earlier (Eq. (2.43)). Combustion can be modeled to begin when the integral of this global reaction rate crosses a threshold value, designated as the Arrhenius threshold. The effect of the pilot injection on combustion is captured as a change in this threshold. It is seen that the relationship between injection timing and combustion phasing can be separated into a linear, analytical component and a nonlinear, empirical component. The assumptions behind this simple model are validated by experimental data.

6.1 Modeling the effect of fuel injection timing

HCCI achieved with exhaust recompression involves closing the exhaust valve early, well before the piston reaches top-dead-center (TDC), thereby trapping a portion of the hot products of combustion within the engine cylinder. This mixture gets compressed and expanded during recompression. This can be seen in Fig. 6.1 which shows a typical in-cylinder pressure trace during this process.

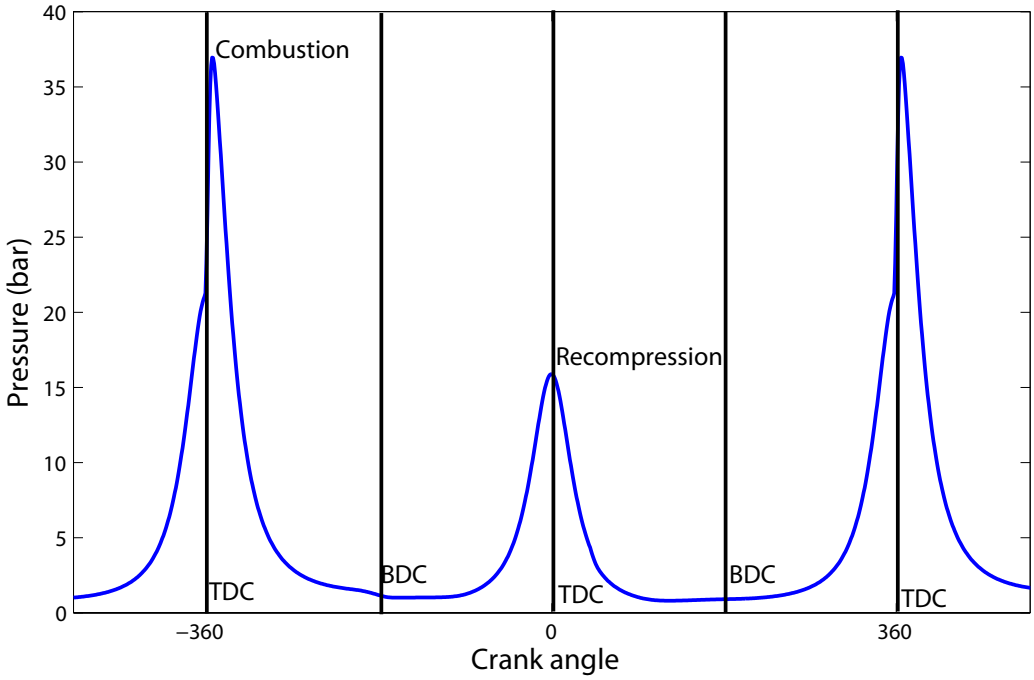

Figure 6.1: HCCI with exhaust recompression - in-cylinder pressure

Any fuel injected into the moderately high pressure and temperature environment that exists during recompression can undergo reaction and thereby affect the characteristics of the main combustion event. The following section presents a brief summary of some of the processes the fuel can go through, so as to facilitate the development of a simple model and control strategy.

6.2 Physical effects of early injection

The effects of fuel injection during recompression can be quite complex and varied. Fuel injected early in the recompression stroke vaporizes and cools the mixture. It can also undergo chemical reaction, especially in the presence of oxygen left over from the main combustion. There are four possible transformations the fuel can go through in the moderately high temperature/pressure conditions that exist in the engine cylinder during recompression. First, the fuel vaporizes, removing energy from the system.

Fuel molecules can then break down into smaller carbon chain molecules (pyrolysis). If there is sufficient oxygen, these smaller chain molecules can also undergo reforming to produce CO and H_2. Finally, in the presence of sufficient oxygen, there can be an exothermic reaction with the formation of end products.

Depending on the extent of reaction, there can be highly varied consequences on the thermal and composition state of the in-cylinder mixture. Fuel vaporization and the breakdown of long-chain hydrocarbon molecules into smaller chains are endothermic processes - therefore if these processes dominate, the overall mixture temperature goes down, which can delay combustion phasing. However, the smaller chain molecules also have a shorter ignition delay during the main combustion. This then has the opposite effect on phasing. If the recompression reaction proceeds to reforming or full reaction, the formation of end products such as CO, H_2, CO_2 and H_2O is exothermic, and so the net effect can be an increase in temperature, which would advance the combustion phasing.

Due to the complex kinetics of the reactions involved, and their sensitivity to the in-cylinder thermal and composition state, different effects are seen to dominate at different operating points. Standing et al. [37] noted that early fuel injection (around exhaust valve closure, EVC) could result in exothermic reactions during negative valve overlap, which were thought to play an important role in affecting the low-load limit of operation. Koopmans et al. [36] mentioned exothermic reaction with early injection, but stressed the generation of intermediate species via reforming reactions. Song and Edwards [38], through tests over a wide operating range, showed the dominance of both fuel breakdown and fuel reforming at different operating conditions.

In summary, the mechanisms by which early fuel injection affects HCCI operation are:

1. charge cooling due to vaporization of the fuel without significant chemical effects
2. fuel breakdown (pyrolysis) into smaller C-chain molecules, lowering the temperature but without significant end-product formation
3. fuel reforming to form partially oxidized products, with little overall thermal changes

4. exothermic reaction, causing an increase in temperature and formation of fully oxidized products.

6.3 Choosing an effective control knob

6.3.1 Single fuel injection

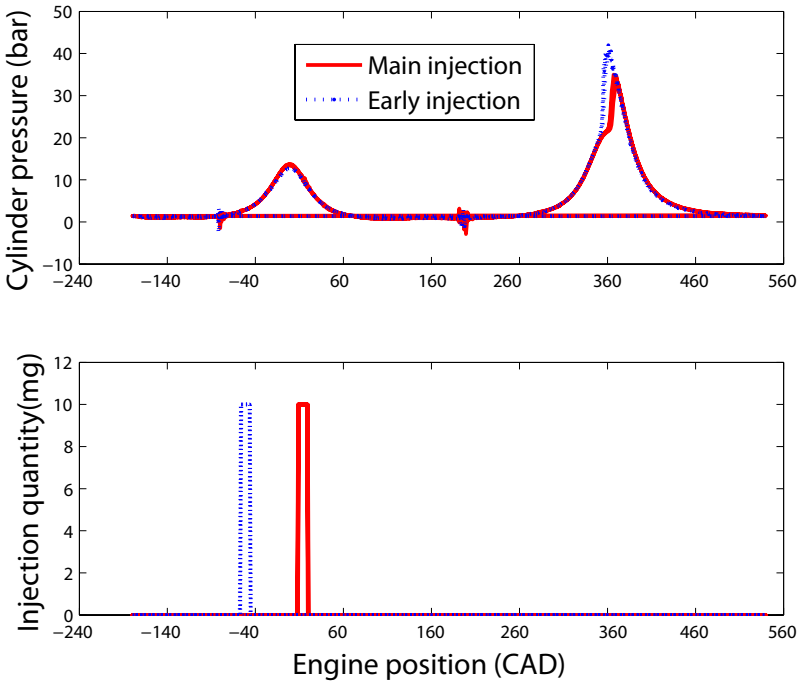

Figure 6.2: Comparison of in-cylinder pressure between main and early injection of fuel (5 engine cycles each)

The operating region chosen for control was a moderately lean condition where, as shown in [38], the fuel pyrolysis effect tends to dominate. Figure 6.2 shows the in-cylinder pressure trace and injection timings for two cases with constant fueling amount - one where all the fuel is injected at the end of recompression (called main injection), and one where all the fuel is injected early in the recompression stroke

(called early injection). All other inputs (such as valve timings) are kept constant. Results shown are from tests run on the multi-cylinded HCCI testbed (plots are shown only for one cylinder). Five engine cycles are plotted for each case.

As seen, the early injection case has a significantly advanced phasing of main combustion as compared to the main injection case, which causes a higher peak pressure. However, the peak pressure during recompression is lower for the early injection case, which indicates that endothermic processes like charge-cooling and fuel-breakdown effects likely dominate.

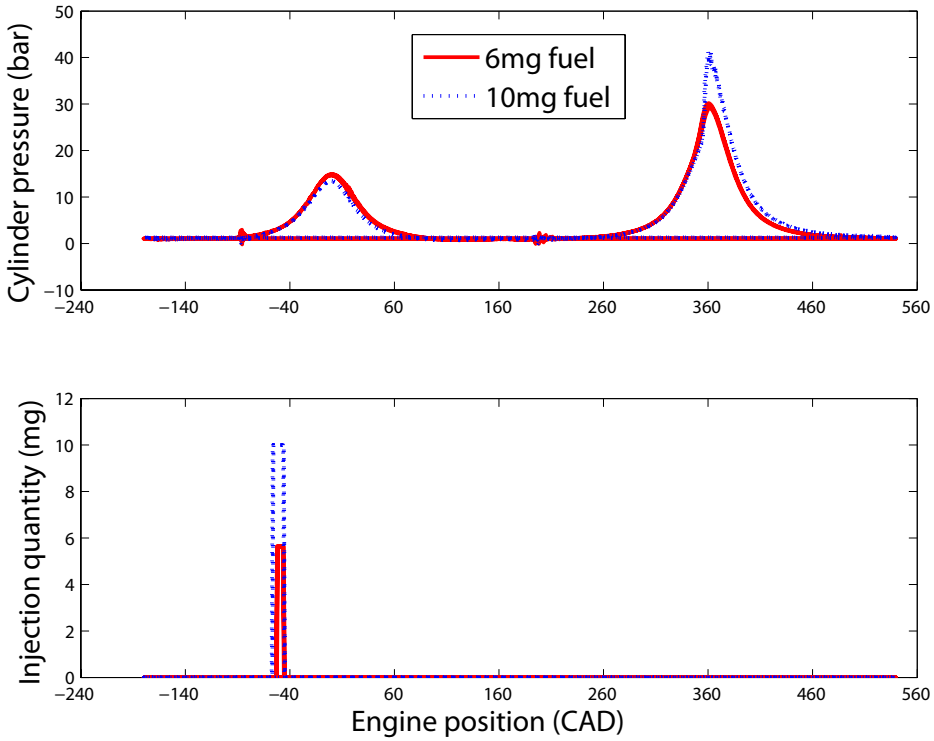

Figure 6.3: Comparison of in-cylinder pressure between 6mg and 10mg early injected fuel (5 engine cycles each)

This is further confirmed by the results shown in Fig. 6.3, where two cases are compared, both with early fuel injection, but with different quantities of fuel (6mg vs 10mg). The 10mg case has a much higher peak pressure (and expansion polytrope)

due to more energy content, but has a lower (and earlier) recompression peak, which again indicates greater endothermicity than the 6mg case.

6.3.2 Split injection

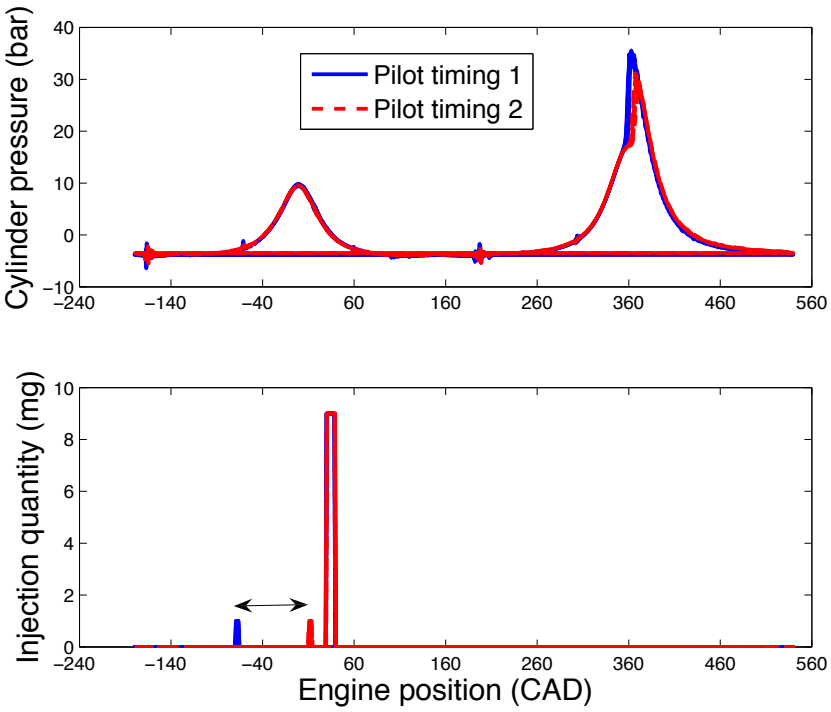

Figure 6.4: Comparison of in-cylinder pressure with different pilot injection timings (5 engine cycles each)

Even a small quantity of fuel injected during the recompression stroke can have a significant effect on the phasing of combustion. Figure 6.4 shows the effect of varying the timing of a 1mg pilot injection on the in-cylinder pressure, while most of the fuel (9mg) is injected after recompression at a fixed timing (60 CAD). This strategy is referred to as a split injection strategy. As seen in Fig. 6.5, a sweep of the pilot injection timing between -50 and 35 CAD commands a combustion phasing range of about 7 CAD, which represents most of the desirable phasing range for HCCI. This

testifies to the power of pilot injection as a control input.

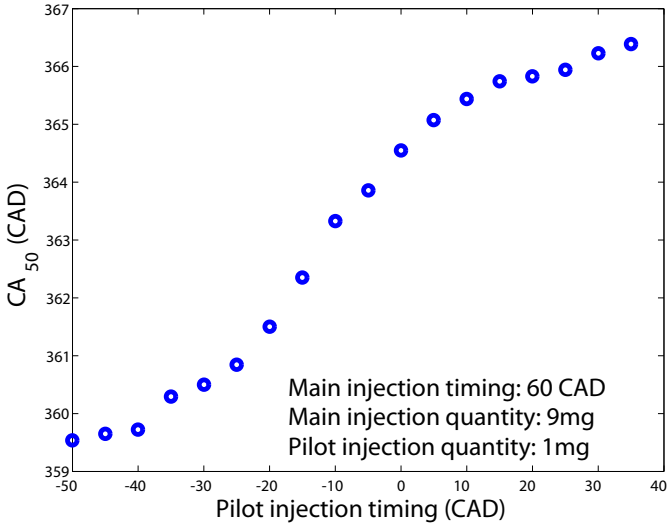

Figure 6.5: Variation of combustion phasing (CA_{50}) with pilot injection timing

The shape of this curve is characteristic of the physical processes that govern recompression reactions. As the injection timing gets later, the conditions in the engine cylinder during injection become more like the conditions during a simple main injection, and the residence time of the pilot fuel is very small. Therefore the effect on combustion phasing is minimal at very late pilot injections. At the other extreme, as the fuel is injected very early in the recompression stroke, the marginal effect on phasing is again small because beyond a point there is little to be gained by allowing the fuel a longer residence time. Therefore the curve flattens out on both ends, and the pilot injection has maximum control authority in the mid-region.

Based on the above results, a split injection strategy was chosen as an effective control knob for HCCI. A physical model for the effect of this injection was then developed and incorporated into the existing control model. It should be noted here that the 1mg pilot injection puts the equivalence ratio during recompression in a range where Song et al [38] saw exothermic reactions dominate. However there is no evidence of this seen in the pressure traces shown in Fig. 6.4.

6.4 Incorporation into existing model structure

The existing control model is a nonlinear dynamic model with four states as shown in Eq. (4.18).

$$\begin{aligned} x_{k+1} &= F(x_k, u_k) \\ y_k &= G(x_k) \end{aligned} \tag{6.1}$$

The states are given by

1. Concentration of oxygen at a fixed location after IVC (θ_s), $[O_2]_{s,k}$
2. Temperature of mixture at θ_s, $T_{s,k}$
3. Concentration of fuel at θ_s, $[f]_{s,k}$
4. Cylinder volume at intake valve closure, $V_{IVC_s,k}$

The states are defined at a fixed crank angle location after intake valve closure - this represents a point where both valves are closed, and all the reactants are present in the cylinder, ready for combustion. Every engine cycle (indexed by k), therefore, is assumed to begin at this fixed crank angle location.

The main outputs of this model are the phasing of combustion (measured in terms of CA_{50}) and the net work output (measured in terms of the net mean effective pressure, $NMEP$). The outputs are controlled using three inputs:

1. *Total moles of fuel injected* in the current cycle, $n_{f,k}$
2. *Cylinder volume at intake valve closure*, $V_{IVC,k}$ and
3. *Cylinder volume at exhaust valve closure*, $V_{EVC,k}$

This model assumes that the fuel is all injected at the end of the recompression stroke (during induction) and so does not consider the effect of a split injection strategy.

Combustion phasing is modeled with a global Arrhenius reaction rate equation. Integrating this global Arrhenius rate equation from the point of state definition to

the point of combustion gives an expression of the form shown in Eq. (4.8)

$$\int RRdt = \int_{\theta_s}^{\theta_{th,k}} \frac{A_{th} e^{\left(\frac{E_a}{R_u T}\right)} [C_7H_{13}]^a [O_2]^b}{\omega} d\theta \tag{6.2}$$

where $\theta_{th,k}$ is the crank angle location at start of combustion.

When the integral in Eq. (6.2) crosses a threshold, K_{th}, combustion is modeled to have begun. For a particular fuel, the values of A_{th}, E_a and K_{th} are fixed.

The integral can be condensed into a map (Eq. (4.9)) that gives the phasing of combustion as a function of the reactant concentrations and temperature at the point of state definition.

$$\theta_{th,k} = F_1([O_2]_{s,k}, T_{s,k}, [f]_{s,k}) \tag{6.3}$$

CA_{50} then is related directly to $\theta_{th,k}$ as the duration of combustion is assumed to be an affine function of the phasing of combustion (Eq. (4.10)).

When fuel is injected early in the recompression stroke, however, it undergoes reactions that lead to the advancing of phasing during the main combustion. Though the chemical changes occuring are fairly complex and depend on factors such as the equivalence ratio during recompression, a simple way of modeling the net effect within the existing model structure would be to lump all these changes into the Arrhenius threshold value, K_{th}. The rationale behind this is that the recompression reactions can be assumed to have lowered the overall threshold for the global reaction.

The relationship between pilot injection timing (or alternately, pilot injection fuel residence time - the amount of time the pilot fuel has to react during recompression) and combustion phasing can then be broken down into two separate relationships:

1. A relationship between the combustion threshold and the phasing of combustion (CA_{50})

2. A relationship between fuel residence time (t_{res}) and the combustion threshold

6.4.1 The relationship between Arrhenius threshold and CA_{50}

The relationship between CA_{50} and the Arrhenius threshold, K_{th} already exists within the existing model structure. However, K_{th} is treated as a constant in the model. With pilot injection, this now becomes variable on every cycle, based on the commanded injection timing.

$$\theta_{th,k} = F_1([O_2]_{s,k}, T_{s,k}, [f]_{s,k}, K_{th,k}) \tag{6.4}$$

Therefore, an additional state, K_{th} is needed to capture the effect of pilot injection timing on the thermochemical state of the in-cylinder mixture before combustion. The full state, input and output vectors are now given by

$$x_k = \begin{bmatrix} [O_2]_s \\ T_s \\ [f]_s \\ V_{IVC_s} \\ K_{th} \end{bmatrix}_k, u_k = \begin{bmatrix} n_f \\ V_{EVC} \\ V_{IVC} \\ u_{th} \end{bmatrix}_k, y_k = CA_{50,k} \tag{6.5}$$

As the oxygen and temperature states on cycle $k+1$ are a function of the combustion phasing on cycle k, Eq. (6.4) implies that $[O_2]_{s,k+1}$ and $T_{s,k+1}$ also depend on $K_{th,k}$. The Arrhenius threshold state, however, is only affected by the pilot injection timing input on the previous cycle. This input can be abstracted to a threshold input, u_{th}, based on the relationship between the Arrhenius threshold and the pilot injection timing (described in the next section). Therefore $K_{th,k+1} = u_{th,k}$.

Incorporating this into the model, and then linearizing about an operating point gives a new set of linear system matrices. The conceptual structure is shown in Eq. (6.6), where X represents a non-zero value (determined by the particular operating

condition):

$$\begin{bmatrix} [O_2]_s \\ T_s \\ [f]_s \\ V_{IVC_s} \\ K_{th} \end{bmatrix}_{k+1} = \begin{bmatrix} X & X & X & X & X \\ X & X & X & X & X \\ 0 & 0 & 0 & 0 & 0 \\ 0 & 0 & 0 & 0 & 0 \\ 0 & 0 & 0 & 0 & 0 \end{bmatrix} \begin{bmatrix} [O_2]_s \\ T_s \\ [f]_s \\ V_{IVC_s} \\ K_{th} \end{bmatrix}_k + \begin{bmatrix} X & X & X & 0 \\ X & X & X & 0 \\ 1 & 0 & 0 & 0 \\ 0 & 0 & 1 & 0 \\ 0 & 0 & 0 & 1 \end{bmatrix} \begin{bmatrix} n_f \\ V_{EVC} \\ V_{IVC} \\ u_{th} \end{bmatrix}_k$$

$$CA_{50,k} = \begin{bmatrix} X & X & X & 0 & X \end{bmatrix} \begin{bmatrix} [O_2]_s \\ T_s \\ [f]_s \\ V_{IVC_s} \\ K_{th} \end{bmatrix}_k \tag{6.6}$$

As seen, the last three states have no dynamics of their own, but are purely dependent on the inputs on the previous cycle (respectively, n_f, V_{IVC} and u_{th}, shown by the 1s in the last three rows of the B matrix). The oxygen and temperature states, however, depend on all the states on the previous cycle, as well as the first three inputs. It is assumed here that they do not depend on the final input, u_{th} - in other words, that the injection of a small quantity of pilot fuel during recompression has a much more significant effect on the combustion threshold than on the oxygen concentration or temperature of the final reactant mixture after IVC. Therefore, though there is possibly some temperature change brought about by the pilot injection, the main effect of this is modeled through the lowering in the Arrhenius threshold.

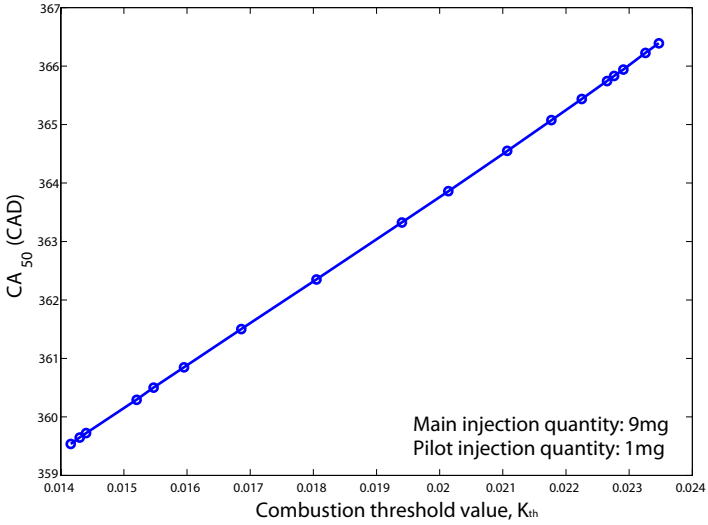

Figure 6.6: Relationship between combustion threshold and combustion phasing

Figure 6.6 shows the relationship between the analytically calculated combustion threshold and the mean measured combustion phasing in steady state on one cylinder of the multi-cylinder HCCI engine testbed. The data is obtained from steady state tests with various pilot injection timings on the multi-cylinder HCCI engine testbed. Results from one engine cylinder are presented (all other cylinders exhibit similar behavior). As seen, the relationship between K_{th} and CA_{50} is highly linear over the entire range of injection timings considered. The slope of this curve, then, represents the element of the C-matrix that relates $CA_{50,k}$ to $K_{th,k}$. This validates the assumption made in linearizing Eq. (6.4) as part of the linear state-space model.

This linear model can now be used to develop a linear controller, that would command a specific set of valve timings and combustion threshold, u_{th} for a desired CA_{50}. The next step is to be able to determine the relationship between this threshold, and the physical input, the pilot fuel injection timing.

6.4.2 The relationship between fuel residence time and combustion threshold

Pilot injection timing, or pilot fuel residence time can be abstracted into the combustion threshold using steady-state engine data, and the Arrhenius map given in Eq. (6.4). The model is first parameterized at a particular operating condition with all the fuel injected during the main injection. Sweeping out a range of pilot injection timings, and inverting the Arrhenius map for each measured value of CA_{50} then gives the corresponding u_{th} value for each value of injection timing/fuel residence time. This gives the functional relationship between the fuel residence time and the threshold input:

$$u_{th,k} = F_2(t_{res,fuel}) \tag{6.7}$$

The residence time here is calculated as the time between the end of the pilot injection, and 420 CAD (which is the end-of-injection timing for the main injection). Hence a main injection would have a residence time of zero for recompression reactions, while an earlier injection would have more time. It is also assumed as before, that the threshold input does not affect the oxygen and temperature states. This allows an inversion of Eq. (6.4) at fixed $[O_2]_s$ and T_s.

The steady state relationship in Eq. (6.7) is used to relate the control input from the linear model, u_{th} on every engine cycle to the physical input, $t_{res,fuel}$ or injection timing.

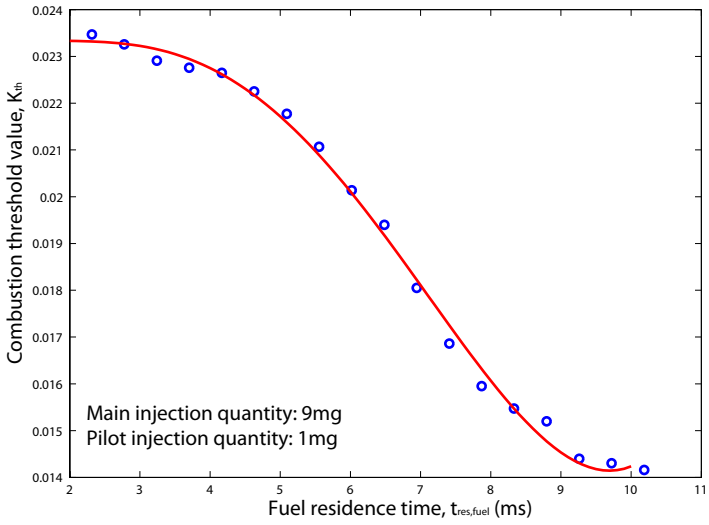

Figure 6.7: Relationship between combustion threshold and fuel residence time

Figure 6.7 shows the relationship between the threshold and the fuel residence time input calculated from experimental steady-state data as described above. This function can be approximated by a polynomial curve as shown.

6.5 Conclusion

The overall model relating pilot injection timing to the phasing of combustion is shown below conceptually.

$$t_{res,fuel} \rightarrow u_{th} \rightarrow CA_{50} \tag{6.8}$$

The model therefore has two distinct parts.

1. $CA_{50,k} = F_1([O_2]_{s,k}, T_{s,k}, [f]_{s,k}, K_{th,k})$, the relationship between the combustion threshold and the phasing of combustion. This relationship is part of a linear, five state model.

2. $u_{th,k} = F_2(t_{res,fuel})$, the relationship between the combustion threshold and

the fuel residence time. This relationship is obtained through steady state experiments, and is described by a nonlinear function.

This model integrates seamlessly with the control model structure developed earlier. The data presented suggests that the nonlinear relationship between fuel injection timing and combustion phasing is an input nonlinearity that can be separated from the state description. A simple linear controller can be used to generate a desired combustion threshold, which can then be related to a commanded fuel residence time through the nonlinear relation F_2. This separability also means that differing behavior in other operating regimes could all potentially be incorporated into the function F_2, while leaving the linear model intact.

The following chapter will explore the development of different control strategies based on this model and demonstrate the power of this split injection strategy as a control knob.

Chapter 7

Control of HCCI with Split Fuel Injection

The focus of this chapter is the application of the expanded model presented in Chapter 6 to the development of controllers for HCCI that use a split fuel injection strategy. As described earlier, fuel injected early in the recompression stroke of an HCCI engine can have a significant effect on combustion. Two different control strategies based on split fuel injection are presented. The timing of this injection is seen to be a powerful control knob within a limited range. This can be seen from the experimental data presented in Fig. 6.5 - pilot injection has maximum control authority in the middle of the region depicted, with its influence on phasing saturating near the extremes. Therefore a controller that uses only the pilot injection timing as a control input is effective in controlling work and combustion phasing in a limited range. By contrast, the exhaust valve timing has a strong influence on combustion phasing over a wide range, but may be impractical to vary on a cycle-by-cycle basis, as most fully flexible valve actuation systems available today are extremely expensive and difficult to package within a vehicle. Therefore a second controller, based on the mid-ranging principle is implemented. Recognizing the practical constraints on valve motion, this controller uses injection timing alone as a fast cycle-by-cycle control input to control the combustion phasing. The exhaust valve timing is then used to gradually bring

the injection timing back to the middle of its range where it has the maximum control authority. This ensures fast, cycle-by-cycle control while at the same respecting constraints on the motion of the valves and the range of the injection timing. The controller enables tracking of desired output trajectories as well as steady operation at low-load conditions. This strategy therefore represents an effective and practical approach to control of HCCI that can be extended to current production engines with existing cam phaser technology.

7.1 Controller development

The overall control framework is the same as that presented in Chapter 5 - as $NMEP$ is almost wholly a function of the total fuel quantity injected, a simple feedforward-integral controller uses fuel quantity to control work output. This controller is used to vary the quantity of fuel injected during the main injection (at a fixed timing of 420 CAD) while keeping the pilot injection quantity fixed at 1mg (but at a varying timing controlled by a model-based feedback controller described below).

To control the phasing with injection timing, the fuel and injection timing inputs need to be separated out in the linear model as was done in Eq. (5.1):

$$x_{k+1} = Ax_k + B_1 u_{1k} + B_2 u_{2k} \tag{7.1}$$

where $u_{1k} = n_{f,k}$, which is commanded by the $NMEP$-fuel map controller, and $u_{2k} = \begin{bmatrix} V_{IVC,k} & V_{EVC,k} & u_{th,k} \end{bmatrix}^T$, which is used to control the combustion phasing. Similar to the formulation in Chapter 5, a reference input tracking controller is designed:

$$u_{2k} = -K_x x_k + (N_u + K_x N_x) r_k \tag{7.2}$$

where r is the reference input (representing the desired output trajectory), N_u and N_x are feedforward matrices and K_x is the controller gain matrix.

Two different control structures are presented here. For the first controller, control gains are selected such that only the Arrhenius threshold input, u_{th} is used, while the

valves are kept fixed. This shows the potential of injection timing as an independent control knob.

However, the range of this input is limited at fixed valve timing due to the saturation seen in Fig. 6.5 - therefore a second control strategy is presented based on the mid-ranging control principle. As stated by Allison et al [65], mid-ranging refers to a class of control problems where there are more manipulated inputs than outputs to be controlled (most commonly, two inputs and one output). Often the inputs differ in their dynamic effect on the output, and the faster input has a more limited range than the slow one. The mid-ranging idea is to have the fast input u_1 controlling the process output, and to use the slower input u_2 to gradually mid-range u_1 to its desired value $u_{1,ref}$. A conceptual block diagram representing a mid-ranging controller is shown in Fig. 7.1.

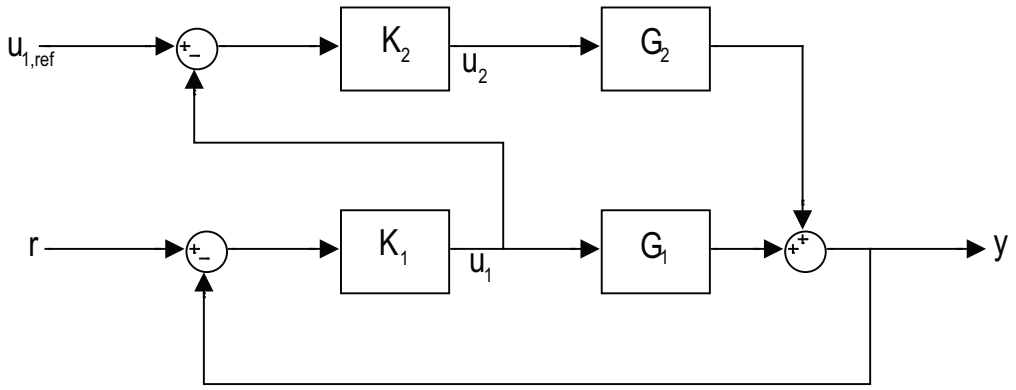

Figure 7.1: Mid-ranging controller - block diagram

For the scenario of HCCI control, the timing of pilot injection is considered the fast input u_1, while the exhaust valve closure timing (EVC) is the slow input u_2. The intake valve is kept fixed in all the tests described here, and is not used as an active input. The controller K_1 is the same reference input tracking controller described in Eq. (7.2). The controller K_2 that controls EVC to mid-range the injection timing is a pure integral controller. The value of the integral gain is determined by the desired maximum slew rate of the valves, and can be set depending on the limitations of the physical system. An anti-windup scheme, as described by Haugwitz et al [66], is added to maintain good performance in the event of saturation.

The controller is combined with a Kalman filter to estimate the oxygen concentration and temperature states, which are not measurable on an engine testbed. The Kalman filter uses the measurement of CA_{50} to estimate the states. This controller-observer system can then be used to track a desired $NMEP - CA_{50}$ trajectory.

7.2 Simulation results

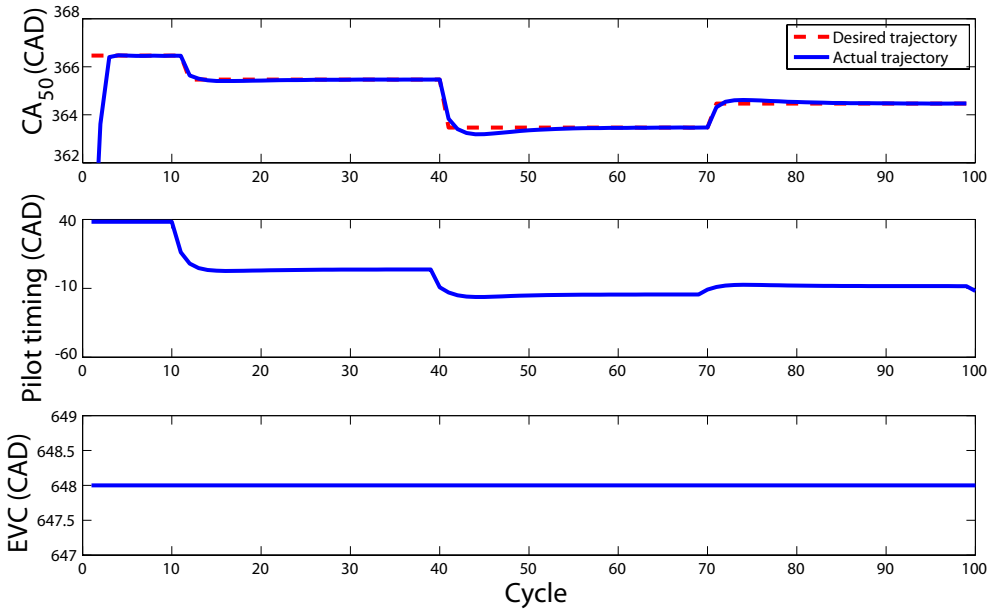

Figure 7.2: Phasing controller without mid-ranging action - simulation results

The two controllers are tested on the continuous time simulation model. Figure 7.2 shows results for a series of step changes in desired combustion phasing with a fixed total fuel quantity using the injection timing controller. The system initially reaches steady state in open-loop starting at a set of initial conditions, and the controller is switched on after 10 engine cycles. As seen, the controller tracks the desired trajectory accurately by changing the pilot injection timing alone, while EVC is kept fixed.

When the mid-ranging control scheme is used, however, to effect the same series of step changes, the EVC value is changed gradually so as to enable the pilot injection timing to track a reference value. This can be seen in Fig. 7.3. The CA_{50} tracking

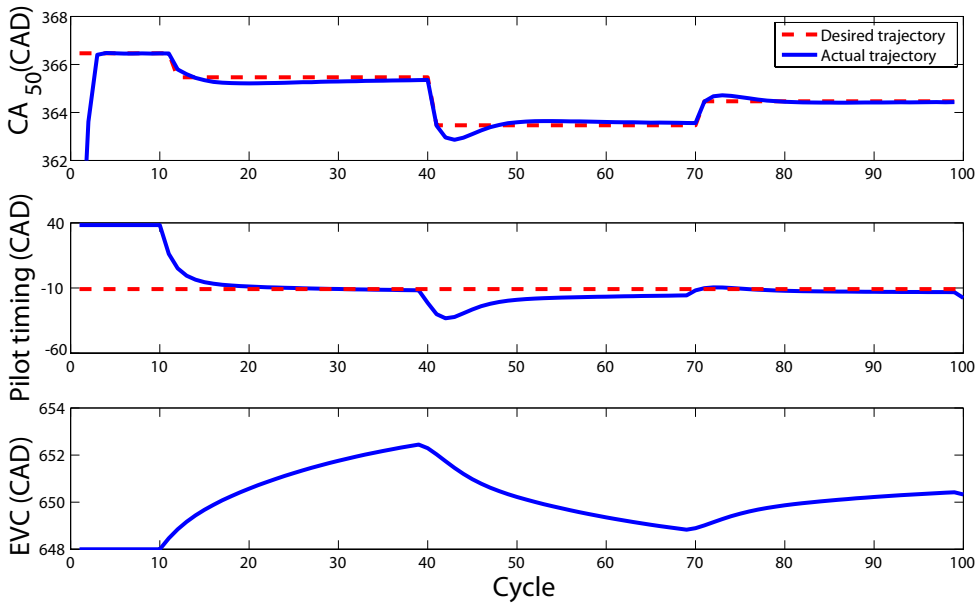

Figure 7.3: Phasing controller with mid-ranging action - simulation results

remains practically unchanged, and the phasing reaches a new steady-state within a few cycles, due to the fast action of the injection timing. Therefore accurate tracking is maintained, while ensuring that the fast control input always stays away from saturation.

7.3 Experimental results

The multi-cylinder engine testbed is used to test the controllers. The controllers run independently on each cylinder of the four cylinder engine. The test conditions for the results presented here are given in Table 7.1.

For the injection timing controller, the exhaust valve opening and closing are kept fixed at 508 and 648 deg CAD respectively. The mid-ranging controller on the other hand varies the EVC timing, and the EVO timing is calculated assuming a fixed valve duration of 140 CAD.

Table 7.1: Test conditions

Parameter	Value	Units
Engine speed	1800	rpm
IVO	70	CAD
IVC	210	CAD
Main injection quantity	Controlled	mg
Main injection timing	60	CAD
Pilot injection quantity	1	mg
Pilot injection timing	Controlled	CAD

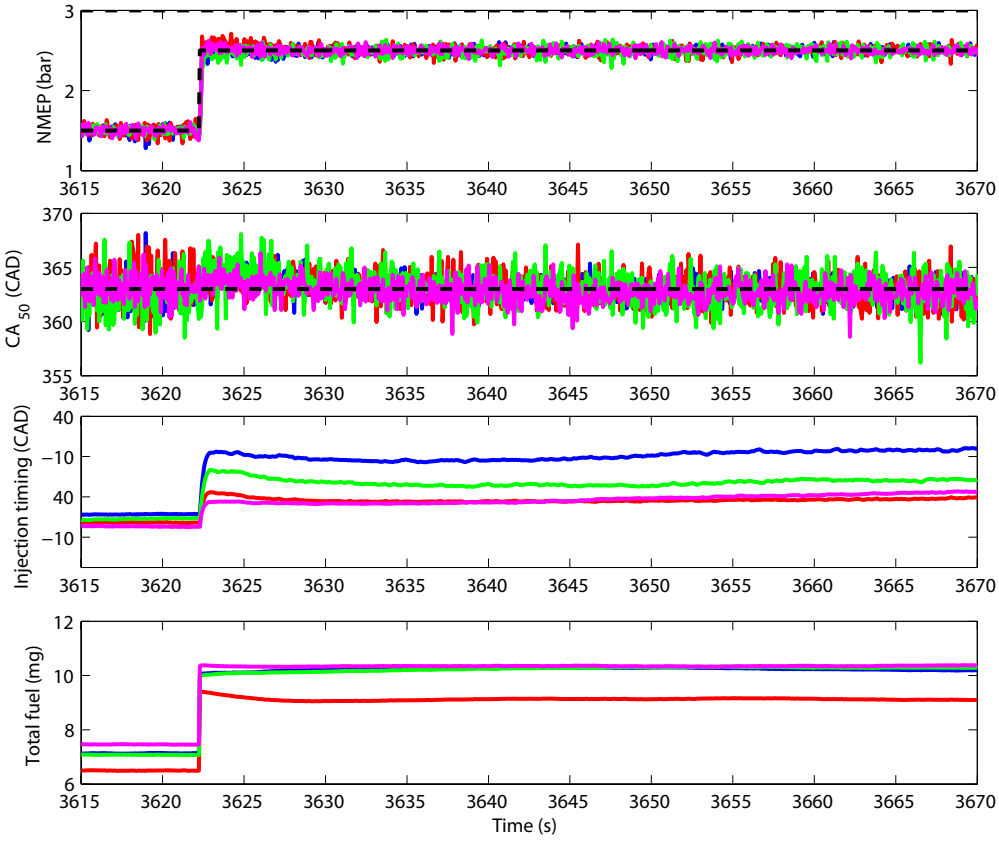

Figure 7.4: Experimental control results - feedback + feedforward + integral controller (dotted line - desired trajectory, solid line - actual trajectory)

Figure 7.4 shows a step change of 1 bar in desired $NMEP$ at constant phasing using the injection timing controller. All the cylinders maintain their timing over the step change, and track the desired work output trajectory exactly. The controller delays the pilot injection timing to compensate for the advanced phasing that a greater amount of fuel injection would cause. As seen, all the cylinders converge to the same steady-state.

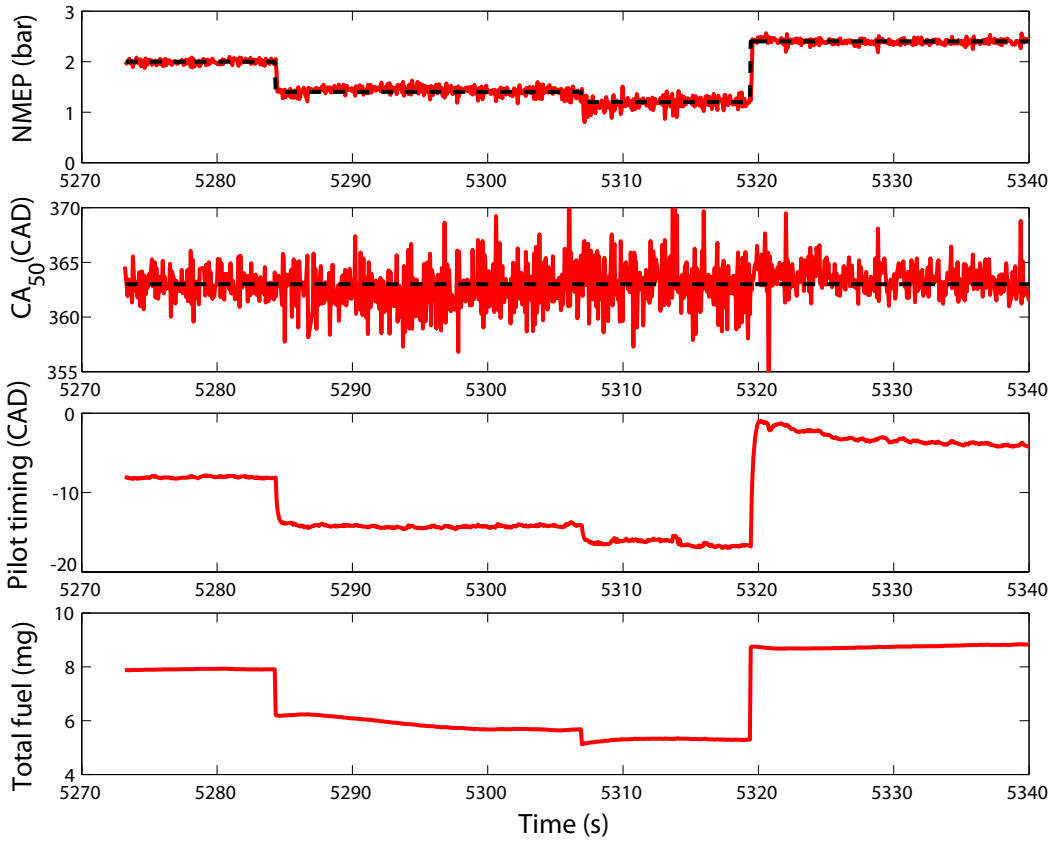

Figure 7.5: Experimental control results - controller range (dotted line - desired trajectory, solid line - actual trajectory)

This controller works effectively over a range of load conditions at this engine speed - from as low as about 1.2 bar to as high as 2.5 bar. Figure 7.5 shows the controller response to a series of step changes on one cylinder. The controller is seen to be very effective at low load conditions and could be useful in expanding the

operating range of HCCI on the low load end.

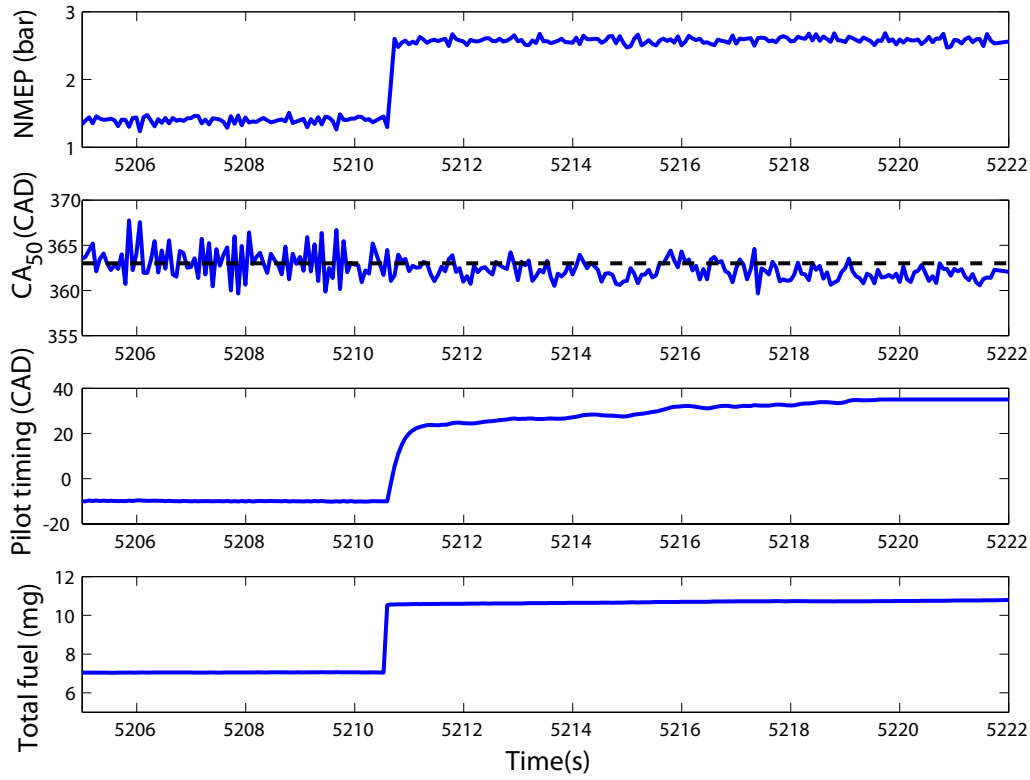

Figure 7.6: Experimental control results - controller limits (dotted line - desired trajectory, solid line - actual trajectory)

For a fixed set of valve timings, this controller reaches its limits when it commands injection timings that fall within the flat part of the curve shown in Fig. 6.5. This effect is seen in Fig. 7.6, when for the particular combination of $NMEP$ and CA_{50} commanded, the injection timing is significantly delayed by the controller. However, even this late injection timing is not sufficient to achieve that CA_{50}, and so the actual phasing trajectory deviates from the desired trajectory. Eventually the input saturates as this late injection timing has no effect on CA_{50}. Accurate tracking beyond this point would require changes in valve timings.

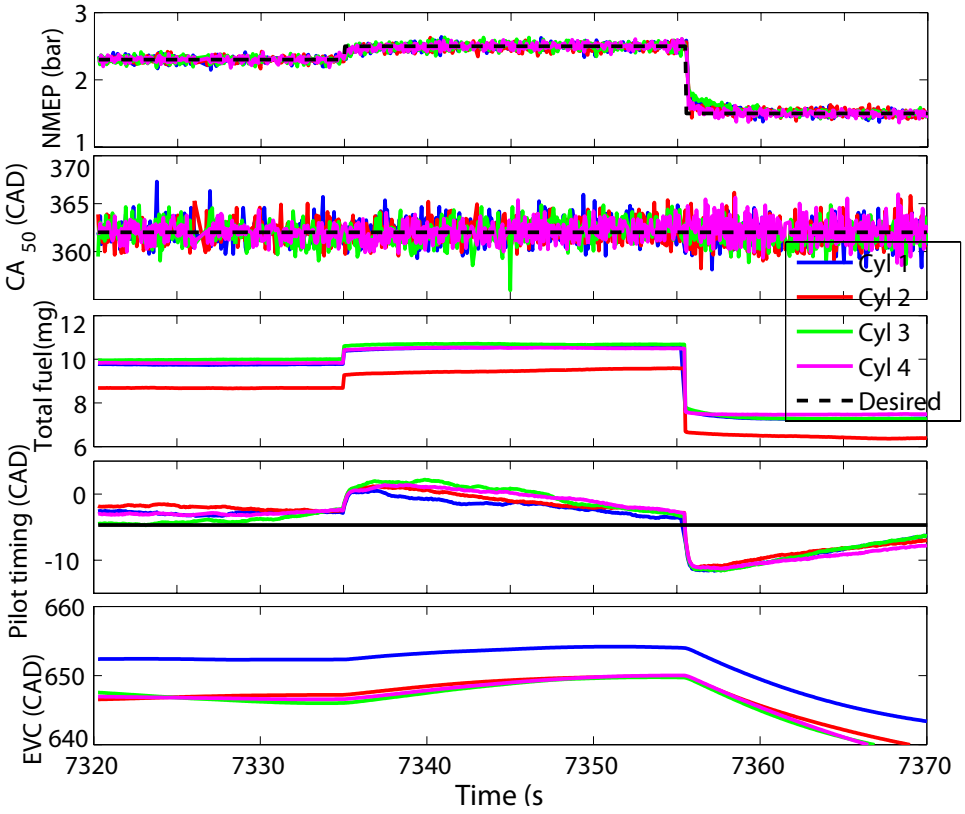

Figure 7.7: Mid-ranging control - experimental results

The mid-ranging control strategy achieves exactly this objective. Figure 7.7 shows the output and input trajectories from a test where a series of step changes in $NMEP$ are commanded at constant combustion phasing. As seen, the controller performs very well on a cycle-by-cycle basis, due to the fast action of the injection timing. The slower EVC motion eventually brings the injection timing back towards its reference value, thereby preventing the kind of saturation seen in Fig. 7.6. As the valve timings on each cylinder are controlled independently, the control action seen does not represent a true cam phaser, which would require that the valve timings on all the cylinders be the same. However the demonstration of this mid-ranging strategy here represents an important step towards the development of a controller that would work with practical cam phaser systems.

Using a pilot injection also makes the controller very effective in stabilizing HCCI

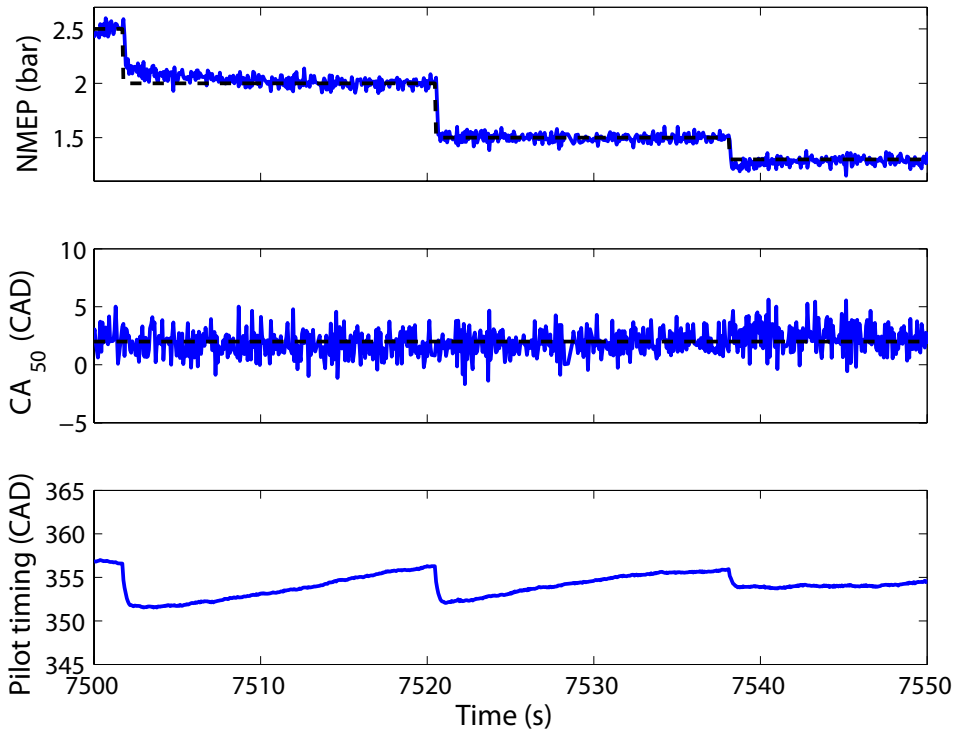

Figure 7.8: Low load operation - Cylinder 3

at low load conditions as seen in Fig. 7.8, where the controller tracks NMEP down to about 1.2bar (results shown for only one of the four cylinders). Steady operation at this low a load without the use of this actuator was not possible on this engine. This shows the ability of this control knob in expanding the operating range of HCCI on the low load end.

Figure 7.9 shows a step change in load at constant phasing for one of the four cylinders, with the plots zoomed in around the step change. As seen, the new steady-state is reached within 3-4 cycles, and there is no discernible change in the combustion phasing due to the increase in fuel quantity. This points to the high fidelity of the model used to capture the effect of varying the pilot injection timing. Again, over the space of a few cycles the EVC value is practically constant as the mid-ranging action occurs over a much longer time scale. The speed of response of the EVC input can be changed by modifying the integral gain K_2.

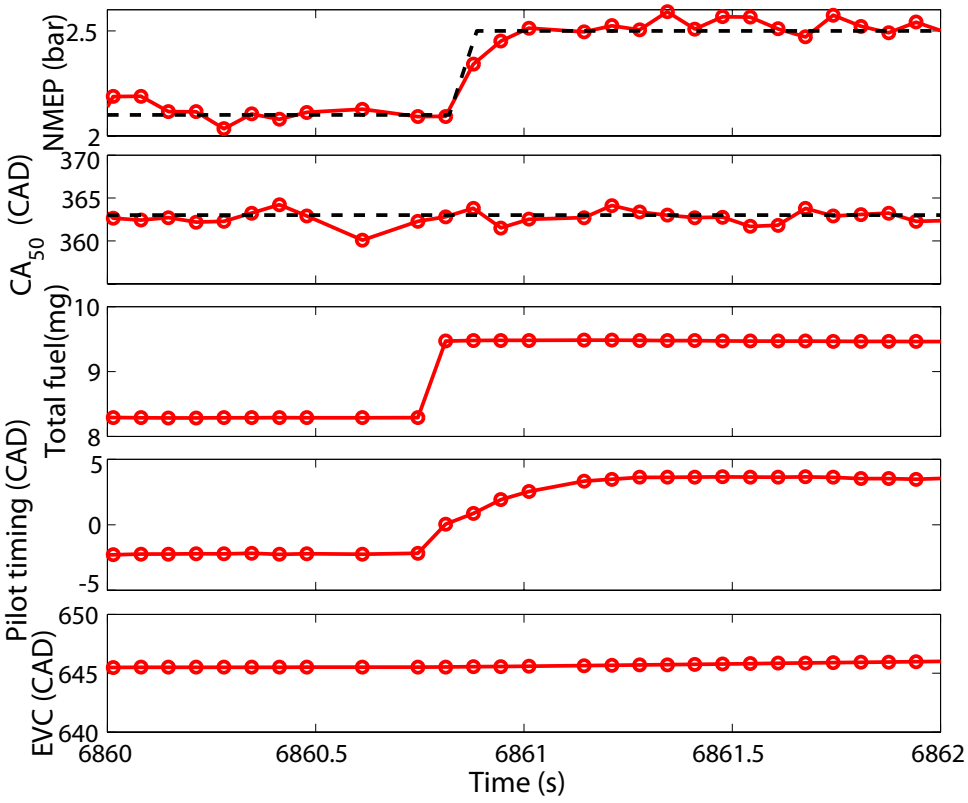

Figure 7.9: Cycle-by-cycle action of mid-ranging controller - Cylinder 2

7.4 Conclusion

As demonstrated in this chapter, the use of fuel injection as a control knob represents a practical way of controlling HCCI combustion on a cycle-by-cycle basis. The two controllers developed here on the basis of the model presented in Chapter 6 are seen to be highly effective in tracking desired load-phasing trajectories. As each engine cylinder has its own direct injector, the injection of pilot fuel can be a powerful control knob for balancing cylinder differences. Its high speed of response also implies the possibility of cycle-by-cycle control of HCCI at minimal cost. The mid-ranging framework in particular is an effective way of satisfying two key objectives - achieving cycle-by-cycle control to track fast transients, and respecting constraints on the available actuators (saturation limits on the pilot injection timing, and slew rate limits

on the valve motion). These results demonstrate the potential of mid-ranging control as a simple and viable control strategy for HCCI engines, enabling the coordination of multiple actuators with different performance characteristics to achieve tracking of the desired outputs in a wide operating range.

The two controllers presented in this chapter show the importance of having a control scheme that recognizes constraints on different actuators, and is able to operate within those limits. The mid-ranging control approach is a simple way to achieve this objective; the next chapter now builds on this and develops a more rigorous approach to controlling HCCI while respecting actuator and other constraints. This is done by framing the entire control problem within a model predictive control (MPC) structure. The MPC formulation provides a way to use the model explicitly in the control scheme. Also, the MPC framework allows specification of input, output and state constraints directly. This is an advantage over the mid-ranging framework, where output and state constraints are not considered and the rather arbitrary choice of the integral control gain provides the only way to address the constraint on valve motion.

Chapter 8

Model Predictive Control of HCCI

So far the focus of the work presented has been the development of a control model of HCCI that captures the essential dynamics of the process, and only simple linear controllers demonstrating the value of the modeling framework have been implemented. Having validated and established the efficacy of the model in controller development, this chapter now describes a much more rigorous approach to model-based control of HCCI. The linear control model is used as the basis for a model predictive control (MPC) strategy that enables explicit treatment of constraints on the system. This is particularly useful in HCCI, where each actuator has its own unique constraints - the pilot injection timing is a powerful knob within a narrow range, while the exhaust valve timing has a much wider range of influence but cannot be actuated on a cycle-by-cycle basis with production cam phaser systems. In addition, it might also be desirable to constrain certain other variables that are not directly controlled, such as the air-fuel ratio within the engine cylinder. As some of the main benefits of HCCI are related to its lean combustion strategy, it is desired to keep the air-fuel ratio away from the rich region, while also ensuring that conditions don't become so lean that combustion stability is impaired. Keeping the air-fuel ratio within certain bounds is also important for effective exhaust aftertreatment. All these different objectives can be formulated easily within the MPC framework, making it an attractive proposition for HCCI control.

Two different MPC strategies are presented in this chapter. The first controls

only the phasing of combustion within the MPC framework while the work output is controlled with the same controller used earlier, a simple feedforward-feedback scheme based on an empirical map relating fuel quantity to $NMEP$. This controller works effectively in simulation and is mostly able to constrain the air-fuel ratio within the desired bounds. However it is seen that the constraints are temporarily violated during transients where a step change in $NMEP$ is commanded. This is because the $NMEP$ controller, being outside the MPC scheme, does not recognize the air-fuel ratio constraint, and so commands step changes in fuel quantity that cannot be compensated for given the restriction on valve motion. Therefore a new controller is designed that incorporates control of $NMEP$ within the MPC framework, thereby addressing this limitation and enabling constraint satisfaction on every engine cycle while maintaining accurate output tracking. The MPC scheme is complemented by a redesigned estimator that uses two measurements - CA_{50} and the measurement from an exhaust oxygen sensor - to estimate the model states. This estimator structure is seen to be much more accurate in simulation than an estimator using only a measurement of CA_{50}.

The predictive controller incorporating $NMEP$ into the framework is seen to perform better in simulation than the first controller, and is therefore tested in experiment on the multi-cylinder engine. An explicit form of this model predictive control scheme is implemented. Results show that the controller is effective in satisfying all the control objectives - the work output and combustion phasing are tracked accurately over a wide range, actuator constraints are respected, and the air-fuel ratio is maintained within respectable bounds. This strategy therefore shows great promise as a practical application of the physical model-based control approach that has been one of the main contributions of this thesis.

8.1 Model predictive control - an introduction

The fundamental basis of model predictive control (MPC) is the generation of inputs as solutions of a real-time optimization problem. The model is used explicitly in calculating the control input, and at every time step a finite horizon optimal control

problem is solved. The solution provides an optimal input sequence over the time horizon considered, where only the first control step is implemented. This process is repeated at each time step with new measurements. Feedback therefore enters indirectly, as the new measurement is used as the initial condition in the optimization.

The MPC concept has been around for several decades. Its origins can be traced back to work done by Propoi [67] in 1963, who proposed the formulation of a receding horizon control approach that is the fundamental basis of MPC. However its widespread use was motivated by its applications in the process industry. In 1978 Richalet et al [68] described the implementation of what they called a model predictive heuristic control strategy in several industrial applications from the chemical industry and commented on its ease of implementation and robustness. Since then its popularity in the chemical process industry has increased steadily, making it one of the few advanced control techniques widely used in industrial control engineering [69]. The main reasons for its success include

1. It can handle MIMO systems easily
2. It can take into account limitations on actuators, states and outputs
3. Compared to conventional control techniques, it can allow operation closer to the constraints, which can be profitable in many applications

Traditional approaches to MPC were developed based on step response models. However Ricker [70] formulated a state space representation of MPC that permits generalization of the approach to more complex cases. Significant progress has also been made in understanding the behavior of model predictive control systems, and a lot of results have been obtained on stability, robustness and performance of MPC [71, 69]. Several reviews of the theory of MPC, different ways of formulating an MPC problem and industrial MPC technology have been published by a number of researchers [72, 73, 74].

A general formulation of MPC with a state space model representation is shown below

Minimize

$$J(k) = \sum_{i=k}^{H_p+k-1} ||y(k+i|k) - r(k+i|k)||_Q^2 + \sum_{i=k}^{H_u+k-1} ||\Delta u(k+i|k)||_R^2$$

subject to

$$\begin{aligned} x_{k+1} &= Ax_k + B_u u_k + B_v v_k \\ y_k &= Cx_k \\ \Delta u_{min} &\leq \Delta u_k \leq \Delta u_{max} \\ u_{min} &\leq u_k \leq u_{max} \\ y_{min} &\leq y_k \leq y_{max} \end{aligned} \tag{8.1}$$

The cost function $J(k)$ consists of two quadratic terms that represent the cost of output tracking errors and input effort. These costs are evaluated over the prediction horizon H_p and the control horizon H_u respectively. Q and R are weighting matrices that can be used to set the relative weights on output errors and input effort. The input sequence $u(k)$ over the control horizon is the optimization variable.

This cost function is then minimized subject to several constraints. The first two constraints specify the linear model that is assumed to represent the plant - therefore over the time horizon considered the system is assumed to evolve according to this model. x, u, v and y represent the states, inputs, known disturbances and outputs respectively. Additionally there are upper and lower limits on the rate at which the inputs can change (Δu_{min} and Δu_{max}) and absolute limits on the values of the control inputs and the outputs (u_{min}, u_{max}, y_{min} and y_{max} respectively). These inequality constraints are all elementwise vector constraints.

As might be expected, the real-time implementation of any general MPC scheme is computationally challenging, due to the necessity of solving an optimization problem at every time step. However, Bemporad et al [75, 76] have developed an explicit representation of the controller that can be derived offline. For discrete-time linear time-invariant systems with constraints on inputs and states, the authors show that

it is possible to determine explicitly a piecewise linear and continuous state feedback control law associated with MPC. This is advantageous, as the online computation is reduced to a simple linear evaluation from a complex quadratic optimization. Additionally, the stability and performance of the explicit representation remains identical to the original model predictive controller. Such an approach has also been extended to control of hybrid systems [77]. The explicit formulation of MPC has been implemented on a wide variety of applications, from the process industry [78] to spacecraft attitude control [79].

8.2 Motivation for MPC in HCCI

There are several reasons why MPC is an attractive proposition for the control of HCCI:

1. With the ability to handle MIMO systems, MPC, like other techniques such as LQR, provides an easy way to trade-off tracking errors on different outputs and the control effort applied by different inputs. This is particularly desirable in HCCI where there are higher costs to actuating some of the inputs vs. others (for example, fuel injection quantity and timing can be easily changed on a cycle-by-cycle basis with injection systems on current production vehicles, while cycle-by-cycle valve motion has a high cost associated with it). Therefore where possible, it is desirable to use fuel injection as the primary input, and move the valves only when necessary.

2. Cam phaser systems, which represent a practical way of achieving variable valve actuation on production engines, have bandwidth constraints that limit how fast they can respond. These are hard constraints - therefore a control scheme that determines the optimal set of control inputs that can best track the desired output trajectory while respecting these constraints is desirable. The MPC framework is such a control scheme, where it is possible to explicitly set constraints on the rate of change of any input to the system.

3. There are also absolute limits on the available inputs in HCCI - for example, when considering the EVC input (represented as V_{EVC}, the cylinder volume at EVC), it is impossible to achieve a cylinder volume greater than the volume at BDC, or lower than the volume at TDC. In reality, the constraints are even tighter - it is desirable to trap at least some exhaust, and so closing the exhaust valve at TDC is unacceptable. Also, as described in Chapter 6 (Fig. 6.5), the pilot injection timing input saturates near the extremes and has little effect in these regions - therefore it is necessary to keep the injection timing within the range where it is most effective. All these input constraints are easy to define within an MPC framework.

4. In addition to constraining inputs, it might also be desirable to bound certain other variables that are not directly controlled for. The most important among these is the air-fuel ratio (AFR). While it is not essential to track AFR to a specific value, it is necessary to keep it away from certain bounds. HCCI combustion is typically lean, and on the low end, an AFR that is less than stoichiometric is to be avoided, as this would imply rich combustion. Rich conditions adversely affect HCCI combustion and significantly reduce the overall efficiency of the process. Also there is a risk of producing high levels of NOx if the mixture is too rich [80]. Very lean combustion is also not desirable as it an have a detrimental impact on combustion stability. Xu et al [81] show that for any given intake valve timing, there is a range of air-fuel ratios where combustion is consistent and the phasing of combustion falls within an acceptable range. Therefore it is necessary to restrict the range of variation of AFR - and it is possible to do this within the MPC framework, by expressing AFR in terms of the states of the control model.

There have been a few instances of the use of MPC in HCCI. Bengtsson et al [52] presented the use of MPC a predictive controller based on a model derived from system identification that controlled both combustion phasing and load-torque. Widd et al [40] used a physical model that included cylinder wall temperature dynamics as the basis of an MPC strategy to control work output and phasing of combustion

on an HCCI engine. This work expands upon these ideas to consider the injection timing of fuel as an input, and the constraints on air-fuel ratio.

8.3 Framing HCCI control as an MPC problem

The main objectives of HCCI control considered in this thesis are the tracking of desired load and combustion phasing trajectories. Based on a linearization of the control model presented in earlier chapters, it is easy to incorporate this control problem in the MPC framework. Two different predictive controllers are presented in this chapter. The first uses the MPC framework to control only the phasing of combustion based on the linear model. Work output is still tracked with the feedforward-integral controller presented earlier. Therefore the total quantity of fuel injected is commanded outside the MPC structure. The second controller incorporates the work output as an output within the linear control model, and therefore controls both load and combustion phasing within the MPC framework.

8.3.1 Combustion phasing control using MPC

A linearized version of the five state model presented in Chapter 6 (Eq. (6.6)) is used as the basis for the predictive controller. The inputs available to control phasing are the valve timings and the timing of the pilot injection. The fuel quantity can be considered a known disturbance to the system, as it is commanded by the NMEP controller outside the MPC structure. In addition, there are several constraints to be considered:

1. Absolute limits on the cylinder volume at intake and exhaust valve closure
2. Absolute limits on the timing of the pilot injection, such that the region of saturation in Fig. 6.5 is avoided
3. A limit on the maximum allowable rate of change of the valve timing
4. Limits on the maximum and minimum allowable air-fuel ratio

The first three constraints involve the control inputs and so can be easily defined while formulating the MPC optimization. The definition of the last constraint is described in the following section.

Incorporating constraints on air-fuel ratio

In this work the constraints on AFR are modeled as constraints on the ratio of oxygen and fuel in the reactant mixture. This is necessary because a conventional definition of air-fuel ratio does not translate directly to the oxygen-fuel ratio in exhaust recompression HCCI because of the presence of trapped exhaust gases. As HCCI combustion is typically lean, these trapped gases have some oxygen - therefore the final oxygen-fuel ratio before combustion is determined both by the quantity of inducted air, as well as the quantity and oxygen concentration of trapped exhaust.

We therefore define lambda (λ) as the ratio of the actual oxygen-fuel ratio and the stoichiometric oxygen-fuel ratio for the particular fuel under consideration. Therefore

$$\lambda = \frac{[O_2]/[F]}{([O_2]/[F])_{stoich}} \tag{8.2}$$

Constraints on AFR therefore are considered equivalent to constraints on λ.

$$AFR_{min} \leq AFR \leq AFR_{max} \Longleftrightarrow \lambda_{min} \leq \lambda \leq \lambda_{max} \tag{8.3}$$

For gasoline fuel modeled as C_7H_{13}, the stoichiometric reaction equation is given by

$$C_7H_{13} + 10.25O_2 + 38.54N_2 \rightarrow 7CO_2 + 6.5H_2O + 38.54N_2 \tag{8.4}$$

Then, based on Eq. (8.4), if $\lambda \leq \lambda_{max}$, then

$$\begin{aligned} \frac{[O_2]}{[F]} &\leq 10.25\lambda_{max} \\ \Rightarrow [O_2] - 10.25\lambda_{max}[F] &\leq 0 \end{aligned} \tag{8.5}$$

Similarly

$$\begin{aligned} \lambda &\geq \lambda_{min} \\ \Rightarrow [O_2] - 10.25\lambda_{min}[F] &\geq 0 \end{aligned} \tag{8.6}$$

Therefore the bounds on the oxygen-fuel ratio can be translated to equivalent bounds on linear combinations of two of the system states - oxygen and fuel concentrations.

Based on the above discussion, the following definitions of the state (x), input (u), disturbance (v) and output (y) vectors are made

$$x = \begin{bmatrix} [O_2] \\ T \\ [F] \\ V_{IVC} \\ K_{th} \end{bmatrix}, u = \begin{bmatrix} V_{IVC} \\ V_{EVC} \\ u_{th} \end{bmatrix}, v = \begin{bmatrix} n_f \end{bmatrix}, y = \begin{bmatrix} CA_{50} \\ y_{AFR,min} \\ y_{AFR,max} \end{bmatrix} \tag{8.7}$$

where

$$\begin{aligned} y_{AFR,min} &= [O_2] - 10.25\lambda_{min}[F] \\ y_{AFR,max} &= [O_2] - 10.25\lambda_{max}[F] \end{aligned}$$

The overall MPC problem then is defined as follows:
Minimize

$$\begin{aligned} J(k) &= \sum_{i=0}^{H_p-1} ||CA_{50}(k+i|k) - CA_{50,des}(k+i|k)||_Q^2 + \sum_{i=0}^{H_u-1} ||\Delta u(k+i|k)||_R^2 \\ &+ \sum_{i=0}^{H_u-1} ||u_{th}(k+i|k) - u_{th,ref}||_{Q_u}^2 + \sum_{i=0}^{H_p-1} \rho||\epsilon||^2 \end{aligned}$$

subject to

$$\begin{aligned} x_{k+1} &= Ax_k + B_u u_k + B_v v_k \\ y_k &= Cx_k \\ \Delta u_{evc,min} &\leq \Delta u_{evc,k} \leq \Delta u_{evc,max} \\ u_{evc,min} &\leq u_{evc,k} \leq u_{evc,max} \\ u_{th,min} &\leq u_{th,k} \leq u_{th,max} \end{aligned}$$

$$\begin{aligned} y_{AFR,min,k} &\geq 0 - \epsilon \\ y_{AFR,max,k} &\leq 0 + \epsilon \end{aligned} \tag{8.8}$$

The cost function in this optimization has four terms. The first two represent costs on errors in CA_{50} and control effort respectively. The input cost matrix R is set such that only two of the three available inputs are used - the intake valve is kept fixed and not controlled. The third term in the cost function imposes a cost on deviations of the pilot injection timing input from a reference - this cost ensures that all things being equal, an input trajectory that maintains the pilot injection timing closer to a reference (set at the middle of its range) will be preferred. Therefore this term serves to achieve some form of mid-ranging action as described in Chapter 7 so as to keep the injection timing in a range where it has maximum control authority. However by incorporating this into the cost function, it is ensured that if necessary, the injection timing can deviate from the reference value - either to lower the cost of output deviations, or to ensure constraint satisfaction. The cost Q_u is set at a value much smaller than the cost Q on the output error, thereby giving priority to output tracking over mid-ranging.

The last term of $J(k)$ imposes a cost on ϵ, which is a slack variable. This slack variable essentially softens the last two constraints, which represent the lower and upper bounds on λ as described earlier. Softening these constraints is necessary to deal with the possibility of infeasibility - a condition that might occur, for example, with an unexpected large disturbance, in which case it might be impossible to keep

the plant within the specified constraints. Introducing the slack variable ϵ ensures that the constraints can be crossed occasionally, but only if really necessary. The relative allowance given for constraint violation can be controlled with the weight ρ - a higher value of ρ makes the constraint relatively "hard" to violate.

The other inequalities represent constraints on the actuators - absolute limits on EVC and injection timing, as well as a rate limit on the EVC. These inequalities are not softened with the slack variable as these represent hardware constraints and therefore should not be violated under any circumstances.

The prediction horizon H_p is set at 3 time steps, while the control horizon H_u is set to be 1. Though these might appear small, the HCCI process typically has little dependence on mixture conditions more than 2-3 engine cycles earlier. This can be understood from the perspective of the trapped exhaust on any engine cycle - the relative quantity of this exhaust that remains trapped within the engine cylinder on successive engine cycles rapidly decreases and becomes insignificant after 3-4 engine cycles. Therefore there is little to be gained with large prediction and control horizons. Widd et al [40] confirm this by testing predictive controllers with different time horizons on an HCCI engine, and conclude that an increase in time horizon beyond 4-5 cycles has no discernible effect on performance, while adding a significant amount of computation time.

The controller is tested on the continuous time simulation model. Figures 8.1 and 8.2 show the output and input trajectories with the predictive controller *without* any constraints on λ, while Figs. 8.3 and 8.4 show results from the same test repeated *with* constraints on λ. The controller in each test is switched on after 10 engine cycles. As seen, in both cases, the control outputs ($NMEP$ and CA_{50}) are tracked well. However in the first case the constrained output λ does not stay within the desired bounds, while in the second it largely remains constrained. Note that the λ here relates to the overall oxygen-fuel ratio in the mixture before combustion as described earlier. The lower and upper bounds here are set arbitrarily at 1.6 and 1.7. Around the nominal operating condition, these bounds correspond roughly to *inducted AFR* λs (ratio of inducted air-fuel ratio to the stoichiometric air-fuel ratio) of about 1.25 and 1.32 respectively. These bounds are chosen to illustrate the controller's response

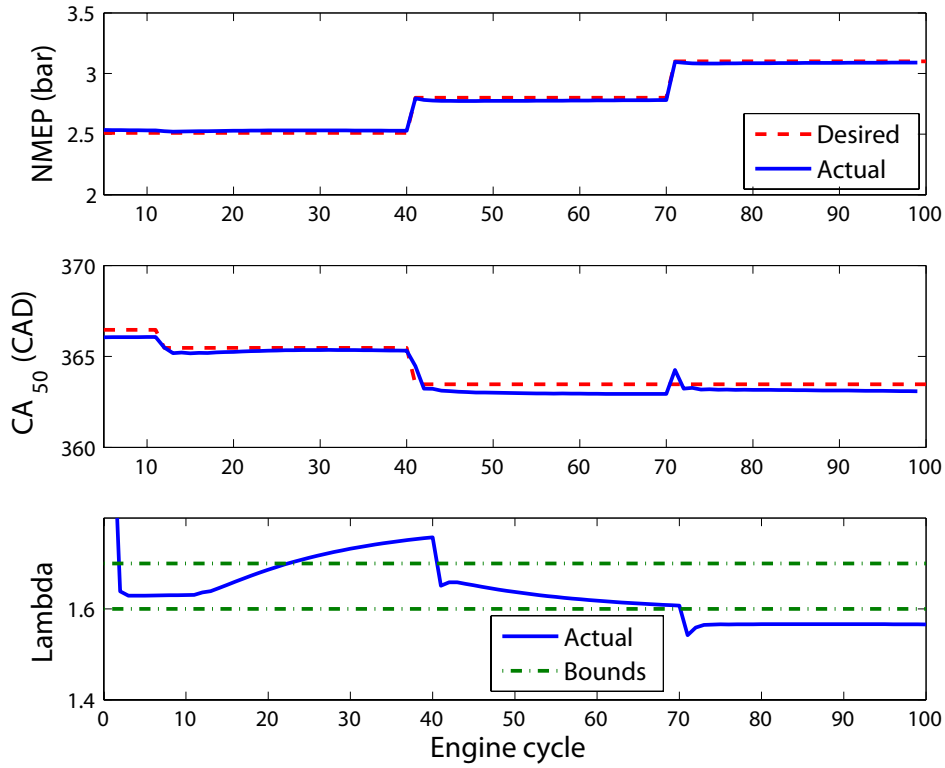

Figure 8.1: Combustion phasing MPC implemented in simulation with no constraint on λ - outputs

to constraints and not to reflect true limits in practice.

The $NMEP$ is controlled directly by the fuel quantity outside the MPC framework - therefore the fuel trajectories seen in Figs. 8.2 and 8.4 relate closely to the actual $NMEP$. The other two inputs - EVC and injection timing - are commanded by the model predictive controller. The EVC input responds over several cycles to step changes in the desired conditions, while the injection timing responds more instantly, due to the constraint on the rate of change of the EVC input. Note that without the additional constraint on λ, a mid-ranging effect is seen with the injection timing going to its reference value over several cycles. However once the λ constraint is added, the injection timing input remains close to its reference value, but does not track it exactly. This is to be expected because of the extra constraint.

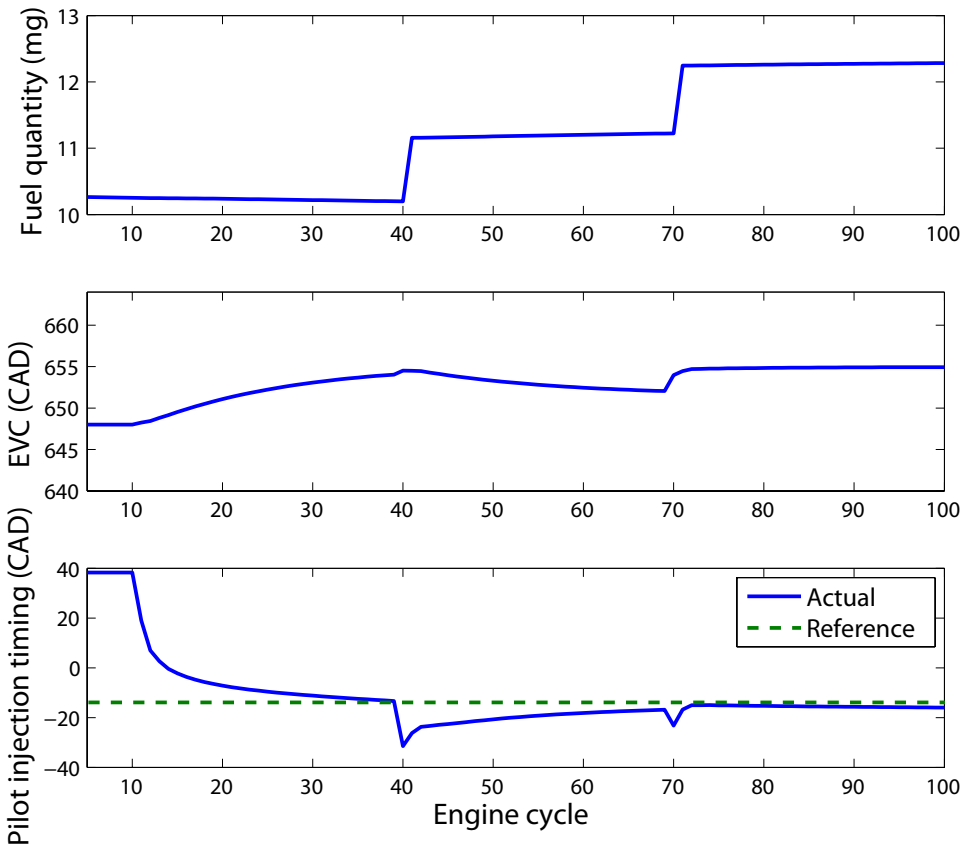

Figure 8.2: Combustion phasing MPC implemented in simulation with no constraint on λ - inputs

These results indicate that this approach is extremely promising in controlling the work output and combustion phasing while satisfying other constraints. However step changes in fuel quantity could cause temporary violation of the constraints on AFR, as seen in Fig. 8.3 around cycles 40 and 70. This is because the NMEP controller operates independent of the MPC scheme, and has no knowledge of the constraints on the other actuators - therefore it commands a step change in fuel when faced with a step change in the desired work output. However slightly slower load tracking - over several engine cycles instead of one - which would require smaller changes in fuel quantity on a cycle-by-cycle basis, would be easier to compensate for in order to

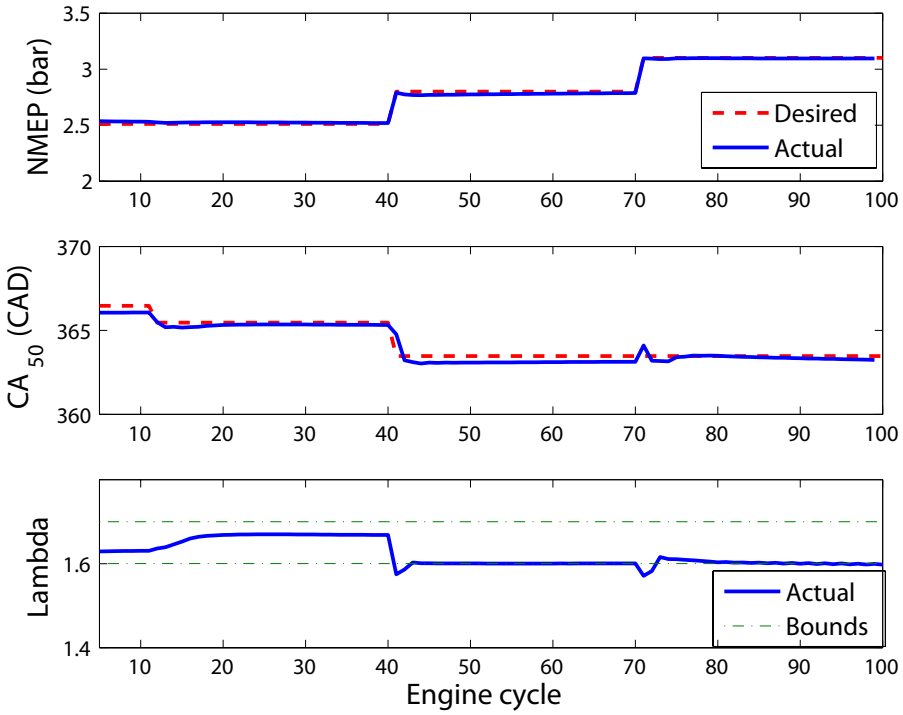

Figure 8.3: Combustion phasing MPC implemented in simulation with constraint on λ - outputs

bound the AFR. This can be achieved by including the control of NMEP within the MPC framework, which would allow the controller to tradeoff fast output tracking with constraint satisfaction during transients. This motivates the second predictive controller described in the next section.

8.3.2 NMEP and Combustion phasing control using MPC

There are several ways to include $NMEP$ as part of the MPC framework. Here a simple approach is taken by linearizing the fuel-$NMEP$ map used as the feedforward controller for work output, and including it as a part of the linearized control model description. Linearizing this map gives an expression of the form

$$NMEP = k[F] \tag{8.9}$$

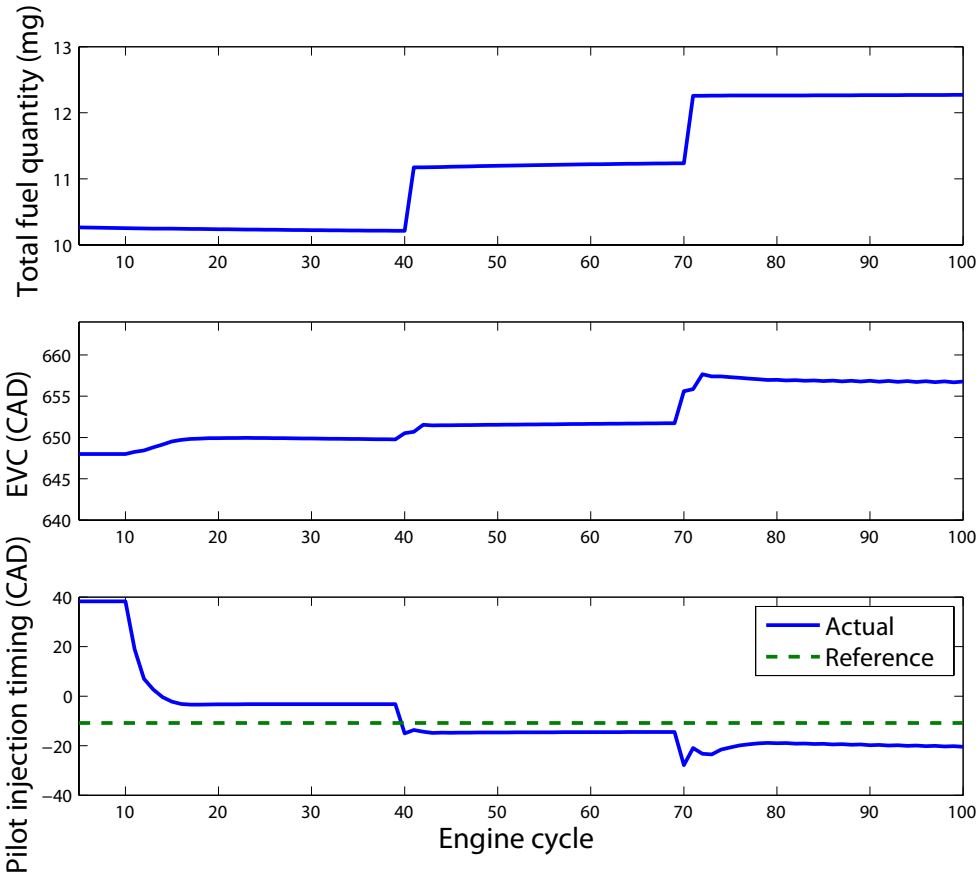

Figure 8.4: Combustion phasing MPC implemented in simulation with constraint on λ - inputs

This can easily be incorporated into the output equation of the linear model as fuel concentration $[F]$ is one of the states. The MPC problem can then be formulated based on the following definitions:

$$x = \begin{bmatrix} [O_2] \\ T \\ [F] \\ V_{IVC} \\ K_{th} \end{bmatrix}, u = \begin{bmatrix} n_f \\ V_{IVC} \\ V_{EVC} \\ u_{th} \end{bmatrix}, y = \begin{bmatrix} NMEP \\ CA_{50} \\ y_{AFR,min} \\ y_{AFR,max} \end{bmatrix} \tag{8.10}$$

The final MPC optimization is

Minimize

$$\begin{aligned} J(k) &= \sum_{i=0}^{H_p-1} ||CA_{50}(k+i|k) - CA_{50,des}(k+i|k)||^2_{Q_1} \\ &+ \sum_{i=0}^{H_p-1} ||NMEP(k+i|k) - NMEP_{des}(k+i|k)||^2_{Q_2} \\ &+ \sum_{i=0}^{H_u-1} ||\Delta u(k+i|k)||^2_R + \sum_{i=0}^{H_u-1} ||u_{th}(k+i|k) - u_{th,ref}||^2_{Q_u} + \sum_{i=0}^{H_p-1} \rho||\epsilon||^2 \end{aligned}$$

subject to

$$\begin{aligned} x_{k+1} &= Ax_k + B_u u_k \\ y_k &= Cx_k \\ u_{fuel} &\geq 0 \\ \Delta u_{evc,min} &\leq \Delta u_{evc,k} \leq \Delta u_{evc,max} \\ u_{evc,min} &\leq u_{evc,k} \leq u_{evc,max} \\ u_{th,min} &\leq u_{th,k} \leq u_{th,max} \\ y_{AFR,min,k} &\geq 0 - \epsilon \\ y_{AFR,max,k} &\leq 0 + \epsilon \end{aligned} \tag{8.11}$$

Figures 8.5 and 8.6 show results from implementing this controller in simulation. This time, both $NMEP$ and CA_{50} are controlled by the predictive controller, which recognizes the constraints on λ. Therefore it slows down the response to a step change in desired $NMEP$ by changing the fuel quantity command more slowly. The other inputs can then be used to ensure that λ stays within the desired ranges on every engine cycle. The tracking of CA_{50} remains very similar to the earlier cases because of the ability of the pilot injection timing to respond quickly to track phasing. Again, this injection timing remains close to its reference value but does not track it exactly because of the λ constraint.

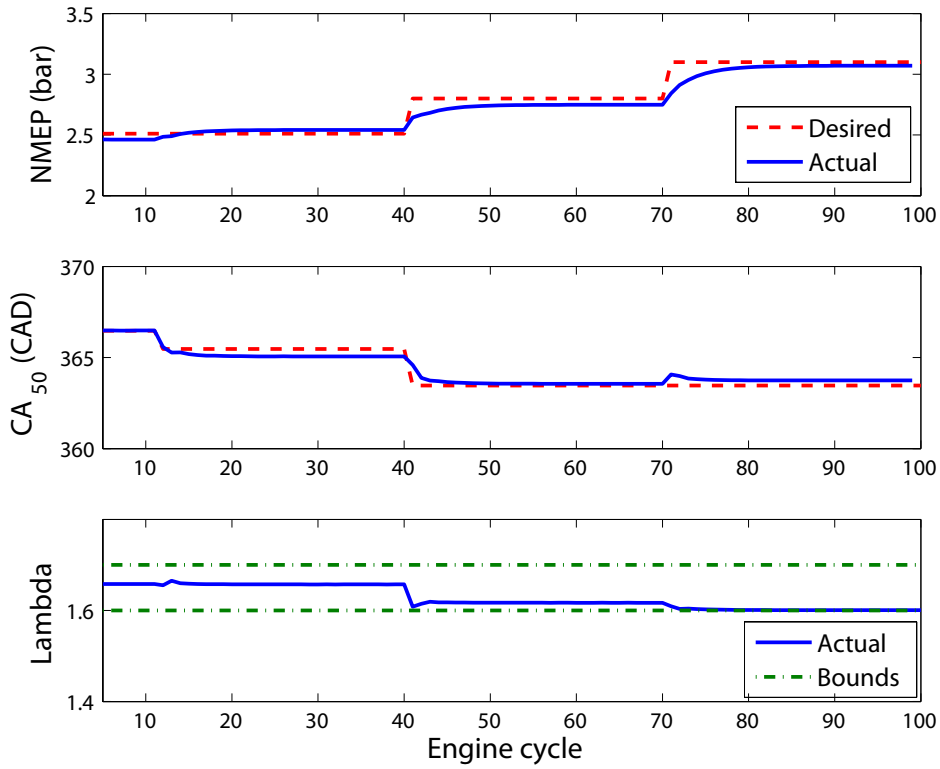

Figure 8.5: NMEP-phasing MPC implemented in simulation with constraint on λ - outputs

8.4 Estimator structure

As detailed in earlier chapters, the two main states, oxygen concentration and temperature, cannot be directly measured and so need to be estimated. In earlier work these were estimated either using simple Luenberger observers or Kalman filters based on a measurement of CA_{50}. However the estimator used here is sufficiently different as to merit a full description.

So far both states have been estimated based on a single measurement of combustion phasing. However an exhaust oxygen sensor can give an independent measurement of the oxygen concentration in the exhaust gas. If the oxygen sensor is located very close to the port, this measurement can serve as a good estimate of the

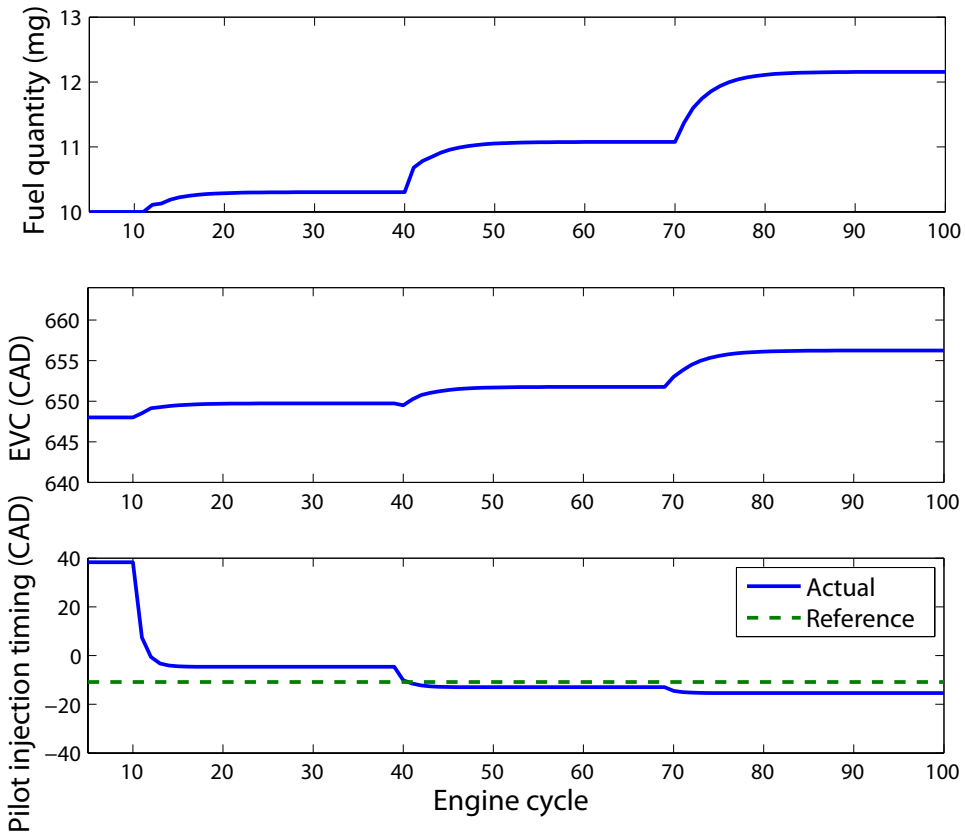

Figure 8.6: NMEP-phasing MPC implemented in simulation with constraint on λ - inputs

oxygen concentration in the trapped exhaust within the engine cylinder. Therefore this measurement can further serve to improve the accuracy of the estimation.

A wide band oxygen sensor typically gives a measurement of the fraction of oxygen in the exhaust gas. This measurement can be compared to an estimate of the fraction of oxygen in the trapped exhaust gas obtained from the control model. As the model steps through each of the distinct states that occur during an engine cycle, it is easy to obtain an expression for the percentage of oxygen in the exhaust gas as a function of the states. The fraction of oxygen in the trapped exhaust is the same as the fraction

of oxygen in the mixture after combustion, and therefore is given by

$$r_{O_2} = \frac{n_{O_2,3}}{N_3} \tag{8.12}$$

where $n_{O_2,3}$ is the moles of oxygen in the post-combustion mixture, and N_3 is the total number of moles after combustion, as described in Chapter 2. Expressions for these are given in Eq. (2.15) and (2.25), and so r_{O_2} can be easily expressed in terms of the model states:

$$r_{O_2} = g([O_2]_s, T_s, [f]_s, V_{IVC,s}) \tag{8.13}$$

The expression in Eq. (8.13) can be linearized analytically and included in the output equation of the linear model. However including a measurement of r_{O_2} in the estimation scheme presents one further hurdle which arises from the fact the measurements of CA_{50} and r_{O_2} are available at different points in the engine cycle. This can be understood by considering the relationship between estimation and control. Typically a Kalman filter estimator involves two steps:

1. *Time update*, where the state estimate is updated based on the model and the applied inputs.
$$\hat{x}_{k|k-1} = A\hat{x}_{k-1|k-1} + Bu_{k-1} \tag{8.14}$$

2. *Measurement update*, where the state estimate is updated based on the measured outputs.
$$\hat{x}_{k|k} = \hat{x}_{k|k-1} + M(y_k - C\hat{x}_{k|k-1}) \tag{8.15}$$

where M is the Kalman filter gain matrix. The state estimate $\hat{x}_{k|k}$ can then be used to determine the control input u_k for cycle k. It is therefore essential that all the measurements y_k be obtained *before* the control input can be determined.

However, as shown in Fig. 8.7, it is only the measurement of CA_{50} that becomes available before the inputs need to be applied - a measurement of exhaust oxygen fraction, r_{O_2} is only available *after* the exhaust process, as the measurement occurs outside the engine cylinder. Based on this observation, the Kalman filter update is performed in three distinct steps, with the measurement update split into two steps.

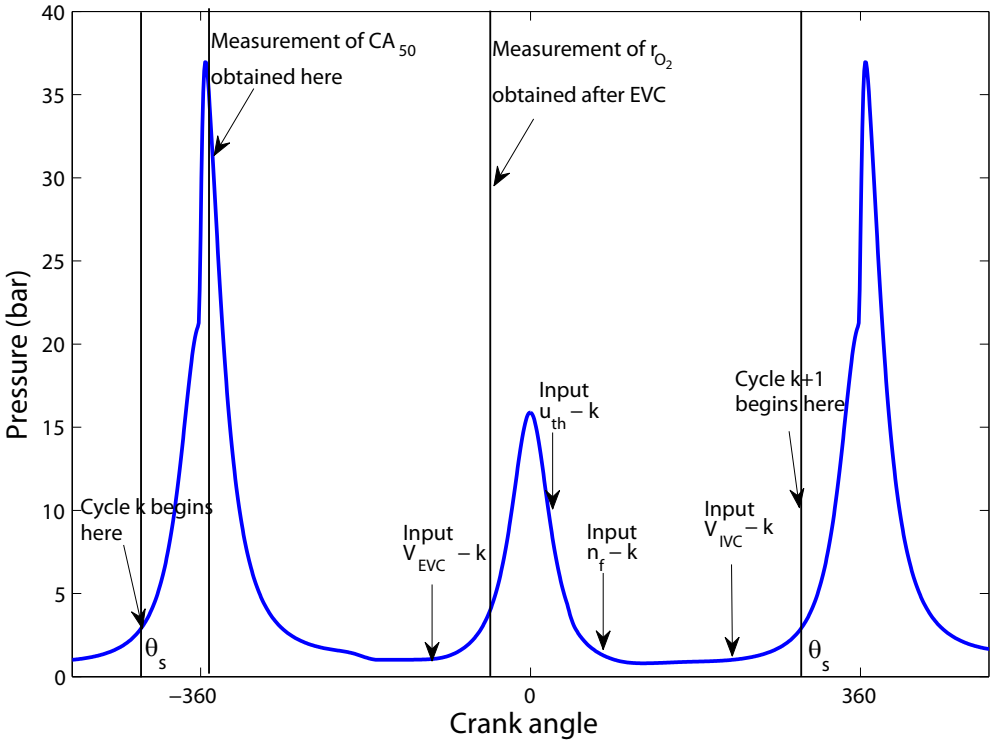

Figure 8.7: Location in engine cycle where measurements are available

1. *Time update*, where the state estimate is updated based on the model and applied inputs.

$$\hat{x}_{k|k-1} = A\hat{x}_{k-1|k-1} + Bu_{k-1} \tag{8.16}$$

2. *Combustion phasing measurement update*, where the state estimate is updated based on the measured CA_{50}.

$$\hat{x}_{k|k,partial} = \hat{x}_{k|k-1} + M_{CA_{50}}(CA_{50,meas,k} - C_{CA_{50}}\hat{x}_{k|k-1}) \tag{8.17}$$

3. *Oxygen sensor measurement update*, where the state estimate is further updated based on the oxygen sensor measurement.

$$\hat{x}_{k|k} = \hat{x}_{k|k,partial} + M_{O_2}(r_{O_2,meas,k} - C_{O_2}\hat{x}_{k|k-1}) \tag{8.18}$$

$M_{CA_{50}}$ and M_{O_2} are the Kalman gain vectors for each of the outputs, CA_{50} and r_{O_2}, while $C_{CA_{50}}$ and C_{O_2} represent the rows of the C matrix corresponding to these two outputs. The third step of this estimation is actually computed on the following time step, once the oxygen sensor measurement is obtained. Therefore the best estimate available to the controller is $\hat{x}_{k|k,partial}$ and uses only one of the two measurements. However this is not a significant problem, as the second measurement still serves to update the estimate before the next time step.

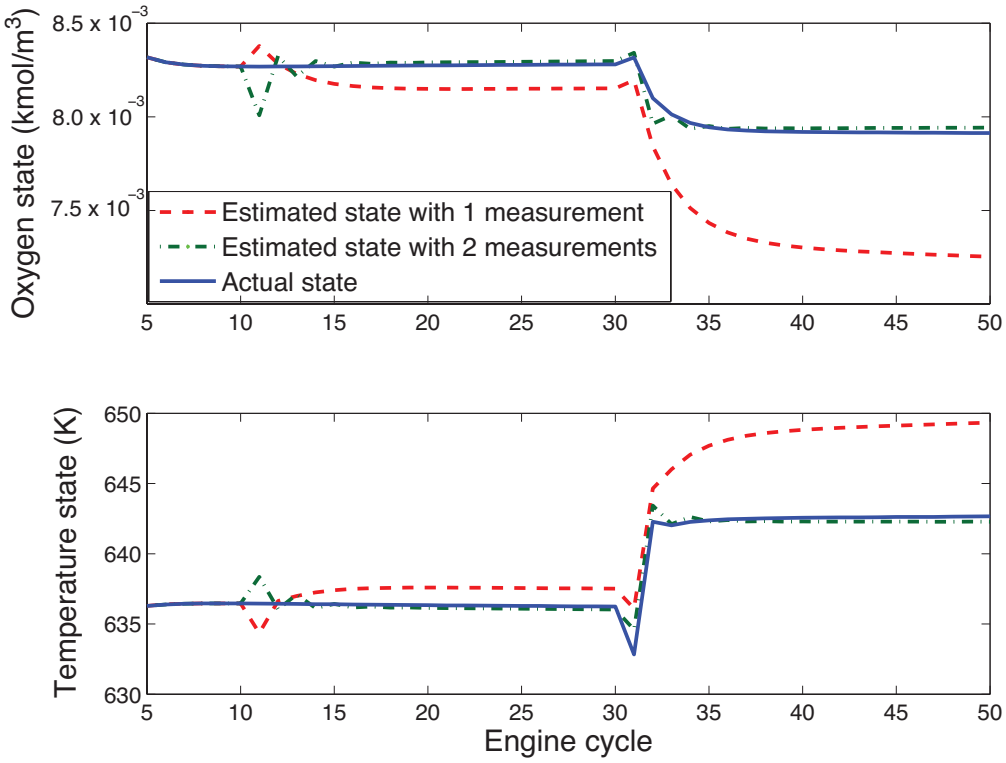

Figure 8.8: Comparison of estimator performance in simulation with one vs. two measurements

Figure 8.8 shows a comparison of the performance of two estimators in simulation, one that uses just the measurement of combustion phasing and one that also uses the measurement of the exhaust oxygen fraction. These responses are plotted for a step increase in fuel quantity, while all other inputs are kept fixed. The estimation is

started after 10 engine cycles. The state estimates plotted here are the estimates used by the controller - therefore for the single measurement case the estimate $\hat{x}_{k|k}$, while for the case with two measurements it is $\hat{x}_{k|k,partial}$. As seen, with two measurements the accuracy of estimation is significantly improved and the estimate tracks the actual state value very closely. Apart from the steady state match, the estimator based on two measurements also captures the dynamic response much better, as seen when the step change in fuel mass is applied after 30 engine cycles.

It should be noted that this estimation strategy assumes a measurement from a wide-band oxygen sensor in the exhaust port of each engine cylinder that can give a fast and accurate measurement of the oxygen concentration in the exhaust stream. Most production engines today are not equipped with such a sensor - and so a more practical estimation approach that can use production-grade sensors would need to be developed before implementation on mass-produced engines. However this analysis does serve to underline the benefits of an estimation scheme that takes into account both the phasing of combustion and the characteristics of the exhaust stream in determining the states.

8.5 Experimental implementation

The model predictive controller structure is implemented on the multi-cylinder HCCI engine testbed. As the second controller presented here, with both $NMEP$ and CA_{50} in the MPC framework, was found to work better in simulation, it was the only one implemented in experiment. Due to the computationally intensive nature of a real-time model predictive control implementation, an explicit representation of the controller as described by Bemporad et al [75] is obtained. Such a representation can be easily obtained for the HCCI controller presented above, and is implemented on the engine through Matlab's hybrid control toolbox. As a proof of concept, the controller was run on only one engine cylinder out of the four. The other three were run at a fixed operating condition.

Figures 8.9 and 8.10 show the output and input trajectories on the cylinder run with the predictive controller over a series of step changes in desired load and phasing.

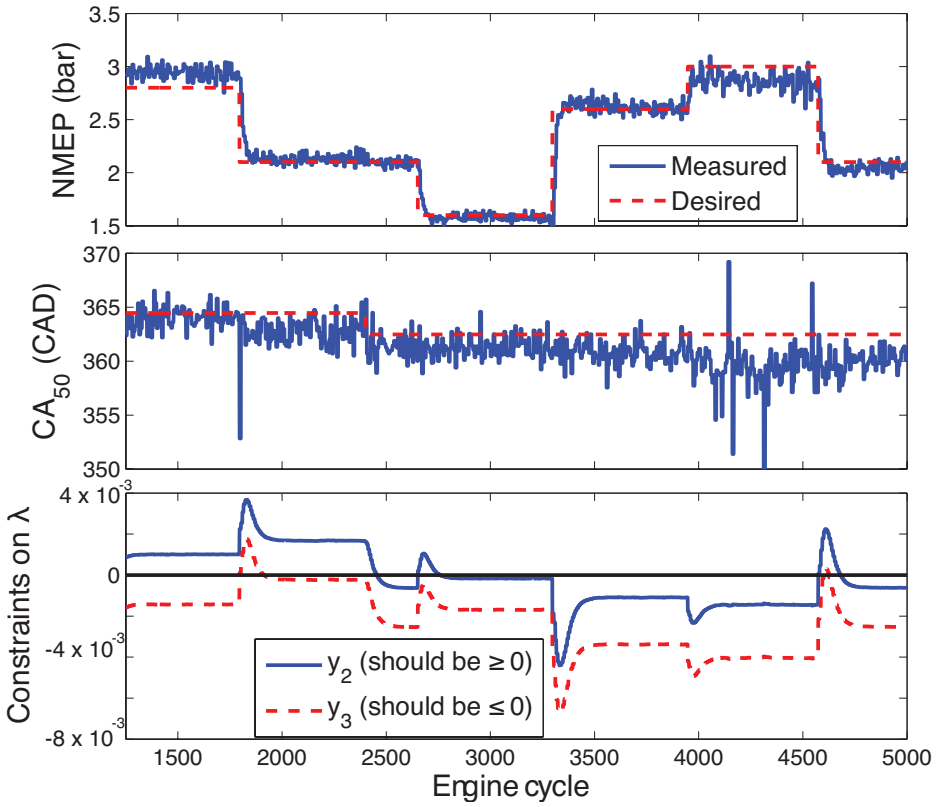

Figure 8.9: NMEP-phasing MPC implemented in experiment without constraint on λ - outputs

This optimization is run without the constraints on λ active. Both work output and phasing are tracked fairly accurately, including over step changes in load as large as 1 bar at constant phasing (around 3400 cycles). There is some steady state error seen at higher loads around 3 bar - this can be attributed to the fact that a single model is used over the entire range, and there is no integral action to correct for linearization errors over such a wide range.

Also plotted in the bottom plot of Fig. 8.9 are the outputs $y_{AFR,min}$ and $y_{AFR,max}$, representing the lower and upper bounds on λ. The lower and upper limits chosen for λ here are $\lambda_{min} = 1.6$ and $\lambda_{max} = 2$, a slightly wider range than in simulation so as to give the controller some flexibility. Based on the optimization problem presented in Eq. (8.11), it is desired to keep $y_{AFR,min} \geq 0$ and $y_{AFR,max} \leq 0$. This would

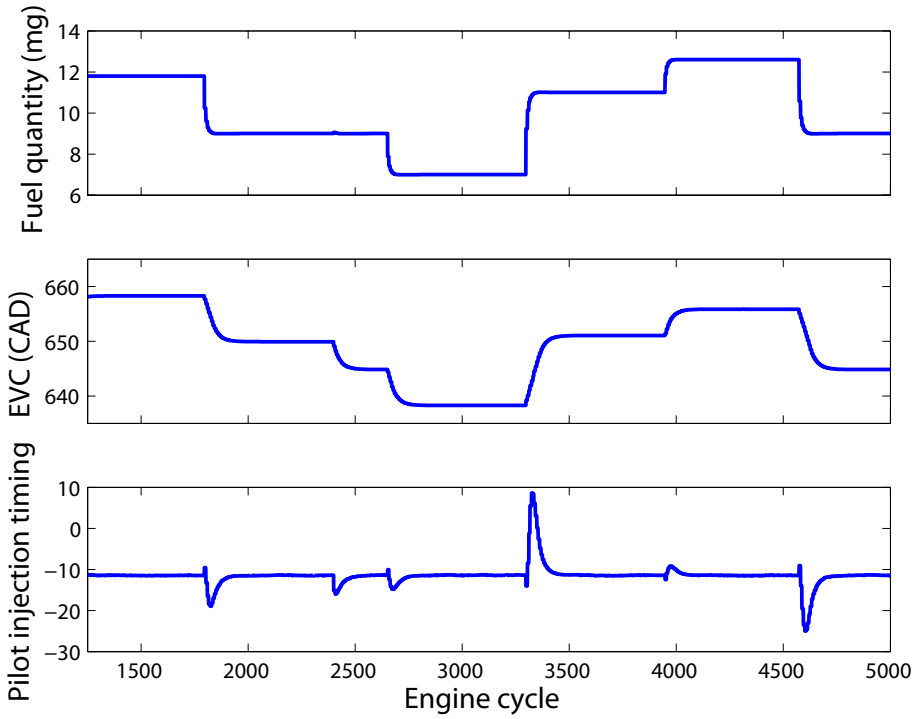

Figure 8.10: NMEP-phasing MPC implemented in experiment without constraint on λ - inputs

ensure that $1.6 \leq \lambda \leq 2$. However it is seen here that the constraints are exceeded significantly several times during the test. This is because the constraints on λ are not active in this test. In particular, large excursions are seen any time step changes in $NMEP$ are commanded. This can be attributed to the step change in fuel quantity - as there are no constraints on λ, the fuel quantity very quickly ramps up/down to the new value desired, while the pilot injection timing also changes quickly to maintain the desired combustion phasing. Over several cycles this input is brought back to its reference value by a slowly changing EVC.

Activating the constraints on λ significantly changes the behavior, as seen in Figs. 8.11 and 8.12. The tracking of the two control outputs, $NMEP$ and CA_{50}, remains as accurate - however the new steady state in $NMEP$ is reached a little slower, especially during large step changes, such as around 3400 cycles. This is

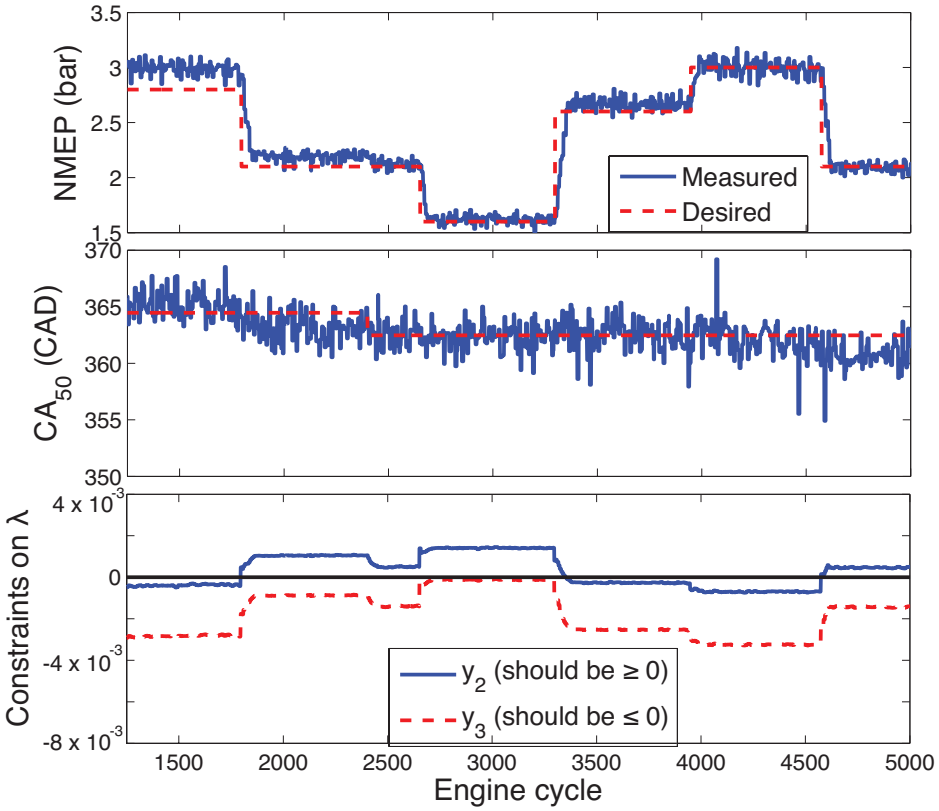

Figure 8.11: NMEP-phasing MPC implemented in experiment with constraint on λ - outputs

because the controller recognizes the constraint on λ and so slows down fuel changes to prevent constraint violation. Additionally, the pilot injection timing no longer tracks its reference value - while it remains close, there are significant deviations seen, especially at higher loads (between 3400 and 4500 cycles). Consequently the constraints on λ are met most of the time, and only at very high loads is there a slight violation of the $y_{AFR,min} \geq 0$ constraint, implying that $\lambda < 1.6$. This is not surprising, as with such a high load demand it is basically impossible to meet all the output requirements while still satisfying the λ constraint. Therefore it is only when something infeasible is demanded of the controller that it allows a violation of the output constraint. One point to be noted though is that even this constraint violation can be avoided by increasing the weight ρ on the slack variable in the optimization,

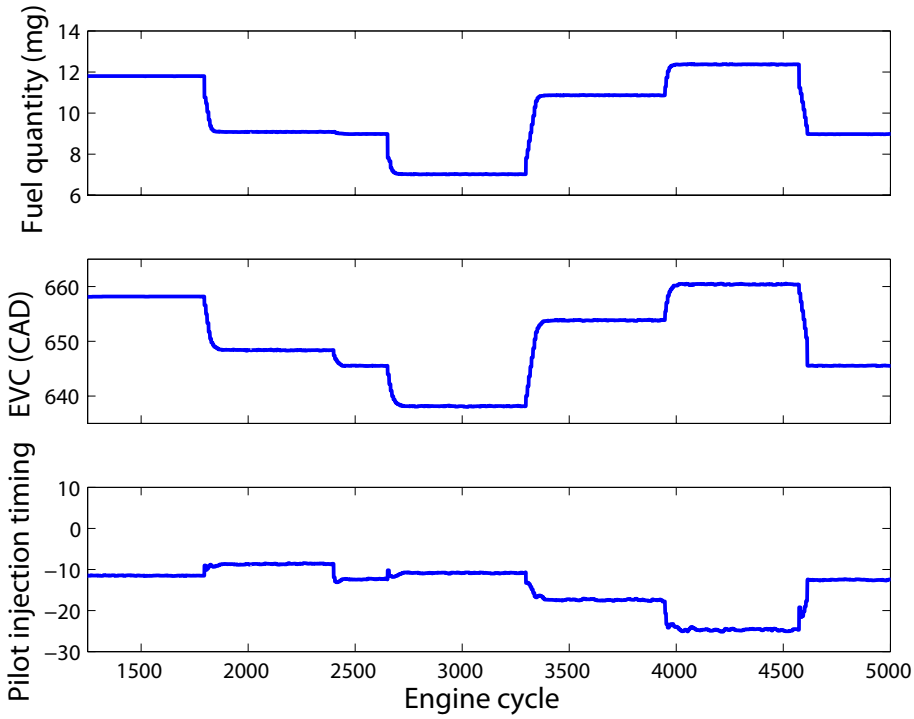

Figure 8.12: NMEP-phasing MPC implemented in experiment with constraint on λ - inputs

ϵ. This would lead to poorer output tracking when faced with an infeasible desired output trajectory. Therefore the relative tradeoff between accurate output tracking and constraint satisfaction can be set at a desired value by changing the value of this weight in the cost function.

8.6 Conclusion

While earlier chapters validated the physical control model and developed simple controllers based on it that were effective on both single and multi-cylinder engine testbeds, the predictive control framework presented in this chapter represents a very practical and yet robust control strategy for HCCI. The key feature of this framework, as shown here, is the ability to explicitly specify actuator and output constraints that

represent real physical limitations on production engines. In particular, the range limitations of the pilot injection timing input, and the bandwidth limitations of a cam phaser system can both be accounted for. Additionally, MPC allows the constraining of outputs, and one important variable in HCCI is the air-fuel ratio. It was seen that constraints on the air-fuel ratio, expressed through the oxygen-fuel ratio in the reactant mixture, could be modeled as constraints on a linear combination of the model states. Inclusion of this as part of the control objective then led to the synthesis of two different control strategies. The first used the MPC framework to only control the phasing of combustion. While this was seen to be effective in output tracking, it was seen that the constraints were occasionally violated, especially during sharp fuel transients commanded by the $NMEP$ controller. Based on these observations, a second and more comprehensive controller is designed that controls both $NMEP$ and CA_{50} within the MPC framework. This controller is able to tradeoff fast load changes with better constraint satisfaction. When implemented on one of four cylinders of the multi-cylinder HCCI testbed, the performance is very similar to that in simulation, with good output tracking and constraint satisfaction. A redesigned estimator that, in addition to combustion phasing, uses a measurement from an exhaust oxygen sensor complements this controller by providing very accurate estimation of the system states.

The work presented in this chapter therefore represents the culmination of the entire physical model-based control approach that has been the focus of this thesis. The model predictive control strategy developed here shows both the value of this approach in understanding and capturing the fundamental behavior of HCCI, as well as its ability to serve as a basis for practical and robust control strategies that could have a significant role to play in the future of HCCI.

Chapter 9

Conclusions and Future Work

The energy and environmental crisis faced by the world today is possibly one of the greatest challenges humanity has ever faced - and to many it is a losing battle, one that we cannot hope to win. The future, however, is not as bleak as some might believe - technological research continues to unveil many promising possibilities for creating a world where our energy needs are met in sustainable ways. The hurdles we face in making these practical and ubiquitous are, however, daunting and will take several years if not decades to be surmounted. In the interim we find ourselves turning to technologies that are easily realizable in a short period of time and yet provide significant benefits over the status quo - and in the automotive sector, HCCI represents one of the most promising engine strategies that fit into this category.

The challenges associated with HCCI, however, necessitate the use of non-trivial closed-loop control strategies to enable its operation over the widest operating range possible - and it is in this realm that the main contributions of this thesis lie. The modeling and control framework developed as part of this research is significant for several reasons.

- It represents a very robust and practical approach to cycle-by-cycle control of HCCI over a wide operating range.
- It enables the coordination of the various actuators available in a way that respects realistic constraints on them.

- The controllers developed contribute to the expansion of the HCCI operating regime in various ways - either through the reduction of cyclic variation at late combustion phasing points, or through enabling steady operation at low loads.
- The physical model serves as a very useful bridge between the fields of thermodynamics and control and is a potentially useful tool for an engine design process that takes into account the requirements of a good control strategy.
- It is an approach that is easily generalizable to different engines with just a simple re-parametrization.

These characteristics make this framework a very flexible approach that takes us a step closer to the implementation of HCCI on mass-manufactured automobiles. The following section presents a more detailed summary of some of the results presented in this thesis that were obtained through the process of deriving this framework.

9.1 Summary of work

Although HCCI is inherently an extremely complex process, the work presented in this thesis suggests that simple lower-order models are sufficient to capture the essential dynamics of HCCI. First, a second-order model was developed in Chapter 2, with its states defined as the moles of oxygen and temperature of the trapped exhaust at EVC. With simplifying thermodynamic assumptions, such as isentropic compression/expansion processes, and instantaneous combustion, this gave a discrete time model that captured the effects of varying fuel quantity and valve timings on the peak pressure and angle of peak pressure in an engine cycle.

A linearized version of this model was used as the basis for an LQR controller that was tested both in simulation and on a single-cylinder HCCI testbed. The implementation of this controller in order to control the peak pressure and angle of peak pressure on every engine cycle was described in Chapter 3. The results validated this approach by showing accurate control of these quantities over a range of operating points. Additionally, it was seen that small changes in fuel injection could lead to a

significant reduction in the variation of combustion at late combustion phasing points. This suggests that there is a systematic nature to the variation seen at these points that is captured well by the model.

This process of controller design and implementation, however, illuminated several features of the model that were not desirable. Chapter 4 took a closer look at these aspects. In particular, it was seen that the definition of states at EVC tied them to a varying input, a characteristic that made them very sensitive to the exact definition of the point of exhaust valve closure. This motivated a revision of the model where the states were defined at a fixed crank angle location after IVC. This location was also seen to tie the states more directly to the output, thereby making estimation easier. The state vector was further expanded to include a measure of fuel concentration and the cylinder volume at IVC in order to ensure there was no direct input feed-through term in the overall model. Finally, some of the thermodynamic assumptions were made more realistic - polytropic processes were assumed instead of isentropic, combustion was modeled as a finite-duration event rather than instantaneous, and a very basic heat transfer model during recompression was introduced. Dynamic comparison of the model with the more complex simulation model showed good agreement between the two.

This model was used to develop a controller for the phasing of combustion, measured as CA_{50} in Chapter 5. As the work output, $NMEP$, is strongly tied to the fuel quantity, a decoupled approach was taken to control of work output and combustion phasing. An empirical feedforward-integral controller commanded the fuel injection quantity to control $NMEP$, while the physical model was used to generate a feedback controller for combustion phasing with variable valve motion. This simple approach worked very effectively both on a single and multi-cylinder engine. On the multi-cylinder engine, the controller was able to balance differences between cylinders, and also stabilize combustion at late phasing points.

The modeling framework was then expanded to include a simple model of fuel injection during recompression in Chapter 6. Due to the complex reactions that are possible during recompression depending on operating regime, the model focused on a split injection strategy, with the timing of a small pilot injection used as the

control input. The relationship between the pilot injection timing and combustion phasing was separated into a linear, analytical component and a nonlinear, empirical component. This model for split injection integrated easily into the overall control model scheme.

Based on the expanded model, two control strategies were presented in Chapter 7 that explored the use of fuel injection as a control knob. The first used only fuel injection to control work output and combustion phasing, without any valve actuation. This worked well, but only within a narrow range where the injection timing had maximum control authority. This motivated a second controller, based on the mid-ranging principle, that made an effort to combine the different actuators available in a way that respected their limitations. The mid-ranging controller used the pilot injection timing as the fast control input, using it to handle sharp transients. It then used a slower variation of the exhaust valve timing to bring the injection timing to the middle of its range, where it is most effective. This strategy enabled HCCI combustion over a wide operating regime, from very low loads to moderately high loads on the multi-cylinder engine. Such an approach could be extended to an engine with cam phasers, where the valve timings cannot be varied on a cycle-by-cycle basis and also need to be the same across cylinders.

Further expanding on the idea of developing practical controllers that respected actuator constraints, Chapter 8 presented a model predictive controller that allowed explicit constraint handling. A measure of the air-fuel ratio in the engine cylinder was also included in the model in order to constrain it away from fuel rich and very lean regions as part of the MPC scheme. The final version of this controller included both work output and combustion phasing as control outputs. A modified estimator was also developed, that could use a measurement from an oxygen sensor located in the exhaust port in addition to the phasing of combustion to generate a very accurate estimate of the states. The predictive controller performed well when implemented on the engine testbed, fulfilling the various control objectives.

9.2 Directions for future research

The research conducted as part of this thesis is a significant step towards practical HCCI implementation - however there are still several open questions to be answered along the path to implementation in automobiles. The first important extension of this work is in the use of the control model to understand more about the various operating regimes in HCCI. Due to its simplicity, the model is an extremely tractable tool for this purpose. Some work along these lines is already being pursued - for example, the model gives a clear picture of the change in temperature dynamics as we move from operating points with very low mixture temperature to very high.

Related to this is the use of the model to understand the effects of various environmental parameters on the combustion process. Any practical HCCI strategy will need to be robust to changes in intake air temperature, humidity and fuel quality as well as changes in heat transfer characteristics with engine wear that a vehicle on the road experiences. Additionally, all the results presented in this thesis have been obtained at a constant engine speed of 1800 rpm. However in reality, engine speed variation is inevitable. The control model already includes many of these parameters as constants - therefore studying the change in HCCI behavior by varying these parameters, and developing a control strategy that would be robust to these changes is an important extension of this work.

Further, the approach taken here to multi-cylinder engine control is the implementation of independent controllers on each cylinder. Taking a more holistic view though, where a single controller is used to control all the different cylinders might yield even better results. For this it would be necessary to expand the framework to explicitly include interactions between cylinders. This might necessitate the inclusion of intake and exhaust manifold models. Also of interest would be a control strategy that uses a cam phaser for all the engine cylinders (and therefore independent valve actuation would be eliminated) while using fuel injection as a cylinder-individual control knob to balance differences.

Finally, a closer look at state estimation would be an interesting avenue of exploration. Further extension of the three step Kalman filter developed in Chapter

8 that explicitly considers exhaust manifold dynamics that might be relevant to the oxygen sensor measurement would be an important step in this direction. Other measurements from the cylinder-pressure sensor, such as the peak pressure during recompression could also provide valuable information about the in-cylinder mixture.

It is the author's hope that these, and other steps, will help bring HCCI to vehicles on the road in the next few years, and provide an efficient and clean alternative to automotive engine technology today.

Bibliography

[1] European Fuel Oxygenates Association. Automobiles and pollution, 2005.

[2] Energy Information Administration. Petroleum products: Consumption, 2008.

[3] Energy Information Administration. Emissions of greenhouse gases report, 2007.

[4] Plunkett Research Ltd. Automobiles and trucks, 2008.

[5] P. A. Caton, A. J. Simon, J. C. Gerdes, and C. F. Edwards. Residual-effected homogeneous charge compression ignition at low compression ratio using exhaust reinduction. *International Journal of Engine Research*, 4(3):163–177, 2003.

[6] J. Martinez-Frias, S. M. Aceves, D. Flowers, J. R. Smith, and R. Dibble. HCCI engine control by thermal management. *SAE paper 2000-01-2869*, 2000.

[7] P. Tunestål, J-O. Olsson, and B. Johansson. HCCI operation of a multi-cylinder engine. *First Biennial Meeting of the Scandinavian-Nordic Section of the Combustion Institute*, 2001.

[8] D. Law, D. Kemp, J. Allen, G. Kirkpatrick, and T. Copland. Controlled combustion in an IC-engine with a fully variable valve train. *SAE paper 2001-01-0251*, 2001.

[9] P. M. Najt and D. E. Foster. Compression-ignited homogeneous charge combustion. *SAE paper 830264*, 1983.

[10] R. H. Thring. Homogeneous charge compression ignition (HCCI) engines. *SAE paper 892068*, 1989.

[11] M. Christensen, P. Einewall, and B. Johansson. Homogeneous charge compression ignition (HCCI) using isooctane, ethanol and natural gas–a comparison with spark-ignition operation. *SAE paper 972874*, 1997.

[12] J. Lavy, J-C. Dabadie, Angelberger C., P. Duret, J. Willand, A. Juretzka, J. Schflein, T. Ma, Y. Lendresse, A. Satre, C. Schulz, H. Krmer, H. Zhao, and L. Damiano. Innovative ultra-low NOx controlled auto-ignition combustion process for gasoline engines : the 4-space project. *SAE paper 2000-01-1837*, 2000.

[13] N. B. Kaahaaina, A. J. Simon, P. A. Caton, and C. F. Edwards. Use of dynamic valving to achieve residual-affected combustion. *SAE paper 2001-01-0549*, 2001.

[14] J. Allen and D. Law. Variable valve actuated controlled auto-ignition: speed load maps and strategic regimes of operation. *SAE paper 2002-01-0422*, 2002.

[15] P. Wolters, W. Salber, J.Geiger, and M.Duesmann. Controlled auto ignition combustion process with an electromechanical valve train. *SAE paper 2003-01-0032*, pages 93–101, 2003.

[16] C. D. Marriott and R. D. Reitz. Experimental investigation of direct injection-gasoline for premixed compression ignited combustion phasing control. *SAE paper 2002-01-0418*, 2002.

[17] H. Zhao, J. Li, T. Ma, and N. Ladommatos. Performance and analysis of a 4-stroke multi-cylinder gasoline engine with CAI combustion. *SAE paper 2002-01-0420*, 2002.

[18] A. Babajimopoulos, D. N. Assanis, and S. B. Fiveland. An approach for modeling the effects of gas exchange processes on HCCI combustion and its application in evaluating variable valve timing control strategies. *SAE paper 2002-01-2829*, 2002.

[19] S. M. Aceves, J. Martinez-Frias, D. L. Flowers, J. R. Smith, and R. W. Dibble. A decoupled model of detailed fluid mechanics followed by detailed chemical

kinetics for prediction of iso-octane HCCI combustion. *SAE paper 2001-01-3612*, 2001.

[20] S-C. Kong and R. D. Reitz. Application of detailed chemistry and CFD for predicting direct injection HCCI engine combustion and emissions. *Proceedings of the Combustion Institute*, 29:663–669, 2002.

[21] Y. Z. Zhang, E. H. Kung, and D. C. Haworth. A PDF method for multidimensional modeling of HCCI engine combustion: effects of turbulence/chemistry interactions on ignition timing and emissions. *Proceedings of the Combustion Institute*, 30:2763–2771, 2005.

[22] S. B. Fiveland and D. N. Assanis. Development and validation of a quasi-dimensional model for HCCI engine performance and emissions studies under turbocharged conditions. *SAE paper 2002-01-1757*, 2002.

[23] S. Tanaka, F. Ayala, and J.C. Keck. A reduced chemical kinetic model for HCCI combustion of primary reference fuels in a rapid compression machine. *Combustion and Flame*, 133:467–481, 2003.

[24] J. Zheng, W. Yang, D. L. Miller, and N. P. Cernansky. A skeletal chemical kinetic model for the HCCI combustion process. *SAE paper 2002-01-0423*, 2002.

[25] M. Jia and M. Xie. A chemical kinetics model of iso-octane oxidation for HCCI engines. *Fuel*, 85:2593–2604, 2006.

[26] G. M. Shaver, J. C. Gerdes, and M. J. Roelle. Modeling cycle-to-cycle coupling and mode transition in HCCI engines with variable valve actuation. *IFAC Journal on Control Engineering Practice (CEP)*, 14(3):213–222, 2006.

[27] F. Sun, X. Chen, D.S-K. Ting, and A. Sobiesiak. Modeling operation of HCCI engines fueled with ethanol. In *Proceedings of American Control Conference*, 2005.

[28] J. Bengtsson, P. Strandh, R. Johansson, P. Tunestål, and B. Johansson. System identification of homogenous charge compression ignition (HCCI) engine dynamics. In *Fourth IFAC Symposium on Advances in Automotive Control*. Elsevier, 2004.

[29] G. M. Shaver, J. C. Gerdes, P. Jain, P. A. Caton, and C. F. Edwards. Modeling for control of HCCI engines. *Proceedings of the 2003 American Control Conference*, pages 749–754, 2003.

[30] N. Jia, J. Wang, K. Nuttall, J. Wei, H. Xu, M.L. Wyszynski, J. Qiao, and M.J. Richardson. HCCI engine modeling for real-time implementation and control development. *IEEE/ASME Transactions on Mechatronics*, 12(6):581–589, December 2007.

[31] A. Widd, P. Tunestål, C.Wilhelmsson, and R. Johansson. Control-oriented modeling of homogeneous charge compression ignition incorporating cylinder wall temperature dynamics. In *Proceedings of AVEC 2008*, 2008.

[32] C. G. Mayhew, K. L. Knierim, N. A. Chaturvedi, S. Park, J. Ahmed, and J. Kojic. Reduced-order modeling for studying and controlling misfire in four-stroke HCCI engines. In *Proceedings of the 48th IEEE Conference on Decision and Control*, 2009.

[33] Y. Choi and J.-Y. Chen. Fast prediction of start-of-combustion in HCCI with combined artificial neural networks and ignition delay model. *Proceedings of the Combustion Institute*, 30:2711–2718, 2005.

[34] M. Shahbakhti and R. Koch. Physics based control oriented model for HCCI combustion timing. *Journal of Dynamic Systems, Measurement, and Control*, 132, 2010.

[35] K. Hiraya, A. Kakuho, T. Urushihara, and T. Ito. A study of gasoline fueled compression ignition engine: Effect of fuel reformation during negative valve overlap. *Proceedings of the JSAE Annual Congress*, 72-02:1–6, 2002.

[36] L. Koopmans, R. Ogink, and I. Denbratt. Direct gasoline injection in the negative valve overlap of a homogeneous charge compression ignition engine. *SAE paper 2003-01-1854*, 2003.

[37] R. Standing, N. Kalian, T. Ma, H. Zhao, M. Wirth, and A. Schamel. Effects of injection timing and valve timings on CAI operation in a multi-cylinder DI gasoline engine. *SAE paper 2005-01-0132*, 2005.

[38] H.H. Song and Christopher F. Edwards. Optimization of recompression reaction for low-load operation of residual-effected HCCI. *SAE World Congress*, SP-2182:79–97, 2008.

[39] G. Haraldsson, P. Tunestål, B. Johansson, and J. Hyvönen. HCCI closed-loop combustion control using fast thermal management. *SAE paper 2004-01-0943*, 2004.

[40] A. Widd, K. Ekholm, P.Tunestål, and R. Johansson. Experimental evaluation of predictive combustion phasing control in an HCCI engine using fast thermal management and VVA. In *Proceedings of Conference in Control Applications*, 2009.

[41] M. Christensen, A. Hultqvist, and B. Johansson. Demonstrating the multi-fuel capability of a homogeneous charge compression ignition engine with variable compression ratio. *SAE paper 1999-01-3679*, 1999.

[42] G. M. Shaver, M. J. Roelle, J. C. Gerdes, J-P. Hathout, J. Ahmed, A. Kojic, P. A. Caton, and C. F. Edwards. A physically based approach to control of HCCI engines with variable valve actuation. *International Journal of Engine Research*, 6(4):361–375, 2005.

[43] L. Shi, Y.Cui, K.Deng, H.Peng, and Y.Chen. Study of low emission homogeneous charge compression ignition (HCCI) engine using combined internal and external exhaust gas recirculation (EGR). *Journal of Energy*, 31:14:2665–2676, 2006.

[44] J-M. Kang, C-F. Chang, J-S. Chen, and M-F. Chang. Concept and implementation of a robust HCCI engine controller. *SAE paper 2009-01-1131*, 2009.

[45] J. Bengtsson, P. Strandh, R. Johansson, P. Tunestål, and B. Johansson. Closed loop combustion control of homogeneous charge compression ignition (HCCI) engine dynamics. *International Journal of Adaptive Control and Signal Processing*, 18:167–179, 2004.

[46] J-O. Olsson, P. Tunestål, G. Haraldsson, and B. Johansson. A turbocharged dual-fuel HCCI engine. *SAE paper 2001-01-1896*, 2001.

[47] G. Haraldsson, P. Tunestål, B. Johansson, and J. Hyvönen. HCCI combustion phasing with closed-loop combustion control using variable compression ratio in a multi-cylinder engine. *SAE paper 2003-01-1830*, 2003.

[48] J.O. Olsson, P. Tunestål, and B. Johansson. Closed-loop control of an HCCI engine. *SAE paper 2001-01-1031*, 2001.

[49] F. Agrell, H-E. Angstrom, B. Eriksson, J. Wikander, and J. Linderyd. Integrated simulation and engine test of closed loop HCCI control by aid of variable valve timings. *SAE paper 2003-01-0748*, 2003.

[50] N. J. Killingsworth, S. M. Aceves, D. L. Flowers, and Miroslav Krstić. Extremum seeking tuning of an experimental HCCI engine combustion timing controller. In *Proceedings of the 2007 American Control Conference*, 2007.

[51] P. Strandh, J. Bengtsson, R. Johansson, P. Tunestål, and B. Johansson. Cycle-to-cycle control of a dual-fuel HCCI engine. *SAE transactions*, (2004-01-0941):589–598, 2004.

[52] J. Bengtsson, P. Strandh, R. Johansson, P. Tunestål, and B. Johansson. Model predictive control of homogeneous charge compression ignition (HCCI) engine dynamics. In *Proceedings of the IEEE International Conference on Control Applications*, 2006.

[53] G. M. Shaver, J. C. Gerdes, M. J. Roelle, P. A. Caton, and C. F. Edwards. Dynamic modeling of HCCI engines utilizing variable valve actuation. *ASME Journal of Dynamic Systems, Measurement and Control*, 127(3):374–381, 2005.

[54] S. Turns. *An Introduction to Combustion: Concepts and Applications*. McGraw-Hill, 2000.

[55] C. K. Westbrook and F. L. Dryer. Simplified reaction mechanisms for the oxidation of hydrocarbon fuels in flames. *Combustion Science and Technology*, 27:31–43, 1981.

[56] J. Chang, O. Gralp, Z. Filipi, D. Assanis, T-W. Kuo, P. Najt, and R. Rask. New heat transfer correlation for an HCCI engine derived from measurements of instantaneous surface heat flux. *SAE paper 2004-01-2996*, 2004.

[57] G. Franklin, J.D Powell, and A. Emami-Naeini. *Feedback Control of Dynamic Systems*. Addison Wesley Publishing Company, 3rd edition edition, 1994.

[58] J. Bengtsson. *Closed-Loop Control of HCCI Engine Dynamics*. PhD thesis, Lund Institute of Technology, 2004.

[59] D. Flowers, S. Aceves, R. Smith, J. Torres, J. Girard, and R. Dibble. HCCI in a CFR engine: Experiments and detailed kinetic modeling. *SAE paper 2000-01-0328*, 2000.

[60] W. Fischer, R. Karrelmeyer, A. Loffler, A. Kulzer, and J-P. Hathout. Closed-loop control of a multi-mode engine with CAI. In *Proceedings of the 2007 IFAC Symposium on Advances in Automotive Control*, pages 495–502, 2007.

[61] H-H. Liao, N. Ravi, A. F. Jungkunz, J-M. Kang, and J. C. Gerdes. Representing recompression HCCI dynamics with a switching linear model. In *Proceedings of the American Controls Conference*, 2010.

[62] A. F. Jungkunz, H-H. Liao, N. Ravi, and J. C. Gerdes. Reducing combustion variation of late-phasing HCCI with cycle-to-cycle exhaust valve timing control.

In *Proceedings of the 2010 IFAC Symposium on Advances in Automotive Control*, 2010.

[63] T. Aroonsrisopon, P. Werner, J. O. Waldman, V. Sohm, D. E. Foster, T. Morikawa, and M. Iida. Expanding the HCCI operation with charge stratification. *SAE paper 2004-01-1756*, 2004.

[64] H. Persson, R. Pfeiffer, A. Hultqvist, B. Johansson, and H. Ström. Cylinder-to-cylinder and cycle-to-cycle variations at HCCI operation with trapped residuals. *SAE paper 2005-01-0130*, 2005.

[65] B. J. Allison and S. Ogawa. Design and tuning of valve position controllers with industrial applications. *Transactions of the Institute of Measurement and Control*, 25, No. 1:3–16, 2003.

[66] S. Haugwitz, M. Karlsson, S. Velut, and P. Hagander. Anti-windup in mid-ranging control. In *Proceedings of the 44th IEEE Conference on Decision and Control, and the European Control Conference 2005*, 2005.

[67] A. I. Propoi. Use of linear programming methods for synthesizing sampled-data automatic systems. *Automation and Remote Control*, 24 (7):837–844, 1963.

[68] J. Richalet, A. Rault, J. L. Testud, and J. Papon. Model predictive heuristic control: Applications to industrial processes. *Automatica*, 14:413–428, 1978.

[69] J. M. Maciejowski. *Predictive Control with Constraints*. Prentice-Hall, Inc., 2002.

[70] N. L. Ricker. Model predictive control with state estimation. *Industrial Engineering Chemical Research*, 29:374–382, 1990.

[71] C. C. Chen and L. Shaw. On receding horizon feedback control. *Automatica*, 18:349–352, 1982.

[72] C. E. Garcia, D. M. Prett, and M. Morari. Model predictive control: Theory and practicea survey. *Automatica*, 25(3):335–348, 1989.

[73] K. R. Muske and J. B. Rawlings. Model predictive control with linear models. *American Institute of Chemical Engineers Journal*, 39(2):262–287, 1993.

[74] S. J. Qin and T. A. Badgwell. A survey of industrial model predictive control technology. *Control Engineering Practice*, 11:733–764, 2003.

[75] A. Bemporad, M. Morari, V. Dua, and E. N. Pistikopoulos. The explicit solution of model predictive control via multiparametric quadratic programming. In *Proceedings of the American Control Conference*, 2000.

[76] A. Bemporad, F. Borrelli, and M. Morari. Model predictive control based on linear programming – the explicit solution. *IEEE Transactions on Automatic Control*, 47 (12):1974–1985, 2002.

[77] A. Bemporad, F. Borrelli, and M. Morari. Piecewise linear optimal controllers for hybrid systems. In *Proceedings of the American Controls Conference*, 2000.

[78] A. Grancharova, T. A. Johansen, and J. Kocijan. Explicit model predictive control of gas - liquid separation plant. In *Proceedings of European Controls Conference*, 2003.

[79] Ø. Hegrenæs, J. T. Gravdahl, and P. Tøndel. Spacecraft attitude control using explicit model predictive control. *Automatica*, 41:2107–2114, 2005.

[80] J.O. Olsson, P. Tunestål, B. Johansson, S. Fiveland, R. Agama, M. Willi, and D. Assanis. Compression ratio influence on maximum load of a natural gas fueled HCCI engine. *SAE paper 2002-01-0111*, 2002.

[81] H. M. Xu, M. L. Wyszynski, A. Megaritis, D. Yap, T. Wilson, J. Qiao, S. Richardson, S. Golunski, and S. Peucheret. Research on expansion of operating windows of controlled homogeneous auto-ignition engines. *International Journal of Engine Research*, 8:29–40, 2007.